

THE EFFECT OF A CHEMOTHERAPY DRUG COCKTAIL ON MYOTUBE  
MORPHOLOGY AND PROTEIN METABOLISM

STEPHEN MORA

A THESIS SUBMITTED TO THE FACULTY OF GRADUATE STUDIES IN PARTIAL  
FULFILLMENTS OF THE REQUIREMENTS FOR THE DEGREE OF  
MASTER OF SCIENCE

GRADUATE PROGRAM IN KINESIOLOGY AND HEALTH SCIENCE  
YORK UNIVERSITY, TORONTO, ONTARIO, CANADA

July 2019

© Stephen Mora, 2019

## **Abstract**

Cachexia, a condition prevalent in many chronically-ill patients, is characterized by weight loss and fatigue resulting from decreases in muscle mass and function. Although development of cachexia is associated with tumour-burden and disease-related malnutrition, studies have suggested a causative link between chemotherapy and cachexia. Day 4 myotubes were treated with vehicle or a chemotherapy drug cocktail consisting of cisplatin, 5-fluorouracil and leucovorin. Myotubes treated with the drug cocktail showed irregular myotube structure and reductions in myofibrillar protein content. Myotubes treated with the drug cocktail showed reductions in the phosphorylation of AKT<sup>Ser473</sup>, S6<sup>Ser235/236</sup> and S6K1<sup>Thr389</sup>. Drug treatments also led to reductions in protein synthesis and mitochondrial complexes cytochrome C oxidase and succinate dehydrogenase. Lastly, reductions in insulin stimulated glucose uptake were found following drug treatment. Findings suggest that it is critical to identify interventions that limit the negative effects of these drugs on muscle protein status and mitochondrial content.

## Acknowledgments

*I would like to thank everyone who has helped me along this Master's Journey. Dr. Adegoke, thank you for this special opportunity and your guidance over these two years. To my friends, family and lab mates, thank you for always supporting me and providing me with motivation to always put out my best work.*

# Table of Contents

Abstract .....	ii
Acknowledgements .....	iii
Table of Contents .....	iv
List of Figures .....	vi
List of Abbreviations .....	vii
 Chapter One: Introduction .....	 1
Chapter Two: Literature Review .....	3
2.1 Skeletal Muscle and Health .....	3
2.1.1 Factors regulating skeletal muscle anabolism.....	3
2.1.1.1 Nutrition and resistance exercise .....	3
2.1.1.2 Anabolic hormones .....	4
2.1.2 Mechanisms of skeletal muscle anabolism .....	5
2.1.2.1 IGF1-AKT.....	5
2.1.2.2 mTORC1.....	6
2.1.2.3 BMP-Smad pathway .....	7
2.1.3 Factors regulating skeletal muscle catabolism.....	8
2.1.3.1 Aging.....	9
2.1.3.2 Muscle disuse.....	9
2.2 Cachexia.....	10
2.2.1 Qualify of life.....	10
2.2.1.1 Weight Loss .....	11
2.2.1.2 Reduced Appetite.....	12
2.2.1.3 Fatigue.....	12
2.2.1.4 Treatment Outcomes.....	13
2.3 Factors regulating cachexia.....	14
2.3.1 Chronic disease .....	14
2.3.1.1 Chronic Heart Failure .....	14
2.3.1.2 Chronic Kidney Disease .....	15
2.3.1.3 Cancer .....	16
2.3.2 Inflammation.....	17
2.3.3 Reactive oxygen species .....	19
2.3.4 Chemotherapy Treatment.....	20
2.3.4.1 Cisplatin .....	21
2.3.4.2 5-Fluourouracil .....	23
2.3.4.3 Leucovorin .....	25
2.4 Mechanisms of skeletal muscle catabolism .....	26
2.4.1 Ubiquitin Proteasome Pathway.....	27
2.4.2 Autophagy.....	27
2.4.3 Apoptosis .....	28
2.4.4 Calcium Calpain.....	29
2.5 Signalling towards mechanisms of skeletal muscle catabolism .....	30
2.5.1 O-type forkhead .....	30
2.5.2 Nf-KB .....	31

2.5.3 Myostatin .....	32
2.5.4 ULK-1 .....	32
2.6 Current treatments.....	32
2.7 Rationale .....	35
2.8 Objectives .....	35
2.9 Hypotheses.....	35
Chapter Three: Manuscript .....	36
Chapter Four: Abstract.....	37
Chapter Five: Introduction.....	38
Chapter Six: Materials and Methods.....	40
6.1 Reagents.....	40
6.2 Cell Culture.....	40
6.2.1 Formation of Chemotherapy Drug Cocktail and Cell Treatment .....	41
6.3 Cell Harvesting .....	42
6.4 Protein Assay, Gels and Western Blot Analysis.....	42
6.5 Protein Synthesis Measurement in Myotubes.....	43
6.6 Myofibrillar and Sarcoplasmic Fractionation of Myotubes.....	45
6.7 Immunofluorescence Microscopy.....	45
6.8 2-Deoxy-Glucose Uptake in Myotubes .....	46
6.9 Graphical Representation of Western Blots and Statistics .....	47
Chapter Seven: Results .....	48
Figure Results. ....	53
Figure 1 .....	53
Figure 2 .....	54
Figure 3 .....	56
Figure 4.....	57
Figure 5.....	58
Figure 6.....	59
Figure 7 .....	61
Figure 8.....	62
Chapter Eight: Discussion.....	63
Chapter Nine: Future Research.....	68
References.....	70
Appendices.....	85
Appendix A - Myofibrillar and Sarcoplasmic Fractionation of Myotubes.....	85
Appendix B - Immunofluorescence Microscopy.....	86
Appendix C - Deoxy-Glucose Uptake in Myotubes .....	87

## List of Figures

<b>Figure 1.</b> A chemotherapy drug cocktail negatively regulates myotube formation and morphology.....	53
<b>Figure 2.</b> A chemotherapy drug cocktail disrupts L6 myofibrillar abundance. ....	54
<b>Figure 3.</b> Myofibrillar protein content is decreased in myotubes treated with a chemotherapy drug cocktail.....	56
<b>Figure 4.</b> mTORC1 signalling is disrupted in myotubes treated with a chemotherapy drug cocktail.....	57
<b>Figure 5.</b> Protein synthesis is reduced in myotubes treated with a chemotherapy drug cocktail. ....	58
<b>Figure 6.</b> Protein synthesis is decreased in fractionated myotubes treated with a chemotherapy drug cocktail .....	59
<b>Figure 7.</b> Mitochondrial Proteins are reduced in myotubes treated with a chemotherapy drug cocktail.....	61
<b>Figure 8.</b> Glucose Uptake is reduced in myotubes treated with a chemotherapy drug cocktail. ....	62

## List of Abbreviations

4E-BP1: eIF4e-binding protein-1

5-Flu: 5-Fluorouracil

AA: Amino Acids

AKT: protein kinase B (PKB)

AMPK: AMP-activated protein kinase

AMP: adenosine monophosphate

ATP: adenosine triphosphate

BCAA: branched-chain amino acids

BW: Body Weight

D0: day 0

D1: day 1

D2: day 2

D4: day 4

D5: day 5

D6: day 6

D7: day 7

DFBS: Dialyzed Fetal Bovine Serum

E3 Protein: E3 ubiquitin ligases

eIF4E: eukaryotic translation initiation factor-4E

eIF4F: eukaryotic translation initiation factor-4F

eIF4G: eukaryotic translation initiation factor-4G

FoxO: forkhead box-O

IGF-1: insulin-like growth factor-1

IGF-2: insulin-like growth factor-2

IL-1: interleukin-1

IL-6: interleukin-6

IRS1: insulin receptor substrate-1

MAPK: mitogen activated protein kinase

MHC-1: myosin heavy chain-1

MPB: muscle protein breakdown

MPS: muscle protein synthesis

mTOR: mammalian target of rapamycin

mTORC1: mammalian target of rapamycin complex-1

MuRF-1: muscle ring finger protein-1

NF- $\kappa$ B: nuclear factor kappa-light-chain-enhancer of activated B cells

REx: resistance exercise

Rheb: ras homolog enriched in brain

ROS: reactive oxygen species

Ser/S: serine

S6/rpS6: ribosomal protein S6

S6K1: p70 ribosomal protein S6 kinase 1

TNF- $\alpha$ : tumor necrosis factor alpha

UPP: ubiquitin proteasome pathway

## Chapter One: Introduction

Cachexia, a condition affecting approximately nine million patients with chronic disease today<sup>68</sup>, is characterized by detrimental loss of body weight and depletion of fat and muscle mass. In addition, this muscle wasting syndrome leads to wide scale fatigue and weakness, associated with decreases in quality of life and increased mortality and morbidity<sup>183, 184</sup>.

Maintenance of skeletal muscle mass is dependent on a balance between protein synthesis and protein degradation. These two processes are highly regulated by multiple signalling events and pathways within skeletal muscle. For example, activation of the insulin receptor substrate 1 (IRS-1)/protein kinase B (AKT)/mechanistic target of rapamycin (mTOR) pathway is well-known to be vital for skeletal muscle growth and the inhibition of skeletal muscle protein degradation<sup>185</sup>. In opposition, stimulation of either the ubiquitin proteasome pathway (UPP) or autophagic mechanisms induce protein degradation within skeletal muscle<sup>186</sup>. Although upstream activators of the UPP, such as forkhead box protein O (FOXO) or nuclear factor kappa-light-chain-enhancer of activated B cells (NFkB) are upregulated in atrophic conditions such as cachexia, signalling events and mechanisms in these pathways are yet to be completely understood.

Past reports have suggested that the development and severity of cachexia is due to the administration of cytotoxic and antineoplastic chemotherapy drugs. Symptoms including nausea, vomiting, poor nutrition and anorexia-like states are often present following chemotherapy treatment. Of these, no side effect matches the debilitating loss of muscle strength and mass, often accompanying chemotherapy regimens in patients.

Although available evidence suggests an association between chemotherapy treatment and cachexia, the mechanisms of chemotherapeutic regimens in the promotion of cachectic

symptoms are not completely clear. Cisplatin, a platinum-containing chemotherapeutic, used in the treatment of testicular, ovarian, head, lung and neck cancers, dramatically increases muscle atrophy F-box (MAFbx) and muscle ring finger-1 (MuRF1) in vivo<sup>158</sup>. In addition, cisplatin also activates nuclear factor kappa-light-chain enhancer of activated B cells (Nf-KB)<sup>159</sup>, linking this chemotherapeutic to the upregulation of the ubiquitin proteasome pathway (UPP) in muscle. 5-Fluorouracil (5-Flu), an antineoplastic agent part of Folfiri and Folfox chemotherapy regimens, upregulates p38 mitogen activated protein kinases (MAPK) resulting in weight loss, muscle loss and reductions in mitochondrial content<sup>160</sup>. Other common chemotherapy drugs, such as CPT-11 or Adriamycin promote tissue injury, either through increased production of inflammatory factors<sup>179</sup> or reactive oxygen species (ROS)<sup>180</sup>.

Better understanding of the mechanisms underlying chemotherapy-induced cachexia may present possible regimens to increase the efficacy of cancer treatment today. Prior to treatment, patients with greater accumulation of muscle mass may be presented with the opportunity for generally more aggressive chemotherapeutic treatment regimens. This opportunity may be lost in patients who have begun to undergo severe muscle wasting or who have faced long term chemotherapy treatment. Therefore, patients with lower levels of muscle mass face the risk of drug toxicity, in accordance with decreased severity of treatment and chance of disease-free survival<sup>181, 182</sup>.

## Chapter Two: Literature Review

### 2.1 Skeletal Muscle and Health

Skeletal muscle contributes to approximately 40% of total body weight<sup>1</sup> and is a major contributor to energy and protein metabolism. The health importance of skeletal muscle stems from its ability to provide support for locomotion, regulate glucose homeostasis<sup>2</sup> and provide a site for fatty acid metabolism and glycogen synthesis<sup>3</sup>. Skeletal muscle mass is associated with overall risk of mortality<sup>4</sup> and loss of skeletal muscle can lead to or worsen chronic, metabolic and muscle wasting associated diseases. Thus, therapeutic interventions that aim to attenuate skeletal muscle loss in all populations is of great interest today.

#### 2.1.1 Factors regulating skeletal muscle anabolism

The maintenance of skeletal muscle is dependent on a balance of two antagonizing processes, muscle protein synthesis and muscle protein breakdown. The balance between these two processes, often termed protein turnover is a major regulator of skeletal muscle mass. When protein turnover reaches a positive balance, increases in muscle protein synthesis will lead to skeletal muscle anabolism. Skeletal muscle anabolism is highly responsive to multiple stimuli: nutrition, resistance exercise and anabolic hormones.

##### 2.1.1.1 Nutrition and resistance exercise

Macronutrient ingestion, specifically protein, remains to be one of the most well-known anabolic regulators of skeletal muscle. Sedentary individuals require 0.8g of protein, per kg/BW/day according to current recommendations<sup>5</sup>. Although this recommendation is the standard in order to satisfy daily requirements, factors such as age, health and physical activity may result in the need for increased protein intake. Due to daily protein recommendations, past studies have investigated the effect of protein on stimulating muscle protein synthesis. Dietary

protein ingestion (specifically amino acids (AA)) have been shown to elicit increases in muscle protein synthesis<sup>6, 7</sup>. Despite an AA induced increase in muscle protein synthesis, overall protein turnover may remain unchanged due to matched increases in muscle protein breakdown. Therefore, in order to elicit muscle hypertrophy, resistance exercise is often the method of choice. Past evidence has shown that resistance exercise stimulates muscle protein synthesis in all populations<sup>8, 9, 10</sup>. In fact, resistance exercise in combination with post-exercise protein supplementation, elicits robust increases in muscle protein synthesis<sup>5, 7, 11, 12, 13, 14, 15, 16</sup>. In fact, past reports have found that bolus protein ingestions of ~20g optimally stimulates muscle protein synthesis following resistance exercise<sup>11</sup>.

### **2.1.1.2 Anabolic hormones**

Insulin is a potent anabolic stimulus within skeletal muscle. Although insulin may not directly stimulate muscle protein synthesis<sup>17</sup>, this hormone plays a pivotal role in multiple intermediary processes. Upon being released from the pancreas in response to hyperglycemia, insulin mediates the uptake of glucose into skeletal muscle. Glucose can then be used for skeletal muscle contraction, stored as glycogen or serve as primary fuel for many metabolic processes, such as protein synthesis. Insulin can also regulate the uptake of other important metabolites into skeletal muscle. As mentioned before, high concentrations of AA in skeletal muscle can elicit increases in muscle protein synthesis<sup>6, 7</sup>. Insulin has been shown to enhance muscle protein synthesis through the uptake of AA into skeletal muscle, but only when AA are highly concentrated in the plasma<sup>18</sup>. Insulin may also have an anabolic effect on skeletal muscle through the inhibition of proteolysis<sup>19, 20</sup>.

Testosterone is an anabolic hormone produced primarily within the gonads of both male and female sexes. This anabolic hormone increases tissue and muscle growth, as well as protein

synthesis. In normal male subjects, 12-week supplementation with testosterone enanthate, an anabolic steroid medication, led to increases in both muscle protein synthesis and muscle mass<sup>21</sup>. While in elderly subjects, 6-months of testosterone treatment prevented the loss of lower limb muscle strength<sup>22</sup>. Testosterone replacement has also been found to enhance skeletal muscle mass and protein synthesis in hypogonadal men<sup>23</sup>.

Growth hormone (GH), secreted by the pituitary gland functions as a crucial regulator of growth and human development. Individual's deficient in GH exhibit decreased muscle mass, strength and increased body fat<sup>24</sup>. In addition, GH can have anti-insulin effects as it decreases the ability of insulin to increase glucose uptake in peripheral tissues such as adipose tissue<sup>263</sup>. GH also functions to stimulate the production of insulin-like growth factor 1 (IGF1)<sup>25</sup>. Similarly to insulin, IGF1 once synthesized and activated begins a cascade of events leading to the eventual phosphorylation on Thr<sup>308</sup> of protein kinase B (AKT)<sup>26</sup>.

### **2.1.2 Mechanisms of skeletal muscle anabolism**

In order to enhance an anabolic state within skeletal muscle, insulin, growth hormone and testosterone must signal through specific mechanisms to augment muscle protein synthesis. Understanding these mechanisms are important as signalling through these pathways have implications in growth and maintenance of skeletal muscle over time. Skeletal muscle anabolism is controlled by signaling through IGF1-AKT, Mechanistic (mammalian) Target of Rapamycin Complex 1 (mTORC1) and Bone Morphogenetic Protein (BMP).

#### **2.1.2.1 IGF1-AKT**

The IGF1-AKT signalling pathway in conjunction with multiple intracellular components plays a pivotal role in skeletal muscle growth. Binding of IGF1 to its cognate IGF1 receptor activates insulin receptor substrate (IRS) leading to the activation of the phosphatidylinositol 3-

kinase (PI3K) family. Once activated, the PI3K family generates phosphatidylinositol-3, 4, 5-trisphosphate (PIP3). PIP3 signals through phosphoinositide-dependent kinase 1 (PDK1) allowing for the subsequent activation of AKT<sup>30</sup>. Once activated, AKT mediates its effect on skeletal muscle anabolism through multiple mechanisms, one being the inhibition of protein degradation. Among others, forkhead box O (FOXO) transcription factors stimulate the production of MAFbx and MURF1, two E3 ligases known to induce muscle atrophy within skeletal muscle<sup>27</sup>. Once phosphorylated on Thr<sup>308</sup>, AKT inhibits protein degradation through the phosphorylation and resulting suppression of FOXO transcription factors<sup>28</sup>.

Aside from inhibiting protein degradation, the IGF1-AKT signaling pathway can stimulate skeletal muscle anabolism through its effect on glycogen synthase kinase  $\beta$  (GSK3 $\beta$ ). GSK3 $\beta$  inhibits protein synthesis via its negative effect on eukaryotic translation initiation factor 2 subunit B (eIF2B). Once activated, AKT phosphorylates GSK3 $\beta$  on Ser21, relieving the inhibitory effect of GSK3 $\beta$  on eIF2B<sup>29</sup>, leading to translation initiation and thus, protein synthesis. The IGF1-AKT pathway also augments its effect on the stimulation of skeletal muscle anabolism through its activation of mechanistic target of rapamycin complex 1 (mTORC1).

### **2.1.2.2 mTORC1**

mTORC1 is a signal integrating hub that plays one of the most important roles in regulating cellular function and skeletal muscle anabolism. Through an indirect mechanism, the IGF1-AKT pathway provides upstream activation of mTORC1. Together, Tuberous Sclerosis Complex 2 (TSC2) and Tuberous Sclerosis Complex 1 (TSC1) form a complex that inhibits mTORC1's activity<sup>31</sup>. Phosphorylation of the TSC2 complex by AKT at S939 and T1462 relieves the inhibitory effect on mTORC1 leading to an increase in mTORC1's kinase activity<sup>32</sup>.<sup>33</sup>. Activated mTORC1 leads to the phosphorylation of p70 ribosomal S6 Kinase 1 (S6K1). Upon

phosphorylation on Thr<sup>389</sup> by mTORC1, S6K1 phosphorylates multiple downstream substrates such as ribosomal protein S6 (S6), eukaryotic translation initiation factor 4B (eIF4B), eukaryotic translation elongation factor 2 kinase (eEF2K) and programmed cell death 4 (PDCD4) resulting in muscle protein synthesis<sup>34, 240</sup>. In addition, mTORC1 can also phosphorylate eukaryotic translation initiation factor 4E-binding protein 1 (4EBP1) on several residues, leading to the dissociation of 4EBP1 from eIF4E. This process allows for eIF4E to upregulate initiation and translation machinery<sup>34, 35</sup> ultimately leading to protein synthesis.

mTORC1 can also be activated directly by high concentrations of AA, specifically leucine. Research from past studies has shown that mTORC1 mediates the AA induced increase in muscle protein synthesis<sup>36</sup>. Once activated by AA, mTORC1 phosphorylates main downstream targets S6K1 and 4EBP1, leading to muscle protein synthesis within skeletal muscle. Perhaps a consequence of low dietary protein, dampened mTORC1 signalling results in decreased gene transcription<sup>37</sup>, cellular growth and muscle protein synthesis.

### **2.1.2.3 BMP-Smad pathway**

Bone morphogenetic proteins (BMPs) are a small group of growth factors primarily functioning in the formation, repair and maintenance of bone. More recently, BMPs has been investigated and established as positive regulators of skeletal muscle anabolism. Signalling through BMPs leads to the phosphorylation of downstream Smad proteins (Smad1/5/8)<sup>38</sup> and the formation of a Smad4 transcriptional complex. This newly formed transcription complex then travels to the nucleus<sup>39</sup> and increases the transcription of genes involved in the IGF1/AKT/mTORC1 pathway<sup>41</sup>.

Dependent on formation of the Smad4 transcriptional complex, activation of the BMP-Smad4 pathway has been shown to regulate muscle growth and inhibit muscle atrophy in

innervated muscle fibers<sup>40</sup>. Part of this effect comes through the BMP-Smad4 pathway operating counter to a common catabolic pathway within skeletal muscle, the Myostatin/Activin pathway. In opposition to the formation of the Smad4 transcriptional complex, the Myostatin/Activin pathway reduces stem cell differentiation and induces fibre atrophy by activating transcription factors Smad 2 or 3<sup>267, 268</sup>. In addition, the Myostatin/Activin pathway increases muscle atrophy through upregulation of MAFbx and MuRF1<sup>178</sup> and this effect is exacerbated when BMP-Smad4 signalling is lost<sup>40</sup>. This shows that the effect of the BMP-Smad4 pathway on skeletal muscle hypertrophy is partly driven by outweighing signals through the Myostatin/Activin pathway. Other studies have also investigated the mechanism of BMP-Smad4 signaling in the promotion of muscle fiber hypertrophy. A novel study in 2013 found that BMP-Smad4 signaling increased the transcription of IGF isoforms and phosphorylation of AKT<sup>S473</sup>, mTOR<sup>S2448</sup>, S6<sup>S235/236</sup> and 4EBP1<sup>T37/46</sup>. Interestingly, this effect of BMP-Smad4 on muscle fiber hypertrophy was dependent on mTORC1, as rapamycin (an mTORC1 inhibitor) completely abolished this effect<sup>41</sup>. This same study also elucidated that in a model of denervation-induced muscle atrophy, BMP-Smad4 signaling both limited muscle wasting and maintained muscle mass over time<sup>41</sup>.

### **2.1.3 Factors regulating skeletal muscle catabolism**

As mentioned before, protein turnover is a major regulator of skeletal muscle mass. Therefore when protein turnover reaches a negative balance, increases in muscle protein breakdown will lead to skeletal muscle catabolism. Aging, muscle disuse and poor nutritional habits are major factors that can regulate skeletal muscle catabolism and lead to muscle atrophy and poor muscle mass maintenance overtime. The multitude of other factors that cause progression of skeletal muscle catabolism will be covered under cachexia.

### **2.1.3.1 Aging**

Aging is associated with a progressive loss of both muscle mass and function. This age associated condition, more commonly known as sarcopenia, causes ~1-2% drop in muscle mass per year in individuals past the age of 50. Sarcopenia can bring about profound consequences in elderly individuals related to negative health outcomes such as loss of functional ability and frailty<sup>42</sup>. Sarcopenia is a multi-dimensional condition caused by multiple environmental, physiological and metabolic changes.

Sarcopenia can be associated with decreased physical activity in the elderly. In both men and women aged 60-80 years of age, reductions in physical activity levels and functional fitness is associated with the aging process<sup>43</sup>. In addition, decreases in protein intake and total caloric requirements are important contributors to sarcopenia in older adults<sup>44</sup>. The effects of sarcopenia can be reduced by the ingestion of dietary proteins above current recommendations<sup>45</sup>.

The reduced muscle mass in the elderly is mainly attributed to decreases in type II muscle fiber size and quadriceps cross sectional area (CSA) compared to young individuals<sup>46</sup>. Additionally, declines in elderly motor neuron activity<sup>47</sup>, exercise capacity<sup>48</sup>, mitochondrial content/activity<sup>48</sup> and hormones necessary for muscle mass maintenance<sup>49</sup> contribute to sarcopenia.

### **2.1.3.2 Muscle disuse**

Overtime, muscle disuse can lead to rapid and detrimental atrophy within skeletal muscle. Muscle disuse atrophy is associated with health complications such as functional decline in physical working capacity, metabolic disorders and increased mortality risk<sup>4</sup>. Muscle disuse atrophy is often driven by either acute or chronic immobilization periods. A study in 2013 found that a 14-week immobilization period in young males led to reductions in quadriceps fiber

strength and CSA<sup>50</sup>. This reduction in fiber size and muscle mass can possibly be accounted for by a suppression or decline in the rate of muscle protein synthesis<sup>51</sup>. In addition, hindlimb immobilization found that muscle protein breakdown is also enhanced during muscle disuse atrophy<sup>52</sup>, but these findings in humans are not yet well defined.

## **2.2 Cachexia**

Associated with exacerbated weight loss and as a sign of forth-coming death, cachexia was first described by Hippocrates during the classical era<sup>53</sup>. Cachexia is a complex muscle or body wasting syndrome characterized by whole-body metabolic and physical abnormalities. An estimate in 2010 reported that approximately nine million people diagnosed with a chronic disease are affected by cachexia<sup>68</sup>. Metabolically, this syndrome is associated with loss of appetite, fatigue, aggravated skeletal muscle catabolism, increases in energy expenditure, large-scale systemic inflammation and negative protein/energy balance<sup>54</sup>. The physical abnormalities of this syndrome include uncontrollable weight loss and is associated with detrimental decreases in fat mass, muscle mass and muscle function<sup>55</sup>. In order to be characterized as having cachexia, an individual needs to have lost more than 5% of their total body weight over 12 months, while being diagnosed with a chronic condition<sup>56</sup>. Although chronic conditions such as congestive heart failure and chronic renal disease positively correlate with cachexia progression, cancer is the dominant chronic disease associated in the development of cachexia. With no effective or accepted treatments today, cachexia plays a massive burden on today's society leading to reductions in quality of life (QOL) and severe complications.

### **2.2.1 Quality of life**

In cancer cachexia, persistent loss of body weight is associated with deteriorating QOL and likely shortens survival time in patients<sup>67</sup>. A study by Fearon et al in 2006 investigated three

distinctive factors related to functional status and prognosis: weight loss, reduced food intake and systemic inflammation. Findings from their study reported that cancer cachectic patients are more likely to score lower on these three measures when compared to their weight stable counterparts<sup>69</sup>. In association, scoring lower on quality of life measures is accompanied by decreases in physical activity and exercise tolerance<sup>70</sup>. Other studies have investigated the prevalence of depression in cancer cachexia. These reports have found that there is a higher prevalence of depression in cancer cachectic patients compared to the general population, but this clinical depression is often overlooked.<sup>71, 72</sup> Lastly, cachexia-induced weight loss also affects body image. Studies have found that the significant weight loss in cachectic patients leads to decreases in both self-identity and self-esteem<sup>73</sup>. These issues potentiate cachectic patients to both self-alienate and socially isolate themselves from personal contact with others<sup>74</sup>. From this, cachexia can affect QOL through complications such as weight loss, reduced appetite, fatigue and treatment outcomes.

### **2.2.1.1 Weight Loss**

Within cachexia, significant body weight loss appears to be the most prevalent and detrimental complication of this syndrome. A study by Ross et al in 2004 investigated the probability of survival in small cell lung cancer patients undergoing chemotherapy treatment. They found that patients with reductions in lean body mass and its associated weight loss, had significantly decreased probability of survival compared to those patients with no weight loss<sup>59</sup>. Although the previous studies have looked at lean body mass, other studies have found that cachectic weight loss is not dependent on adipose tissue wasting, as obese patients with cachexia still exhibit large reductions in muscle weight<sup>57, 58</sup>. From this, cachexia associated weight loss can be attributed mainly to adverse reductions in lean body mass, specifically skeletal muscle.

With the health importance of skeletal muscle mentioned earlier, it is clear why weight loss within cachexia is major problematic complication of this syndrome. The loss of body weight experienced by cachectic patients can coincide with other complications including reductions in food intake, decreased appetite, increased fatigued and decreased physical activity.

### **2.2.1.2 Reduced Appetite**

In normal individuals, eating a healthy well-balanced diet while satisfying all the daily nutrient recommendations leads to the maintenance of weight. As seen in some conditions such as anorexia, reductions in food intake and therefore energy consumption leads to detrimental weight loss. In cachectic patients, symptoms of both early satiety and decreased appetite are of high prevalence<sup>60</sup>, but are often overlooked<sup>61</sup>. Although it can be thought that the weight loss experienced in cachexia is in part due to reductions in food intake and energy consumption, this is not the case. Multiple past reports have found that in cancer cachectic patients, dietary counselling<sup>62</sup>, oral nutritional support<sup>63</sup> and dietary treatments<sup>64</sup> did improve caloric intake, but had no significant effect on increasing body weight. Therefore, malnutrition is not a major determinant in the development of cachexia as improvements in nutrient and caloric intake do not rescue the adverse weight loss. Although cachexia is not due to malnourishment, complications such as early satiety and decreased appetite experienced by patients can lead to poor eating behaviours and consumption of nutrients below normal requirements. Therefore, these unfavourable changes in eating habits can generate a potential negative protein balance leading to muscle protein breakdown, further contributing to weight loss.

### **2.2.1.3 Fatigue**

A third well-known complication experienced by cachectic patients is severe weakness and fatigue. Approximately 70-100% of all cancer patients with cachexia experience fatigue

throughout the course of their disease<sup>65</sup>. With fatigue, cachectic patients often experience declines in the levels of physical activity due to decreased energy levels. Therefore, cachectic patients may avoid being physically active in order to conserve energy levels. Unfortunately, immobilization due to constant feelings of fatigue potentially lead to deconditioning and the worsening of exercise tolerance<sup>66</sup>. With this, strategies attempting to reduce fatigue and increase physical activity in cachectic patients are of great value. Regimens to increase physical activity and lessen feelings of fatigue include walking programmes, exercise sessions, reductions in stress levels and psychosocial support<sup>65</sup>. The inability to rescue long term fatigue in cachectic patients can lead to immobilization and muscle disuse contributing further to weight and muscle loss that is already aggravated in this condition due to other complications.

#### **2.2.1.4 Treatment outcomes**

The possibility of having successful treatment of any chronic condition represents one of the most favourable ways to increase quality of life in patients. Unfortunately, cachexia can negatively impact treatment outcomes in a spectrum of different chronic diseases. For example, in cancer where chemotherapy is the most common treatment, cachexia-induced weight loss leads to decreased treatment doses and increased likelihood of drug toxicity<sup>200</sup>. In contrast, weight stable cancer patients respond better to cancer therapy, resulting in a greater chance of survival following treatment<sup>201</sup>. In patients requiring surgical treatment, cachexia increases surgical risk factors associated with post-operative complications, surgical complications and longer hospital stays<sup>202, 203</sup>. In addition, due to the array of metabolic disruptions and factors leading to cachexia progression, it is unlikely that a single treatment modality would provide successful treatment for cachectic patients<sup>204</sup>.

## **2.3 Factors regulating cachexia**

Similar to the factors regulating skeletal muscle catabolism, factors leading to cachexia progression potentiate a negative balance within protein turnover. A negative protein balance can lead to extreme proteolysis matched with debilitating muscle atrophy. Chronic disease, inflammation, reactive oxygen species (ROS) and chemotherapy are all factors regulating cachexia development and progression.

### **2.3.1 Chronic disease**

Chronic disease represents one of the major determinants in the development of cachexia today. Individuals diagnosed with chronic diseases such as chronic heart failure (CHF), chronic kidney disease (CKD) and cancer will face one or more of the symptoms of cachexia throughout the duration of their disease. Cachexia affects a large majority of the patients diagnosed with these diseases and in the United States, more than 5 million people are affected by this muscle wasting syndrome<sup>97</sup>. From this, cachexia is a significant public health issue and interventions that attenuate the onset or progression of cachexia could provide vast therapeutic benefits.

#### **2.3.1.1 Chronic Heart Failure**

CHF is a well-known cardiovascular disease leading to higher rates of morbidity and mortality in elderly populations<sup>98</sup>. Cardiovascular diseases effects ~2% of the population<sup>100</sup> and the likelihood of developing CHF doubles after the age of 55. Majority of the individuals diagnosed with CHF are burdened by symptoms including shortness of breath, tiredness and irregular heartbeat. Unfortunately, treatment and therapeutic options for this disease are minimal and revolve around palliative care and pharmacological support<sup>241</sup>.

Approximately 5-15% of all elderly patients diagnosed with CHF experience cardiac cachexia, characterized by loss of muscle mass and function compared to healthy elderly

people<sup>99</sup>. CHF patients may also experience loss of fat tissue and bone density, all of which contribute to reduced body weight. Studies have also found that CHF patients with cachexia have a very poor prognosis leading to an impact on quality of life<sup>101</sup>. From a pathophysiology viewpoint, CHF patients are observed to have increased plasma levels of cortisol and inflammatory cytokines, specifically TNF- $\alpha$ , that aggravate muscle wasting<sup>102</sup>. Further, a study in 2016, investigated the effect of cardiac cachexia on heart health in CHF patients. Cardiac cachexia was associated with higher rates of atrial fibrillation, as well as impairments in posterior wall thickness and left ventricular ejection fraction<sup>103</sup>. These negative effects induced by cardiac cachexia potentiate higher blood pressure, an important complication and contributor to mortality rates in CHF patients.

### **2.3.1.2 Chronic Kidney Disease**

CKD affects approximately 850 million people worldwide and contributes to an increase in morbidity and mortality of elderly individuals<sup>104</sup>. CKD is a common term used to describe an illness characterized by a loss of kidney function. Although CKD is often asymptomatic, this disease is most often accompanied or diagnosed with other comorbidities such as diabetes or cardiovascular disease<sup>105</sup>. Diagnosis of CKD may also expose individuals to an increased likelihood of acute kidney injury, further contributing to greater morbidity and mortality risk. Novel nutritional based therapeutic interventions are on the rise, but early detection may be important in reducing future risk.

With 18-75% of patients with CKD showing evidence of muscle wasting, cachexia is relatively prevalent in this disease<sup>106</sup>. The large range of cachexia incidences is due to the different comorbidities that can be present in CKD. Multiple factors and signalling molecules have been reported in the pathogenesis of cachexia in CKD patients<sup>107-111</sup>. Although malnutrition

does not solely induce wasting, studies have investigated the link between appetite controlling hormones and the prevalence of cachexia in CKD. One study found that in CKD patient's leptin levels were severely increased in the blood, leading to hyperleptinemia and cachexia<sup>107, 108</sup>. Other studies have reported that ghrelin, a hunger hormone, is decreased in CKD patients leading to early satiety and decreased appetite<sup>109</sup>. Aside from appetite control, studies have also investigated the presence of inflammatory cytokines in CKD. These studies find that compared to healthy patients, inflammatory cytokine levels are much higher in kidney disease patients<sup>108, 110</sup>. Lastly, upregulation of proteolytic mechanisms, specifically the caspase-3 and the ubiquitin proteasome pathway are also implicated in the progression of cachexia in CKD<sup>111</sup>.

### **2.3.1.3 Cancer**

Every year, approximately ten million people or more are diagnosed with cancer around the world<sup>112</sup>. This makes cancer the second leading cause of death worldwide behind cardiovascular disease. Contributing to a larger mortality risk, cancer of the lung, female breast, bowel and prostate are the most common diagnosed. Cancer can be defined as chronic mutated and uncontrollable cell growth within a given tissue. As symptoms often depend on the type of cancer diagnosis, common signs may include unforeseen or persistent lumps, bloody urine, hoarseness, difficulty swallowing and unexpected, but extreme weight loss<sup>242</sup>. With the potential for negative treatment outcomes, cancer may soon be the biggest health burden in today's society, especially for elderly populations<sup>112</sup>.

Cachexia occurs in 80% of all cancers<sup>113</sup>, making cancer the leader in disease-associated cachexia. Cancer of the pancreas, oesophagus, stomach, lung and liver account for the majority of cancer deaths worldwide<sup>114</sup>, and it comes as no surprise that cachexia is largely associated with each of these cancer types. The cachectic weight loss although mainly comes from skeletal

muscle wasting, adipose tissue, specifically brown adipose tissue is seen to have an important role in cachexia<sup>122</sup>. In addition to having a severe negative impact on QOL, cancer patients with cachexia respond poorly to chemotherapy treatment compared to weight-stable patients<sup>115, 116</sup>. Pathophysiology of cancer cachexia partly revolves around disruptions and imbalances in protein metabolism. In cancer cachexia, the rate of catabolism significantly outweighs the rate of anabolism in skeletal muscle leading to net protein breakdown and muscle atrophy<sup>118, 119</sup>. Increases in energy expenditure and consequently resting energy expenditure is also implicated as contributing to the wasting process, especially in pancreatic and lung cancer<sup>120, 121</sup>. Lastly, during cancer progression, there is undoubtedly a significant increase in the levels of pro-inflammatory cytokines tumour necrosis factor-alpha (TNF- $\alpha$ ), interleukin 6 (IL-6) and interleukin 1 (IL-1)<sup>117</sup>.

### **2.3.2 Inflammation**

Systemic inflammation indicated by the production of pro-inflammatory cytokines is arguably the biggest contributor to the regulation of cachexia<sup>117</sup>. Cachectic patients exhibit elevated levels of TNF- $\alpha$ , IL-6 and IL-1 and these pro-inflammatory cytokines are all positively correlated with causing cachexia-like effects<sup>76</sup>. Although these three cytokines may have differing mechanisms of action, TNF- $\alpha$ , IL-1 and IL-6 can all readily cross the blood brain barrier and affect appetite<sup>77</sup>.

The pro-inflammatory cytokine TNF- $\alpha$  is one of the most well-known and studied mediators of cachexia. A study in 2005 by Li et al investigated the effect of TNF- $\alpha$  on the expression of atrogin1, a gene responsible for skeletal muscle atrophy. The study found that in vitro, TNF- $\alpha$  actively works via the expression of atrogin1 to induce myotube atrophy<sup>78</sup>. Other in vitro studies have shown that TNF- $\alpha$  is implicated in the production<sup>79</sup> and signalling<sup>80</sup> of reactive

oxygen species (ROS). In vivo, studies have found that tumour-bearing mice result in increased levels of TNF- $\alpha$  and this cytokine is responsible for muscle protein breakdown in skeletal muscle<sup>81</sup>. Interestingly, although TNF- $\alpha$  leads to increased proteolysis and decreased protein synthesis<sup>76</sup>, inhibition of this cytokine does not stop or slow cachexia progression<sup>82</sup>.

Aside from TNF- $\alpha$ 's effect on cachexia, TNF- $\alpha$  also augments the formation of another pro-inflammatory cytokine, IL-1<sup>76</sup>. Over time, IL-1 has been implicated in causing anorexic states in cachectic patients. An in vivo study by Dunn AJ in 1988 found that intraperitoneal injections of IL-1 increased tryptophan levels throughout the brain<sup>83</sup>. The IL-1 induced increase in tryptophan levels leads to subsequent increase in serotonin levels. From this, increased serotonin levels have been shown to both suppress hunger and limit appetite<sup>84</sup>. It is through this indirect mechanism of hunger and appetite suppression that IL-1 can regulate cachexia. Aside from this mechanism, IL-1 can also induce the production of IL-6.

Although IL-6 is an anti-inflammatory myokine, IL-6 is also a well-known mediator of cachexia. A study by Strassmann et al in 1992 found that in tumour-bearing mice, cachexia progression was associated with increased levels of IL-6. In tandem, this same study also elucidated that a monoclonal antibody to IL-6 reduced cachexia progression in vivo<sup>85</sup>. In cachectic patients, levels of IL-6 appear to be lower in weight-stable patients compared to their cachectic counterparts<sup>76</sup>. While in human trials of cancer patients, IL-6 is associated with weight loss in some patients<sup>86</sup>, but not all<sup>87</sup>.

It is clear from the literature that pro-inflammatory cytokines have diverse systemic effects and mechanisms that regulate cachexia. It is also worth addressing that the relationship between inflammation and cachexia is a complex interplay of multiple factors and mechanism that regulate cachexia as a whole. Therefore, further studies elucidating the effects of multiple

pro-inflammatory cytokines on cachexia development and progression should be of great interest today.

### **2.3.3 Reactive oxygen species**

Reactive oxygen species (ROS) are highly reactive oxygen-derived molecules normally produced as by-products from cellular metabolism or mitochondrial activity. The most common types of ROS include superoxide ( $O_2^-$ ) and hydrogen peroxide ( $H_2O_2$ ). In a healthy cellular environment, ROS helps to maintain normal physiological functioning mainly through its interaction with cysteine residues on protein<sup>89</sup>. However, due to complications such as environmental stress, metabolic alterations and disease, increases in ROS levels can lead to oxidative damage<sup>90</sup>. Previous studies have reported that uncontrolled ROS levels can contribute to cellular impairments, skeletal muscle atrophy, macromolecule damage, DNA damage and pathogenesis of disease<sup>91</sup>. Fortunately, the human body has well-structured antioxidant defences that help control against extreme levels of oxidative stress. Common antioxidant enzymes include superoxide dismutase (SOD), catalase and glutathione peroxidase (GPx). From this, imbalances through either increases in ROS or decreases in antioxidant enzyme activity will perpetuate oxidative damage<sup>90, 92</sup>.

Overtime, elevated oxidative damage has been implicated in the progression and development of cachexia. Both in vitro and in vivo studies have reported the association between ROS and cachectic states. A study by Russell et al in 2007 found that increases in ROS formation induced by proteolysis-inducing factor and angiotensin II led to total protein degradation in murine myotubes<sup>93</sup>. Similarly, a study by Barreiro et al in 2005 investigated levels of protein carbonylation in tumour-bearing mice. The study found that in the muscles of tumour-bearing mice, protein carbonylation was significantly greater compared to control muscles,

signifying increases in oxidative damage<sup>96</sup>. Other studies have reported decreases in antioxidant enzyme activity in cachectic states. A study by Sullivan-Gunn et al in 2011 investigated the enzyme activity of SOD1 and SOD2 in the muscle of mice with cancer cachexia. Cancer cachectic mice were associated with decreases in SOD1 and SOD2 enzyme activity matched with increases in O<sub>2</sub> levels<sup>94</sup>. Likewise, past reports have also shown decreases in the levels of antioxidant enzymes catalase<sup>95</sup> and GPx<sup>94</sup> in cachexia studies. Taken together, these studies suggest that cancer cachectic patients not only experience elevated ROS levels, but also reductions in the antioxidant protective properties normally guarding against oxidative damage.

### **2.3.4 Chemotherapy Treatment**

Chemotherapy is one of the most common cancer treatments today. With cancer being the leader in disease-associated cachexia, it is important to discuss and understand how common chemotherapy drugs can regulate cachexia. Broadly, chemotherapy acts through the induction of death in tumour cells<sup>123</sup>, by damaging DNA necessary for cell division. Unfortunately, due to the complexity of cancer and the fact that anticancer strategies, specifically chemotherapy are not specific to the tumour itself<sup>124</sup>, many other bodily processes are affected. For instance, administration of single chemotherapy drugs in cancer patients often leads to drug toxicity and resistance, resulting in treatment failure and often death<sup>125</sup>. From this, resistance to cancer chemotherapy is a major problem in cancer therapy. To account for this problematic feature, cancer therapy has turned to combining multiple chemotherapy drugs, administered as a cocktail. Combining multiple chemotherapy drugs have been shown to not only reduce drug toxicity and resistance, but also reduce side effects as separate drugs can be administered at lower concentrations<sup>126</sup>. In addition, combining multiple chemotherapy drugs can lead to increases in the bioavailability of drugs<sup>127</sup>, leading to the enhanced effect of these drugs on killing cancer

cells. Among others, common treatment regimens that utilize combinations of chemotherapeutic drugs include folfiri, a combination of Leucovorin (Leu), 5-Fluorouracil (5-Flu) and irinotecan and folfox, a combination of Leu, 5-Flu and oxaliplatin. Nonetheless, chemotherapy treatment, used in combination or not, is still associated with side effects, including nausea, vomiting, appetite changes, constipation and hair loss. Of all these effects, none match the detrimental skeletal muscle wasting and atrophy that can ensue through chemotherapy treatment.

#### **2.3.4.1 Cisplatin**

Cis-diamminedichloroplatinum (II), better known as cisplatin, is a platinum-containing compound present as a yellow crystalline powder at room temperature. Dating back to cisplatin's first scientific investigation in the 1960s by Rosenberg<sup>128</sup>, the focus on using platinum containing compounds as anti-cancer agents has increased drastically. In 1978, cisplatin became the first platinum compound to gain FDA approval for the use as cancer treatment<sup>129</sup>. Since then, cisplatin has become best known for being a potent chemotherapeutic drug used most commonly in treatment of testicular, ovarian, head, lung and neck cancers.

It is relatively clear that the main mechanism of cisplatin's anti-cancer effect comes primarily through the targeting of deoxyribonucleic acid (DNA). Once cisplatin enters a cell, often through passive permeation<sup>130</sup>, previous reports have linked cisplatin's cytotoxic action with the induction of intrastrand DNA adducts<sup>131, 132</sup>. Often times, DNA adducts not removed from the cellular environment could give rise to problematic mutations. Therefore, in response to DNA adducts, p53 and mitogen-activated protein kinase (MAPK) signalling pathways become activated, inducing cellular apoptosis. Specifically, cisplatin has been shown to activate MAPK c-jun terminal kinase (JNK), leading to the transcription of fas ligand (FasL) and the induction of cisplatin-mediated apoptosis<sup>264</sup>. In addition, p53 can also have an effect on cell cycle

checkpoints, causing arrest in the G, G1 and S phases of the cell cycle<sup>132</sup>. This effect is particularly important as cisplatin, a chemotherapeutic drug should have positive effects on reducing the abnormal and uncontrolled cell growth present in cancer cells.

Unfortunately, cisplatin has at least two problematic side effects. Under cisplatin administration, patients can experience drug toxicity leading to ineffective treatment and negative health outcomes. Normally, patients receive cisplatin treatment every 3-4 weeks at a dose of about 50-100mg/m<sup>2</sup> intravenously. Dosage can depend on multiple factors: renal function, age, muscle mass, cancer type and combination with other antineoplastic agents<sup>133</sup>. Inadvertently, cisplatin overdose leading to toxicity can also become apparent in patients when dosage amounts reach upwards to 480mg/m<sup>2</sup><sup>134</sup>. Symptoms of cisplatin toxicity may include nausea, vomiting, nephrotoxic associated renal insufficiency and myelosuppression<sup>133</sup>. Management of cisplatin toxicity is therefore critical in order to support proper health outcomes in patients. Such management includes antiemetic support, aggressive hydration, red blood cell transfusions, supportive therapies and avoidance of other drugs that may bring about similar symptoms<sup>133</sup>. Aside from drug toxicity, patients receiving cisplatin treatment overtime may also face unforeseen resistance to this anti-cancer agent. Cisplatin resistance is associated with a myriad of cellular changes that reverse the mechanism of cisplatin's effect. Constant exposure of cisplatin leads to the development of a phenotypic self-defence system that allows cells to escape the cytotoxicity of cisplatin. These phenotypic changes include decreases in platinum derived DNA-adducts, as well as changes in gene expression associated with apoptosis, DNA-damage repair, mitochondria metabolism and the cell cycle<sup>135, 136, 137</sup>. Of all the changes that occur, reductions in the accumulation of cisplatin in cells presents a defining feature of cisplatin resistance. This is evident in human cisplatin resistant cells, where significant reductions in

platinum-induced DNA-adducts are found<sup>138</sup>. In addition, the reduced accumulation and resistance of cisplatin, may also be a factor of impaired uptake or increased efflux of platinum compounds within cells<sup>139, 140, 141</sup>.

With regards to the effect of cisplatin on inducing cachexia, one of the most common side effects or symptoms of cisplatin treatment is muscle fatigue. A study by Sakai et al in 2014 investigated the effect of 3mg/kg of cisplatin on muscle atrophy in mice over four days. Compared to vehicle, cisplatin treated mice exhibited decreased body weight associated with reductions in quadriceps muscle mass, coinciding with dramatic increases in Muscle atrophy F-Box (MAFbx) and Muscle RING Finger-1 (MuRF1)<sup>158</sup>. Cisplatin has also been shown to induce the expression of nuclear factor kappa-light-chain-enhancer of activated B cells (Nf-KB)<sup>159</sup>, pointing to a likely mechanism of protein ubiquitination and degradation in muscle. Due to side effects of drug resistance, toxicity and muscle fatigue, cisplatin can often be used in combination with a separate chemotherapy drug, 5-Flu. In combination, cisplatin and 5-Flu can effectively treat cancer of the head, neck, anus and esophagus.

#### **2.3.4.2 5-Fluourouracil**

5-Fluourouracil (5-Flu) is a well-known analog of uracil possessing both immunological and anti-metabolic properties. This compound is a fluorinated pyrimidine present as a white crystalline powder at room temperature. Since being first synthesized in 1957 by Heidelberger et al<sup>142</sup>, investigations into the antineoplastic activity of 5-Flu became of great interest. Today, 5-Flu is a well-studied chemotherapeutic drug used both singularly and in combination with other chemotherapy drugs. Specifically, 5-Flu is used for the treatment of colon, pancreatic, breast, gynecological, head and neck cancers<sup>143</sup>.

Similar to cisplatin, the antineoplastic activity of 5-Flu comes primarily through the

action of this compound on DNA. The discovery of 5-Flu came through the finding that hepatoma tumours from rats formed DNA from uracil at a more rapid pace than healthy tissue. Therefore, Heidelberger and colleagues designed 5-Flu to differ from uracil by substituting uracil's hydrogen at the carbon-5 position with a fluorine atom<sup>142, 144</sup>. Once incorporated into the cell, either through non-facilitated diffusion or facilitated nucleobase transport<sup>145</sup>, 5-Flu undergoes a myriad of changes as 5-Flu by itself is inactive. Intracellularly, 5-Flu is converted into 5-fluoro-2'-deoxyuridine-5'-monophosphate (FdUMP), a critical nucleotide metabolite in 5-Flu's mechanism of action. Once formed, FdUMP inhibits thymidylate synthase, a regulatory enzyme that is responsible for DNA synthesis<sup>146</sup>. Due to this mechanism, TS, especially with 5-Flu treatments becomes a critical target for cancer chemotherapy<sup>142</sup>. In addition, 5-Flu can be converted into 5-fluorodeoxyuridine-5'-triphosphate (FdUTP) leading to inhibition of DNA synthesis and function<sup>146</sup>. Additionally, 5-Flu can also be converted into 5-fluorouridine-5'-triphosphate (FUTP) leading to inhibition of RNA synthesis and mRNA translation<sup>147</sup>.

Again similarly to cisplatin, treatment with 5-Flu can overtime leads to an increase in drug resistance, drug toxicity and ultimately decreased effectiveness. On average, patients receive bolus 5-Flu treatment every 4 weeks at a dose of about 500mg/m<sup>2</sup> intravenously<sup>152</sup>. Different dosages can depend on factors such as cancer type, dosage schedule and combinations with other chemotherapy drugs. Due to the fact that 5-Flu can be metabolized and excreted rapidly within the human body, determining toxicity can be both difficult and challenging. Nonetheless, the major cause of 5-Flu toxicity is due to a deficiency in Dihydropyrimidine dehydrogenase, the rate limiting enzyme in 5-Flu catabolism<sup>153</sup>. Deficiency of this enzyme occurs in about 3-5% of all patient populations<sup>155</sup>, leading to symptoms of 5-Flu toxicity such as leukopenia, diarrhea, stomatitis and nausea<sup>154</sup>. In addition to drug toxicity, many past reports

have also found 5-Flu resistance as another problematic feature of this drug. Increases in the catabolic activity of enzymes responsible for breaking down FdUMP, FdUTP and FUTP may result in decreased accumulation of active 5-Flu<sup>144</sup>. In addition, reductions of 5-Flu incorporation into both DNA and RNA may lead to drug resistance<sup>148</sup>. With regards to thymidylate synthase specifically, 5-Flu treatment augments increases in thymidylate synthase protein content and protein synthesis, leading to increased requirements for 5-Flu dosages<sup>149, 150</sup>. Lastly, any mutation in the coding region of thymidylate synthase may affect the ability of FdUMP to bind and inhibit this enzyme<sup>151</sup>.

Interestingly, not much research has been conducted on the effects of 5-Flu by itself on muscle atrophy. Nonetheless, similarly to cisplatin, fatigue plays a crucial role in 5-Flu treatment symptomatology. In 2014, a study by Barreto et al investigated the mechanisms of Folfiri and Folfox, two 5-Flu combinatory cocktails on chemotherapy-induced cachexia in mice. The study reported that both chemotherapy regimens led to concurrent weight and lower-limb muscle loss, associated with upregulation of p38 mitogen activated protein kinases (MAPK) and reductions in mitochondrial content<sup>160</sup>. From this and the above mechanisms, it is clear that drug toxicity, drug resistance and even metabolism of 5-Flu can be problematic features that inhibit the effect of this chemotherapy drug on killing cancer cells. Specifically, one medication, leucovorin, has been shown to be mechanistically important to increase the effectiveness of 5-Flu. The effects of a 5-Flu and leucovorin cocktail are outlined below.

### **2.3.4.3 Leucovorin**

Leucovorin, also known as folinic acid, is a medication that can be used to treat folate deficiency and also to decrease the toxicity of certain chemotherapy agents. Of all the effects, leucovorin is most commonly used clinically in combination with 5-Flu. When used with 5-Flu,

leucovorin is often administered just prior to 5-Flu's intravenous infusion with a dose of 20mg/m<sup>2</sup> 5 times over 4 weeks or 400mg/m<sup>2</sup> once over 2 weeks. Intracellularly, leucovorin is reduced to folate 5, 10-methylenetetrahydrofolate and in this form, reduced leucovorin can bind and form a complex with FdUMP, a major metabolite of 5-Flu. The FdUMP-leucovorin complex can now better bind to thymidylate synthase, leaving this enzyme in a maximally inhibited state and ultimately significant reductions in DNA biosynthesis<sup>146</sup>. Interestingly, since 5-Flu is often metabolized and excreted from the body rapidly, the increased binding to thymidylate synthase allows 5-Flu to be present in the cell for longer allowing for increased effectiveness. Multiple past reports have also supported the efficacy of a leucovorin and 5-Flu combination. Work by Sotos et al, found that the cytotoxic action of 5-Flu was enhanced when used in combination with leucovorin<sup>156</sup>. Other studies have also supported the notion of significantly higher response rates with 5-Flu and leucovorin together opposed to 5-Flu alone<sup>157</sup>. It should also be noted that although leucovorin is not a chemotherapy drug, symptomology with this medication is still prevalent as leucovorin is almost always used in combinations with other chemotherapy drugs.

## **2.4 Mechanisms of skeletal muscle catabolism**

In order for a cachexia to occur, factors such as chronic disease, inflammation, reactive oxygen species and chemotherapy treatment must signal through specific mechanisms to elicit muscle protein breakdown. Skeletal muscle catabolism can occur through a shift in protein equilibrium, either through an increase in protein degradation or a decrease in protein synthesis. Unfortunately, the mechanisms associated with the pathophysiology and development of skeletal muscle catabolism and cachexia are often complex, multidimensional and very poorly understood. Understanding the complex mechanisms of cachexia development and progression may shed light on potential therapeutic interventions to manage cachexia-induced muscle loss.

### **2.4.1 Ubiquitin Proteasome Pathway**

The Ubiquitin Proteasome Pathway (UPP) accounts for the vast majority of protein degradation in mammalian cells<sup>161</sup>. Within this pathway, the 26S proteasome, is a crucial protein complex necessary for degrading proteins that have been tagged for degradation<sup>161</sup>. Before the 26S proteasome can degrade proteins, substrates must be conjugated by multiple units of ubiquitin by a cascade of enzymes. First, ubiquitin is activated by an activating-enzyme (E1) and transferred to a ubiquitin carrying molecule (E2). Next, E2 bound ubiquitin can recognize E3 ligases and in turn, E3 ligases can bind and form ubiquitin chains on protein substrates. Two of the most common and studied E3 ligases have been identified to actively contribute to proteolysis and associated muscle loss are MAFbx/atrogen-1 and MuRF1<sup>163</sup>. Only once a protein has been conjugated with a chain of ubiquitin by the E3 ligases can the 26S proteasome act to degrade the protein substrates<sup>162</sup>.

Within cachexia, multiple past reports have found that the UPP is severely upregulated<sup>164</sup>,<sup>165</sup>, showing a pivotal role of this pathway in protein degradation. In addition, in catabolic models of fasting, diabetes and cancer cachexia, the upregulation of E3 ligases MAFbx and MuRF1 have been deemed essential for associated muscle protein loss<sup>163, 166, 167</sup>. Therefore, much research has attempted to identify upstream transcription factors of these E3 ligases.

### **2.4.2 Autophagy**

Autophagy is a highly regulated recycling process present in all mammalian cells. Since autophagy is involved in protein and cellular recycling, autophagy has been well recognized as vital to maintenance and survival of cells<sup>244</sup>. There are three primary forms of autophagy: microautophagy, macroautophagy and chaperone mediated autophagy, all of which function to transport substrates to the lysosome for recycling<sup>245</sup>. The most commonly studied,

macroautophagy, involves the formation of a double-membraned vesicle, an autophagosome, which engulfs substrates and transports them to the lysosome<sup>246</sup>. Often induced by nutrient or energy starvation, autophagy may be a cytoprotective mechanism to maintain cellular function and growth. Unfortunately, dysregulated autophagic mechanisms is associated in the progression of human pathologies such as cancer and metabolic diseases, such as diabetes<sup>244, 247</sup>.

Since autophagy involves the recycling and breakdown of protein substrates, past reports have investigated the relationship between cachexia and autophagic mechanisms. A study in 2016 by Aversa et al investigated the levels of autophagy markers in the skeletal muscle of cancer cachectic patients. In cancer cachectic patients, both beclin-1 and LC3B-II protein levels were significantly increased, signifying autophagy induction and autophagosome formation respectively<sup>248</sup>. Mitochondrial selected autophagy, also known as mitophagy, also showed a trend to be increased in cancer cachectic patients<sup>248</sup>. Other past reports have also found autophagic degradation as a significant contributor to muscle wasting in lung<sup>249</sup> and esophageal<sup>250</sup> cancer cachectic patients.

### **2.4.3 Apoptosis**

Also known as programmed cell death, apoptosis is a vital process necessary for normal immune system activity, as well as proper cellular homeostasis, development and turnover. Since apoptosis is involved in cell death, great interest is focused on how the mechanisms of apoptosis is regulated in skeletal muscle. Intrinsically, the process of apoptosis is initiated by DNA damage or cellular stress caused by factors such as hypoxia, toxins and radiation<sup>205</sup>. In turn, these stress stimuli augment mitochondrial permeabilization, the release of cytochrome c and the formation of the apoptosome. The apoptosome leads to the irreversible activation of caspase 9 and caspase 3 leading to cellular disassembly, degrading of intracellular substrates and cell death<sup>205, 206</sup>.

Although homeostatic levels of apoptosis can be critical to normal cellular functioning, levels of apoptosis can be increased in normal aging<sup>207</sup>, muscle denervation<sup>208</sup> and cancer cachexia<sup>209</sup>. Increased levels of apoptosis in muscle atrophy conditions suggest that apoptosis may play a role in loss of muscle mass over time. A study by Belizario et al in 2001 investigated the activation of caspase-induced apoptosis in tumour-bearing mice affected by cachexia. Compared to non-tumour-bearing mice, the study found that tumour-bearing mice had significantly increased caspase 1, 8, 3, 6 and 9 in the gastrocnemius muscle. In addition, cytochrome c was found to be released from mitochondria, providing further evidence of increased apoptosis in cancer cachexia-induced muscle loss<sup>209</sup>.

#### **2.4.4 Calcium-Calpain**

Calpains are calcium-dependent proteases, regulated by a wide variety of factors within skeletal muscle. As the name implies, calpains are regulated by calcium<sup>223</sup>, as well as phospholipids and calpastatin<sup>224</sup>, a calpain inhibitor. The mechanisms of calpain-induced muscle damage is multifactorial, but the end result of protein degradation remains constant. Activation of the calpains is associated with sarcomeric disturbances, resulting in damaged and degradation of myofilaments by the 26S proteasome<sup>225</sup>. In addition, calpain activity can lead to the promotion of two factors involved in muscle wasting, TNF- $\alpha$ <sup>226</sup> and Nf-KB<sup>227</sup>. Recent studies have also shown an inhibition of AKT by the calpains<sup>228</sup>, resulting in protein degradation by the 26S proteasome either through a suppression of mTORC1 or upregulation of FOXO proteins and GSK3 $\beta$ . Aside from an indirect effect on the 26S proteasome, past reports suggest that calpains may directly regulate the 26S proteasome with the calcium ionophore A23187<sup>229</sup>.

Due to the above mechanisms, it is relatively clear why investigating the effects of calpains in skeletal muscle atrophy is critical. Studies from sepsis-induced cachexia show both

indirect and direct evidence of calpain expression in skeletal muscle<sup>230, 231, 232, 233</sup>. In cancer cachexia, both calpain mRNA expression<sup>234</sup> and proteolysis through calcium-dependent mechanisms<sup>235</sup> were upregulated in tumor bearing rats. More recently, as study in 2017 by Lin et al investigated whether calpain inhibitors would ameliorate cachectic effects in tumour-bearing mice. In tumour-bearing mice, calpain activity was associated with decreased body weight, gastrocnemius muscle mass and increases in MuRF1 and atrogen-1 gene expression. Interestingly, calpain inhibitors were able to reverse the expression of atrophic genes, leading to improved weight and survival outcomes in tumour-bearing mice<sup>239</sup>. Calpain mechanisms have also been reported to play a role in other conditions such as sarcopenia<sup>236</sup>, muscle unloading<sup>237</sup> and chronic heart failure<sup>238</sup>.

## **2.5 Signalling towards mechanisms of skeletal muscle catabolism**

During cachexia, skeletal muscle catabolic mechanisms can be driven by the upregulation of transcription factors and enzymes. Associated with cachexia and muscle loss, O-type forkhead (FOXO), Nf-KB and Myostatin are three families of transcription factors that can upregulate MAFbx/atrogen-1 and MuRF1 expression. In addition, enzymes such as caspases (mentioned previously) and Unc-51 Like Autophagy Activating Kinase 1 (ULK-1) also upregulate skeletal muscle catabolism.

### **2.5.1 O-type forkhead**

Expressed within skeletal muscle, FOXO is a family of transcription factors made up of FOXO1, FOXO3a and FOXO4. Specific to skeletal muscle, past reports have found that FOXO transcription factors are highly expressed during atrophic conditions<sup>167, 168, 169</sup>. Once activated either by c-Jun N-terminal kinase (JNK) or macrophage stimulating 1 (MST1) regulators<sup>243</sup>, FOXO transcription factors travel to the nucleus and have the ability to activate E3 ligases

MAFbx and MuRF1<sup>170, 171</sup>, enhancing protein degradation through the UPP. Past reports have also investigated the transcriptional activity of FOXO in cachectic models. A study by Reed et al in 2012, investigated the regulation of gene transcription and muscle fiber atrophy by FOXO in two cachexia conditions, cancer and sepsis. The study found that cachexia increased the mRNA expression and transcriptional activity of FOXO family members. In addition, FOXO activation was required for cachexia-induced muscle fiber atrophy associated with increased expression of atrophy related genes MuRF1 and MAFbx<sup>172</sup>. These findings point to a crucial role of FOXO in the transcriptional upregulation of key atrophy related genes in cachectic conditions.

### **2.5.2 Nf-KB**

Nf-KB is a family of transcription factors involved in cell survival, inflammation and immunity. Normally, Nf-KB is bound to inhibitory protein of  $\text{KB}\alpha$  ( $\text{IKB}\alpha$ ) and stuck in the cytoplasm. Once phosphorylated by inhibitor of kappa light polypeptide gene enhancer in B-cells (IKK),  $\text{IKB}\alpha$  is unbound and degraded by the 26S proteasome and NF-KB is free to translocate to the nucleus<sup>173</sup>. Upon nuclear accumulation, NF-KB can upregulate the expression of E3 ligases MAFbx and MuRF1<sup>174</sup>, leading to ubiquitination and greater activity through the UPP. Unfortunately, the exact role of Nf-KB in cachexia and muscle wasting is poorly defined. A study in 2011 found that in cancer cachectic mice, NF-KB bound near transcription start sites of MAFbx, MuRF1 and caspase 3 showing the requirement NF-KB signaling in cancer cachexia<sup>175</sup>. In addition, studies have also shown that NF-KB transcription factors can be regulated upstream by the formation of ROS<sup>176</sup>. From this, a possible mechanism of cachexia through NF-KB is introduced. As mentioned previously, elevated ROS in cachexia, either through direct increases in ROS levels or decreased antioxidant enzyme activity, may lead to downstream activation of NF-KB, increased expression of E3 ligases, augmenting 26S proteasome activity and protein

degradation.

### **2.5.3 Myostatin**

Also known as growth differentiation factor 8, myostatin is a myokine part of the TGF $\beta$  superfamily and a known negative regulator of muscle growth. Often increased through glucocorticoid stimulation, myostatin inhibits activation of AKT by inhibiting IGF-1<sup>265</sup>, leading to the upregulation of atrophy related genes MAFbx and MuRF1 through FOXO3<sup>178</sup>. Therefore the mechanism of myostatin's effect on muscle atrophy through the UPP is similar to that of FOXO3 and NF-KB. In vitro, myostatin has been found to have a negative effect, decreasing both size and numbers of myotubes<sup>178</sup>. Interestingly, systemic overexpression of myostatin induces body weight, muscle and fat loss in mice<sup>177, 178</sup> comparable to the losses observed in cancer cachexia.

### **2.5.4 ULK-1**

Unc-51 like Autophagy Activating Kinase 1 (ULK-1) is a serine/threonine protein kinase necessary for autophagy signalling, as disruption of the ULK-1 complex can inhibit autophagy<sup>254, 255</sup>. One of the most known upstream regulators of ULK-1 is mTORC1, as amino acid activation of mTORC1 phosphorylates ULK-1, inhibiting ULK-1's kinase activity<sup>256, 257</sup>. In contrast, activation of ULK-1 by amino acid starvation<sup>258</sup>, AMP activated protein kinase (AMPK)<sup>259</sup> or glycogen synthase kinase 3<sup>260</sup> can keep ULK-1 in the dephosphorylated state, ultimately activating autophagy. Related to cachexia, a previous report has shown that in tumour-bearing mice, ULK-1 plays a crucial role in autophagy induction mediated by p38 $\beta$  MAPK<sup>261</sup>.

## **2.6 Current treatments**

It should first be stated that there are currently no effective or accepted treatments for cachexia. In addition, due to the multi-array of cachectic factors experienced by patients, it is

often necessary to develop forms of treatment specific to each patient. A study in 2001 suggested that with cancer patients, treatment of cachexia relied solely on curing the cancer itself<sup>75</sup>. With the option to cure cancer not always viable, multiple reports have focused on developing effective treatments for cachexia.

During the mid-1990s, studies focused on the maintenance of lean body mass by attempting to decrease the levels of a TNF- $\alpha$ , a known factor in the development of cachexia. Two human trials, focused on using either drugs such as pentoxifylline<sup>210</sup> or hormones such as melatonin<sup>211</sup>, but both showed little efficacy in limiting cachexia-induced muscle loss. More recently, studies have attempted to use combinations of nutritional and pharmaceutical based supplements in treating cachexia. In a phase II trial by Mantovani et al, treatment included a diet high in polyphenols, antioxidants, polyunsaturated fatty acids mixed with celecoxib and a dose of medroxyprogesterone acetate pharmaceuticals. After four months, the treatment had a positive effect on body weight, lean body mass, appetite, fatigue and in addition, led to decreased inflammatory cytokine levels IL-6 and TNF- $\alpha$ <sup>212</sup>.

In addition to these nutritional combination therapies, studies have also examined the potential to increase skeletal muscle anabolism through testosterone therapy in cachectic patients. Two studies conducted within the same lab in 2013 and 2018, investigated the effect of adjunct testosterone compared to placebo in cachexia-related muscle loss. In 2013, the study found that testosterone led to greater total body mass associated with positive changes in lean body mass<sup>213</sup>. In 2018, with a similar study design, testosterone led to 3.2% increases in lean body mass, as well as positive outcomes in activity levels and quality of life. Unfortunately, both placebo and testosterone treated groups did not differ in overall survival<sup>214</sup>.

Since testosterone positively impacted lean body mass, but did not increase survival

outcomes, past reports have also looked at the inhibition of skeletal muscle catabolism through modulation of the UPP. Eicosapentaenoic acid (EPA) is a health promoting agent often investigated in cachectic environments due to the fact that EPA is the only known nutritional supplement that acts on the UPP<sup>215</sup>. Treatment with EPA has been shown to reduce inflammatory cytokines<sup>216</sup>, mitigate the activity of Nf-KB<sup>217</sup> and reduce critical subunits involved in mechanisms of proteolysis<sup>218</sup>. In animal trials, EPA supplementation leads to increases in SOD activity following chemotherapy treatment<sup>219</sup> and positively affects muscle function in tumor bearing mice when combined with leucine<sup>220</sup>. In addition, EPA treatment when compared to megestrol acetate improved lean body mass<sup>221</sup> and positively affected weight gain, survival and quality of life<sup>222</sup>. Unfortunately, findings surrounding the anti-cachectic effects of EPA can suffer from attrition and variability<sup>222</sup>.

Although cachexia has been seen to be a major determinant of quality of life and survival, it is important to state again there are currently no effective treatments for this skeletal muscle wasting disorder. The inability to have effective treatments likely stems from the insufficient knowledge of the underlying causal and biological mechanisms.

## **2.7 Rationale**

Although previous research has linked chemotherapy with the induction of cachexia, the mechanisms underlying this association are not completely understood.

The chemotherapy drug cocktail I used for my study consisted of 20µg/mL of cisplatin, 50µg/mL of 5-Fluourouracil and 10µg/mL of leucovorin. I used these drug concentrations as similar drug concentration have been used recently and found to be effective in their ability to induce myotube atrophy<sup>160, 266</sup>. I combined chemotherapy drugs as this approach is common in the clinical setting today. This is because combining multiple chemotherapy drugs not only reduces drug toxicity and resistance<sup>126</sup>, but also results in a greater bioavailability of chemotherapy drugs<sup>127</sup>. Further, I treated myotubes with the chemotherapy drug cocktail once, similar to a clinical setting, in which cancer patients receive chemotherapy doses in single cycles lasting approximately 3-4 weeks<sup>133, 152</sup>.

## **2.8 Objectives**

- i. Examine the effect of a chemotherapy drug cocktail on myotube morphology, abundance of myofibrillar proteins and anabolic signalling mechanisms.
- ii. Study whether the associated loss of protein abundance is linked to altered rates of protein synthesis, mitochondrial content and glucose uptake in chemotherapy drug treated myotubes.

## **2.9 Hypotheses**

- i. A chemotherapy drug cocktail will have a negative effect on myotube growth and protein abundance.
- ii. A chemotherapy drug cocktail will cause a decrease in the rate of protein synthesis coinciding with reductions in mitochondrial content and glucose metabolism.

## Chapter Three: Manuscript

### THE EFFECT OF A CHEMOTHERAPY DRUG COCKTAIL ON MYOTUBE MORPHOLOGY AND PROTEIN METABOLISM

**Stephen Mora<sup>1</sup>, Olasunkanmi A.J. Adegoke<sup>1</sup>**

Muscle Health Research Centre, School of Kinesiology and Health Science, York University,  
Toronto, ON, M3J 1P3

**Corresponding Author: Dr. Olasunkanmi A.J. Adegoke**

Muscle Health Research Centre, School of Kinesiology and Health Science, York University,  
Toronto, ON, Canada. Tel: 416-7362100 Ext 20887. Fax: 416-736- 5774. Email:  
oadegoke@yorku.ca

**Key Words:** Cachexia, Chemotherapy, Protein Synthesis

## Chapter Four: Abstract

Cachexia, a condition prevalent in many chronically-ill patients, is characterized by weight loss and fatigue resulting from decreases in muscle mass and function. Although development of cachexia is associated with tumour burden and disease-related malnutrition, other studies have suggested a causative link between chemotherapy treatment and cachexia. In order to understand the mechanisms of chemotherapy-induced cachexia, we investigated the effects of a common chemotherapy drug cocktail on myotube morphology and myofibrillar protein abundance. On day 4 of differentiation, myotubes were treated with vehicle or a chemotherapy drug cocktail (a mixture of cisplatin (20µg/mL), leucovorin (10µg/mL), and 5-fluorouracil (50µg/mL)). Compared to myotubes treated with vehicle, those treated with the drug cocktail showed irregular myotube structure. Drug treatment also induced significant reductions in Myosin Heavy Chain (MHC) (n=5, p = 0.0003), troponin (n=4, p < 0.0001) and tropomyosin (n=4, p = 0.0059) by day 6 of differentiation. To explore the reasons for the low abundance of myofibrillar proteins, we examined treatment effects on mTORC1 (mammalian/mechanistic target of rapamycin complex1) signalling. Myotubes treated with the drug cocktail showed ~2-fold reduction in the phosphorylation of mTORC1 activator AKT<sup>Ser473</sup> (n=4, p = 0.0058) and ~3-fold reduction in phosphorylation status of mTORC1 substrates ribosomal protein S6<sup>Ser235/236</sup> (n=3, p = 0.0178) and its kinase, S6K1<sup>Thr389</sup> (n=3, p = 0.0025). Drug treatments also led to reductions in protein synthesis, as well as further reductions in mitochondrial proteins cytochrome C oxidase (COX IV) and succinate dehydrogenase (SDHA) (n=4, p < 0.05). Lastly, due to reductions in phosphorylation of AKT, insulin-stimulated glucose uptake was measured and found to be reduced in myotubes treated with the drug cocktail (n=5, p = 0.06). The above findings suggest that it is critical to identify interventions that can limit the negative effects of these drugs on muscle protein status and mitochondrial content.

## Chapter Five: Introduction

Cachexia, a condition affecting approximately nine million patients with chronic disease worldwide<sup>68</sup>, is characterized by detrimental loss of body weight and depletion of fat and muscle mass. In addition, this muscle wasting syndrome leads to wide scale fatigue and weakness, associated with decreases in quality of life and increased mortality and morbidity<sup>183, 184</sup>.

Maintenance of skeletal muscle mass is dependent on a balance between protein synthesis and protein degradation. These two processes are highly regulated by multiple signalling events and pathways within skeletal muscle. For example, activation of the insulin receptor substrate 1 (IRS-1)/protein kinase B (AKT)/mechanistic target of rapamycin complex 1 (mTORC1) pathway is well-known to be vital for skeletal muscle growth and the inhibition of skeletal muscle protein degradation<sup>185</sup>. In opposition, stimulation of either the ubiquitin proteasome pathway (UPP) or autophagic mechanisms induce protein degradation within skeletal muscle<sup>186</sup>. Although upstream activators of the UPP, such as forkhead box protein O (FOXO) or nuclear factor kappa-light-chain-enhancer of activated B cells (NFkB) are upregulated in atrophic conditions, signalling events and mechanisms in these pathways are yet to be completely understood.

Past reports have suggested that the development and severity of cachexia is due to the administration of chemotherapy drugs. Symptoms including nausea, vomiting, poor nutrition and anorexia-like states are often present following chemotherapy treatment. Of these, no side effect matches the debilitating loss of muscle mass, accompanying chemotherapy treatment regimens.

Although available evidence suggests an association between chemotherapy treatment and cachexia, the mechanisms of chemotherapeutic regimens in the promotion of cachectic symptoms are not completely clear. Cisplatin, a platinum containing chemotherapeutic, used in the treatment of testicular, ovarian, head, lung and neck cancers, dramatically increases muscle

atrophy f-box (MAFbx) and muscle ring finger-1 (MuRF1) in vivo<sup>158</sup>. In addition, cisplatin also activates nuclear factor kappa-light-chain enhancer of activated B cells (Nf-KB)<sup>159</sup>, linking this chemotherapeutic to the upregulation of the UPP in muscle. Other drugs, such as 5-Fluorouracil (5-Flu), part of Folfiri and Folfox chemotherapy regimens, upregulates p38 mitogen activated protein kinases (MAPK) resulting in weight loss, muscle loss and reductions in mitochondrial content<sup>160</sup>. Other common chemotherapy drugs, such as CPT-11 or Adriamycin promote tissue injury, either through increased production of inflammatory factors<sup>179</sup> or reactive oxygen species (ROS)<sup>180</sup>.

Better understanding of the mechanisms underlying chemotherapy-induced cachexia may present possible regimens to increase the effectiveness of cancer treatment today. Prior to treatment, patients with greater accumulation of muscle mass may be presented with the opportunity for generally more aggressive chemotherapeutic treatment regimens. This opportunity may be lost in patients who have decreases in muscle mass. Therefore, patients with lower levels of muscle mass face the risk of drug toxicity, in accordance with decreased severity of treatment and chance of disease-free survival<sup>181, 182</sup>.

The purpose of this study was to investigate the factors of common chemotherapy drugs on the promotion of cachexia. In vitro, we explored the effects of a combinatory drug cocktail made up of chemotherapeutic agents cisplatin, 5-Flu and leucovorin. In this, we assessed L6 myotube morphology, myofibrillar protein abundance and the modulation of anabolic signalling pathways. In addition, rates of protein synthesis, mitochondrial content and glucose metabolism were measured in drug exposed myotubes. Findings from this study present possible mechanisms of chemotherapy's effect on muscle protein status, metabolism and mitochondria.

## Chapter Six: Materials and Methods

### 6.1 Reagents

$\alpha$ -Modification of Eagle's Medium (AMEM) was purchased from Wisent (#310-010-CL). Growth media (GM) was created by supplementing AMEM with 10% fetal bovine serum (FBS) from Gibco (#26050-088) and 1% Antibiotic-Antimycotic purchased from Wisent (#15240-062). Differentiation media (DM) was created by supplementing AMEM with 1% Antibiotic-Antimycotic and 2% horse serum (HS) purchased from Gibco (#26050088). Phosphate buffered saline (PBS) (#311-010-CL) and trypsin (#325-043-CL) were both purchased from Wisent. Protease inhibitor (#P8340) and phosphatase inhibitor (#P5726) were purchased from Sigma Aldrich. Dithiothreitol (DTT) was purchased from Research Organics (#2190D-A101X). Chemotherapeutic drugs Cisplatin (#PHR1624-200MG) and 5-Fluorouracil (#F6627-1G), along with Folinic acid calcium salt hydrate (Leucovorin) (#F7878-500MG) were purchased from Sigma Aldrich. Dimethyl sulfoxide (DMSO) was purchased from Sigma Aldrich (#D5879-100ML). 1X DMEM lacking Methionine, Cysteine, L-Glutamine and sodium pyruvate, but supplemented with 4.5g/L D-Glucose was purchased from Gibco (#21013-024). Radioactive <sup>35</sup>S express protein labelling mix was purchased from Perkin Elmer (#NEGO72007MC). [<sup>3</sup>H]-2-deoxyglucose was purchased from Perkin Elmer (#NET549). Triton was purchased from MP Biomedicals, LLC (#M2528).

### 6.2 Cell Culture

All experiments were completed using L6 rat skeletal muscle cell lines purchased from American Type Culture Collection. Cells were thawed from -80°C storage and cultured in T75 flasks purchased from Gibco (#E18033C5). Cells were grown in 15mLs/flask of GM and placed in a cell culture incubator set at 37°C and 5% carbon dioxide. Once cells reached 70-80%

confluency, cells were incubated in trypsin for 5 minutes and passed by adding 200,000 cells into a new flask. Cells were then re-incubated for 48 hours until experiments were ready to begin. On experiment start dates (Day -2), cells were counted and seeded  $2 \times 10^5$  (200,000) cells/well in 6-well plates or  $10^5$  cells/well in 12-well plates. Cells were then left to incubate and proliferate for 48 hours until the cells became 90-100% confluent. Once confluency was obtained (Day 0), cells were washed with 1mL/well PBS and shifted into 2mL/well of DM. Fresh DM was replenished every 24-48 hours until Day 4 when experiments were performed on myotubes.

### **6.2.1 Formation of Chemotherapy Drug Cocktail and Cell Treatment**

The chemotherapy drug cocktail used for all experiments was made up of a combination of three chemotherapeutic agents: Cisplatin, 5-Fluorouracil and Leucovorin. Stock concentrations were first made for each chemotherapy drug: 50mg Cisplatin dissolved in 1mL DMSO, 50mg 5-Fluorouracil dissolved in 1mL DMSO and 20mg Leucovorin dissolved in 1mL DDH<sub>2</sub>O. Each stock concentration was then aliquoted into 20 $\mu$ L, 30 $\mu$ L and 25 $\mu$ L amounts for Cisplatin, 5-Fluorouracil and Leucovorin respectively. Each aliquot was then stored at -80°C until needed. DMSO was chosen as the suitable vehicle for all experiments as the drugs were dissolved in this solution. Upon thawing and using of each drug aliquot, the remaining amount was discarded. On Day 4, myotubes were separated into a drug or vehicle group. In the drug group, myotubes were exposed to fresh DM in conjunction with a chemotherapy drug cocktail consisting of 20 $\mu$ g/mL Cisplatin, 50 $\mu$ g/mL 5-Fluorouracil and 10 $\mu$ g/mL Leucovorin. Myotubes in the vehicle group were exposed to fresh DM supplemented with 1.4 $\mu$ L/mL of DMSO. The vehicle group served as control for all experiments. Myotubes were differentiated until day 7 for western blot analysis and day 6 for immunofluorescence, protein synthesis and glucose metabolism measurements.

### 6.3 Cell Harvesting

Myotube morphology was monitored by light microscopy daily and cell harvesting took place on Day 0, 4, 5, 6 and 7 for western blot analysis. Following washing with 1mL/well of PBS, 100 µL of lysis buffer [1mM EDTA, 2% sodium dodecyl sulphate (SDS), 25 mM Tris-HCL pH 7.5, 10µL/mL protease inhibitor, 10µL/mL phosphatase inhibitor and 1mM DTT] was added to each well of the 6-well plate. A cell scraper was then used to collect the cells. In order to lyse the cells, all cell lysates were passed up and down using a 1mL syringe fitted with a 26-gauge needle. Each vehicle and drug lysate were then stored at -20°C for future analysis. Cell harvesting for protein synthesis and myotube fractionation are described below (See 6.5 and 6.6)

### 6.4 Protein Assay, Gels and Western Blot Analysis

Following sample collection, the Pierce BCA Protein Assay Kit purchased from Thermo Scientific (#23225) was used to determine protein concentrations for each sample. Equal amounts of protein (~25µg) were then heated, vortexed and loaded into either 10% or 15% SDS-page gels. Following gel electrophoresis, all proteins were transferred onto polyvinylidene difluoride (PVDF) membranes and left overnight at 4°C. The following day, the quality of transfer was measured by exposing each PVDF membrane to ponceauS (purchased from Sigma Aldrich, #81460) dye treatment for 15 minutes. In order to block non-specific antigen binding, membranes were incubated in a milk solution (5% milk powder in TBST) at room temperature for 1 hour. Each membrane then underwent a 3x5 minute wash in TBST followed by overnight incubation at 4°C in the primary antibody of interest. See table below.

<b>Primary Antibody</b>	<b>Dilution</b>	<b>Purchased From</b>	<b>Secondary Antibody</b>
ph-S6K1 <sup>thr389</sup>	1:1000	Cell Signaling #9205	Anti-rabbit (CST #7074)

ph-S6 <sup>Ser235/236</sup>	1:1000	Cell Signaling #4858	Anti-rabbit (CST #7074)
ph-Akt <sup>Ser473</sup>	1:1000	Cell Signaling #9271	Anti-rabbit (CST #7074)
Gamma-Tubulin	1:1000	Sigma Aldrich #T6557	Anti-mouse (CST #7076)
MHC	1:500	Developmental Hybridoma	Anti-mouse (CST #7076)
Troponin	1:400	Developmental Hybridoma	Anti-mouse (CST #7076)
Tropomyosin	1:400	Developmental Hybridoma	Anti-mouse (CST #7076)
COX IV	1:1000	Cell Signaling #4850	Anti-rabbit (CST #7074)
Succinate Dehydrogenase	1:1000	Cell Signaling #11998	Anti-rabbit (CST #7074)
HSP60	1:1000	Cell Signaling #12165T	Anti-rabbit (CST #7074)
GAPDH	1:1000	Cell Signaling #2118S	Anti-rabbit (CST #7074)

Following the overnight incubation in primary antibody, membranes went through a second 3x5 minute wash in TBST. Anti-rabbit (CST #7074) and Anti-mouse (CST #7076) antibodies purchased from Cell Signaling Technologies were diluted in the milk solution described earlier at a dilution of 1:10000. Each membrane was then incubated in the corresponding secondary antibody for 3 hours at room temperature. Following the 3 hour incubation time, membranes were washed 3x5 minutes in TBST. Lastly, HRP chemical luminescent substrate purchased from BioRad (#1705060S) was applied to each membrane and BioRad ChemiDoc XRS+ was used for signal visualization. Images were quantified using image lab software v7.

### **6.5 Protein Synthesis Measurement in Myotubes**

On Day 5 and Day 6 of treatment, vehicle and drug treated myotubes were exposed to a protein synthesis labelling mix consisting of 1mL/well of 1X DMEM lacking Methionine and Cysteine, 2µci/mL of <sup>35</sup>S protein labelling mix and 2% Dialyzed FBS (DFBS). Each well

received 1mL of the protein synthesis labelling mix and was then placed in the cell culture incubator for 1 hour. Following the 1 hour, the incubation media (1mL) from each well was collected and later counted for scintillation to ensure equal levels of radioactivity in each well. Each well then underwent 5X washes in 1mL/well of ice cold PBS to wash away any <sup>35</sup>S residue on the cell surface. The steps for cell harvesting including the addition of lysis buffer and cell scraping then commenced, similar to that of Western Blot Analysis (See 6.3).

Protein assay, creating gels and gel electrophoresis for western blot analysis of proteins have all been described previously (See 6.4). Following gel electrophoresis on a separate pair of gels, gels were stained with Coomassie Brilliant Blue Solution for 1 hour (0.1g Coomassie Blue R-250 dissolved in 100ml of methanol, acetic acid and DDH<sub>2</sub>O solution). Following the 1 hour Coomassie blue staining, 4x15minute washes with a destaining solution (60% DDH<sub>2</sub>O, 20% Methanol, 10% Glacial Acetic Acid) was used to wash the Coomassie blue solution away. Overnight incubation at 4°C in the destaining solution then commenced. The following day, a Coomassie blue blot (CBB) of the stained membrane was taken by the Typhoon FLA 9500 imager and the gel was then dried for 1 hour using a Model 583 Gel Dryer from BIO-RAD. Gels were dried in between a piece of filter paper and saran wrap. 1 hour later, the dried gel (with radioactive samples/proteins within) was placed inside an autoradiography cassette (FBCA 810) purchased from Fisher Scientific and exposed to a 20x25cm phospho imaging screen purchased from Fujifilm (#An28956475) for 1-2 weeks. Following the exposure period, the imaging plate was imaged using Typhoon FLA 9500 imager. Typhoon FLA 9500 software program was used for signal visualization and images were quantified using Quantity One software from BIO-RAD.

## **6.6 Myofibrillar and Sarcoplasmic Fractionation of Myotubes**

On day 5 and 6 of treatment, vehicle and drug-treated wells were incubated for 1 hour in a protein synthesis mix described previously. Three drug and three vehicle treated wells were then incubated in trypsin for 5 minutes and cells were collected into one 15mL test tube per condition. 15mL tubes were then centrifuged at 2000rpm for 5 minutes, washed and then re-suspended in 500 $\mu$ L/tube of a Triton solution (PBS, 1% Triton, 10 $\mu$ L/mL protease inhibitor, 10 $\mu$ L/mL phosphatase inhibitor, 1mM EDTA). Of the 500 $\mu$ L Triton solution, 100 $\mu$ L was extracted and set aside for protein assay measurement. Fractionation began by centrifuging the triton solution (now 400 $\mu$ L) at 1200g for 5 minutes followed by the removal and storage of the sarcoplasmic (supernatant) portion. Steps were then taken to prepare a concentrated myofibrillar sample (See Appendix A for full procedure). Gel electrophoresis, western blot analysis, comassie blue staining and protein synthesis measurement procedures described previously (see 6.4 and 6.5) were then completed.

## **6.7 Immunofluorescence Microscopy**

L6 myoblasts were seeded into 12-well plates and grown on top of cover slips purchased from Fisher Scientific (#092815-9). Once 90-100% confluency was reached (Day 0), cells were washed and shifted into DM until Day 4 of differentiation. On Day 4, myotubes were exposed to fresh DM in conjunction with either Vehicle or Drug treatment. On Day 5 and 6 of differentiation, cover slips with cells were fixed with 1mL/well of a paraformaldehyde (PFA) solution (4% PFA in PBS), permeabilized with 1mL/well of a Triton solution (0.03% Triton X-100 in PBS) and incubated with 400 $\mu$ L/well of a blocking solution (10% horse serum in PBS). Cover slips were then exposed overnight to 500 $\mu$ L/well of diluted MHC primary antibody solution (2.5 $\mu$ g/ml of MHC in 1% BSA in PBS). The following day, cover slips were washed

3x5minutes with PBS and then exposed to 500 $\mu$ L/well of a diluted Texas Red anti-mouse IgG secondary antibody before DAPI staining (for nuclei) and cover slip mounting on a microscope slides. Slides were then imaged using the EVOS FL Auto microscope from Life Technologies along with the EVOS FL Auto program for signal capturing and exposure (See Appendix B for full procedure). For quantification purposes, all images were transformed into an 8-bit gray scale image and mean gray value of each sample was measured within a 0-255 range using image j.

### **6.8 2-Deoxy-Glucose Uptake in Myotubes**

2-deoxyglucose (2-DG) was used for all glucose uptake assays. This is due to the fact that once 2-DG is taken up into the cell, it cannot be fully metabolised and accumulates within the cell. By using radiolabelled 2-DG ( $[^3\text{H}]$ -2-deoxyglucose), both the radioactively tagged 2-DG and unlabelled 2-DG can enter the cell. Therefore, by measuring the level of radioactivity within cells, we can determine the levels of glucose uptake either with or without the presence of insulin.

L6 myoblasts were seeded into 12-well plates until 90-100% confluency was reached (Day 0). On Day 0, cells were washed and shifted into DM until Day 4 of differentiation. On Day 4, myotubes were exposed to fresh DM in conjunction with either Vehicle or Drug treatment. On Day 5 and 6 of differentiation, myotubes in both conditions were incubated in starvation media (complete starvation medium, free of amino acids and serum), plus their respective treatments for three hours. Following the three hour starvation period, myotubes in each condition were incubated with or without 100nM of insulin diluted in starvation media and their respective vehicle or drug treatments for 20 minutes. Post 20 minute insulin exposure, cells were rinsed 2X in HEPES (4-(2-Hydroxyethyl) piperazine-1-ethanesulfonic acid) buffered saline and then incubated for 5 minutes at 37.1 $^{\circ}$ C in 300 $\mu$ L of transport solution (HEPES buffer, 10 $\mu$ M

2-deoxyglucose, 0.5  $\mu\text{Ci/mL}$  [ $^3\text{H}$ ]-2- Deoxyglucose). After 5 minutes, the glucose uptake reaction was stopped through constant exposure to ice and by washing the cells 3X in ice-cold stop solution (1ml/well of 0.9% Saline). 1mL of 0.05M NaOH was then added to the cells for scraping and collection. Two-hundred  $\mu\text{L}$  was set aside and frozen at  $-20^\circ\text{C}$  for future protein assay analysis. The leftover 800 $\mu\text{L}$  was pipetted into scintillation fluid (Ecolite+, MP Biomedicals #01882475) and respectfully labelled scintillation tubes (see Appendix C for full procedure). A liquid scintillation counter (Tri-Carb Liquid Scintillation Counter) was used to count and measure the radioactivity from samples in each vial. Protein assay protocol (described above) and results were than used and rate of glucose transport was expressed picomole per  $\mu\text{g}$  of protein.

## **6.9 Graphical Representation of Western Blots and Statistics**

Western blotting for MHC, troponin, tropomyosin, P-AKT, P-S6K1, P-S6, COXIV, SDHA and HSP60 were adjusted by their respective gamma tubulin values and then normalized to the Vehicle group on Day 5. All graphs were designed using Prism Computer Software Version 7.

Unpaired t-tests with a welch-correction was used to analyze immunofluorescence results and to compare D0 myoblasts to D4 myotubes. Two-way ANOVA across all groups was used to compare vehicle and drug treated myotubes on Day 5, 6 and 7, as well for glucose uptake results to measure the significance of differences followed by a Tukey's Post-Hoc Test. Differences were found to be significant when p-value  $< 0.05$ . All results expressed as means  $\pm$  SEM.

## Chapter Seven: Results

### A chemotherapy drug cocktail negatively regulates myotube formation and morphology

Due to the literature outlining the negative relationship between chemotherapy treatment and skeletal muscle<sup>158, 160</sup>, I examined the effect of a chemotherapy drug cocktail on L6 myotube formation. On Day 0, control myoblasts (Fig.1A) were co-treated with fresh DM and either DMSO (Vehicle) or a chemotherapy drug cocktail (Drug). By day 4 of differentiation, myoblasts exposed to the chemotherapy drug cocktail did not form myotubes likely due to reductions in cell number (Fig.1B). Due to the inability of chemotherapy drug-treated myoblasts to grow and differentiate, I turned to investigate the effect of the chemotherapy drug cocktail on myotubes differentiated over four days. I also believed that adding the drug to fully formed myotubes would present a more real life scenario as patients undergoing chemotherapy treatment have functionally formed muscle prior to treatment. On day 4, control myotubes (Fig.1C) were treated with fresh DM and either vehicle or drug treatments. By day 5 of differentiation, myotubes treated with the drug cocktail began to show small, but noticeable abnormalities in myotube structure compared to vehicle (Fig.1D). Forty-eight (Fig.1E) and 72 (Fig.1F) hours after commencement of drug treatment, abnormalities in myotube morphology were aggravated. Due to the possibility that the myotubes treated with the drug cocktail may exhibit disruptions in total protein concentration, I next measured and compared the protein concentrations of each treatment. Although protein concentration significantly differed between D0 myoblasts and D4 myotubes ( $n=4$ ,  $p = 0.006$ ), there were no significant differences found with regards to protein concentrations in vehicle and drug-treated myotubes on Day 5, 6 and 7 (Fig. 1G). Although the evidence presented here is clear on the negative effect of a chemotherapy drug cocktail on myotube morphology, the mechanisms behind this relationship remain unclear.

### A chemotherapy drug cocktail disrupts L6 myofibrillar abundance

Due to the significant morphological changes observed under light microscopy in myotubes treated with the drug cocktail (Fig. 1), I next used immunofluorescence to examine the expression of myosin heavy chain (MHC). MHC staining of vehicle and drug treatments is shown in both D5 and D6 treated myotubes (Fig 2A). On day 5 of differentiation, a small non-significant decrease is seen in MHC staining of myotubes treated with the drug cocktail (Fig 2B). However, by Day 6 of differentiation, detrimental loss of myofibrillar abundance, shown through a significant decrease in MHC staining ( $n=4$ ,  $p = 0.0209$ ) is present in the drug group compared to vehicle (Fig. 2C). DAPI staining of nuclei is equal in both treatments across both days of differentiation (Fig. 2A-C). Coinciding with the images seen under light microscopy, the drug cocktail is clearly having a negative effect on L6 myofibrillar abundance.

### Myofibrillar protein content is decreased in myotubes treated with a chemotherapy drug cocktail

Due to the negative effect of the drug cocktail on MHC staining (Fig. 2), I next investigated via western blotting, the abundance of myofibrillar proteins MHC, troponin and tropomyosin. Compared to myotubes treated with vehicle, those treated with the drug cocktail showed significant reductions in MHC ( $n=5$ ,  $p = 0.0003$ ), troponin ( $n=4$ ,  $p < .0001$ ) and tropomyosin ( $n=4$ ,  $p = 0.0059$ ) by day 6 of differentiation. By day 7 of differentiation, myotubes treated with the drug cocktail showed significant reductions in MHC ( $n=5$ ,  $p < .0001$ ), troponin ( $n=4$ ,  $p < 0.0001$ ) and tropomyosin ( $n=4$ ,  $p = 0.0095$ ) compared to vehicle (Fig.3A-C). This data demonstrates that the abnormalities in myotube structure caused by the drug cocktail may be attributed to a decrease in the levels of myofibrillar protein content.

### mTORC1 signalling is disrupted in myotubes treated with a chemotherapy drug cocktail

I next sought to investigate factors associated with the decrease in myofibrillar proteins

found in myotubes treated with the drug cocktail. I examined proteins involved in signalling towards mTORC1, a master regulator of protein synthesis. Upstream activator AKT, along with two key downstream substrates S6 and S6K1 were the signalling proteins examined to help determine mTORC1 activity (Fig.4). Compared to D0 myoblasts, phosphorylation of AKT<sup>Ser473</sup>, S6<sup>Ser235/236</sup> and S6K1<sup>Thr389</sup> were all increased in D4 myotubes (Fig. 4A-C). Compared to myotubes treated with vehicle, those treated with the drug cocktail showed significant reductions in the phosphorylation of AKT<sup>Ser473</sup> (n=4, p = 0.0058), S6<sup>Ser235/236</sup> (n=3, p = 0.0178) and S6K1<sup>Thr389</sup> (n=3, p = 0.0025) by day 6 of differentiation. By day 7 of differentiation, myotubes treated with the drug cocktail showed significant decreases in the phosphorylation of AKT<sup>Ser473</sup> (n=4, p < 0.0001), S6<sup>Ser235/236</sup> (n=4, p = 0.0309) and S6K1<sup>Thr389</sup> (n=4, p = 0.0190) (Fig.4A-C). The data presented shows that a decrease in myofibrillar protein content may be a result of a decrease in mTORC1 activity.

#### Protein synthesis is reduced in myotubes treated with a chemotherapy drug cocktail

Although myotubes treated with the drug cocktail exhibited significant decreases in mTORC1 signalling (Fig. 4), it is still undetermined whether this relationship is due to a decrease in protein synthesis or an increase in proteolysis. Therefore, I next measured the rate of protein synthesis in myotubes treated with the drug cocktail using <sup>35</sup>S Methionine incorporation. On both Day 5 and 6 of differentiation, myotubes under drug treatment showed a decrease in the levels of <sup>35</sup>S methionine incorporation into proteins compared to vehicle (Fig. 5A), signifying a decrease in protein synthesis. Protein concentrations in both treatment groups are shown across both days of differentiation represented by the  $\gamma$ -tubulin blot (Fig. 5B) and the comassie blue blot (CBB) (Fig. 5C). Due to the equal concentrations of protein in each treatment, these results point to a decrease in the rates of total protein synthesis in myotubes treated with the drug cocktail.

### Protein synthesis is decreased in fractionated myotubes treated with a chemotherapy drug cocktail

Due to the negative effect of the drug cocktail on myofibrillar protein abundance (Fig.3), I next wanted to determine whether the decrease in total protein synthesis (Fig.5), was specific to myofibrillar and sarcoplasmic fractions. I therefore fractionated L6 myotubes from both treatments into three fractions: total lysate (Load), Myofibrillar (Myofib) and sarcoplasmic (Sarco) fractions. We then measured the rates of protein synthesis using  $^{35}\text{S}$  Methionine incorporation. On both Day 5 and 6 of differentiation, levels of  $^{35}\text{S}$  Methionine incorporation were decreased in all drug treated fractions compared to vehicle (Fig 6A). In accordance with the above protein synthesis results, protein concentrations in both treatment groups were equal across both days of differentiation represented by the  $\gamma$ -tubulin blot (Fig. 6C) and CBB blot (Fig. 6B). Successful fractionation of myotubes was identified via western blotting of MHC for myofibrillar fractions and GAPDH for sarcoplasmic fractions (Fig. 6C).

### Mitochondrial Proteins are reduced in myotubes treated with a chemotherapy drug cocktail

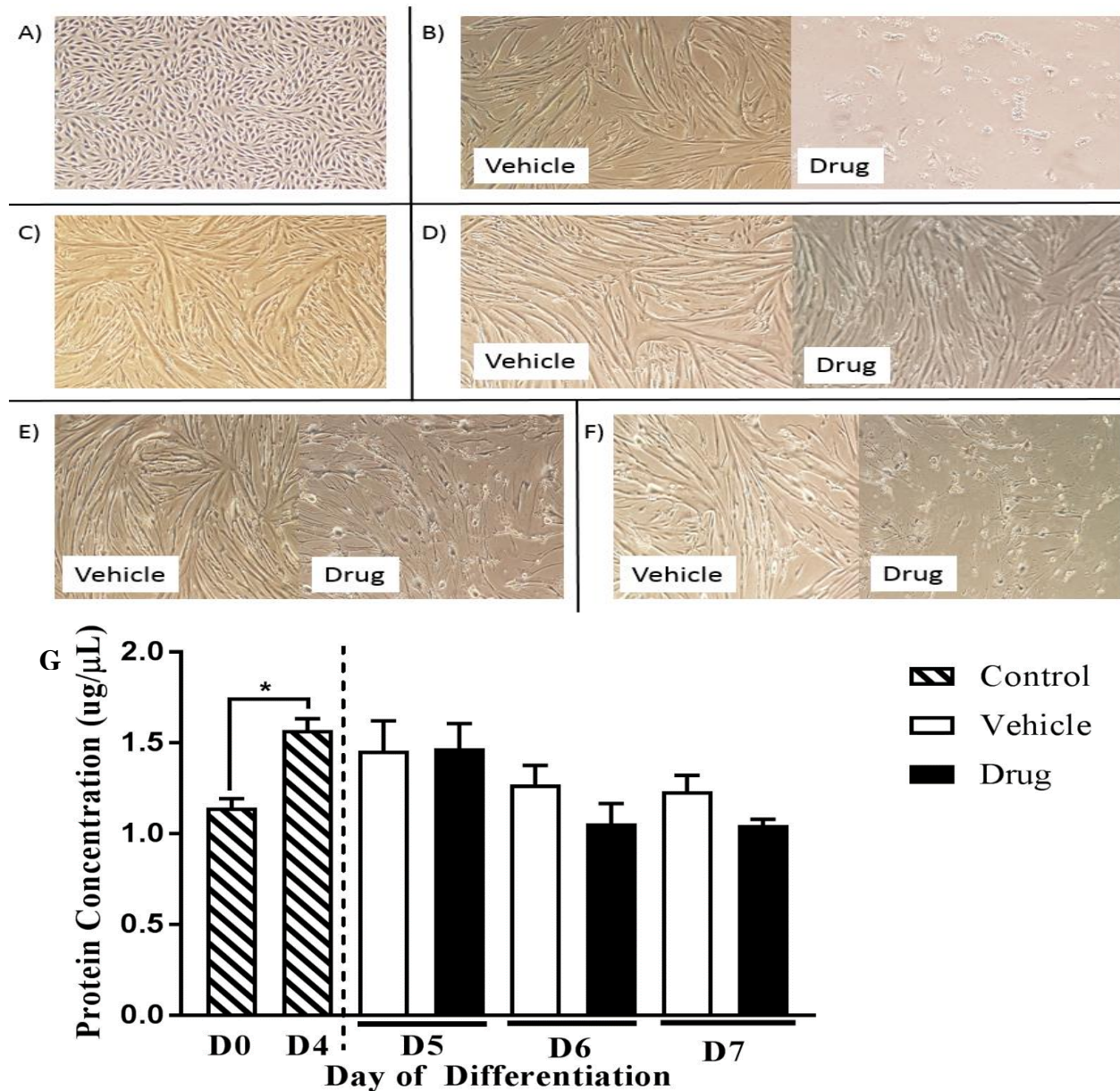
I next investigated the modulation of mitochondrial proteins as mitochondrial proteins are associated with skeletal muscle maintenance and growth. Compared to D0 myoblasts, Succinate Dehydrogenase and COXIV, but not HSP60 were increased in D4 myotubes (Fig. 7A-C) Compared to myotubes treated with vehicle, those treated with the drug cocktail showed a significant decrease in Succinate Dehydrogenase (n=4, p = 0.0018) by day 6 of differentiation (Fig. 7A). By day 7 of differentiation, myotubes treated with the drug cocktail exhibited decreases in COX IV (n=4, p < 0.0001) and Succinate Dehydrogenase (n=4, p < 0.0001) compared to vehicle (Fig. 7A-B). Interestingly, myotubes treated with the drug cocktail showed a significant increase in HSP60 (n=3, p = 0.0053) by day 6, but not day 7 of differentiation compared to vehicle (Fig. 7C).

### Glucose Uptake is reduced in myotubes treated with a chemotherapy drug cocktail

Due to the presence of GLUT4 in L6 muscle cells and the finding that the phosphorylation status of AKT was reduced in myotubes treated with the chemotherapy drug cocktail (Fig. 4A), I next investigated insulin stimulated glucose uptake in both treatment groups. By day 5 of differentiation, there were no differences in the levels of glucose uptake across treatments (Fig. 8A). In contrast, by day 6 of differentiation, myotubes treated with the chemotherapy drug cocktail exhibited reductions in insulin-stimulated glucose uptake ( $n=5$ ,  $p < 0.06$ ) compared to vehicle (Fig. 8B).

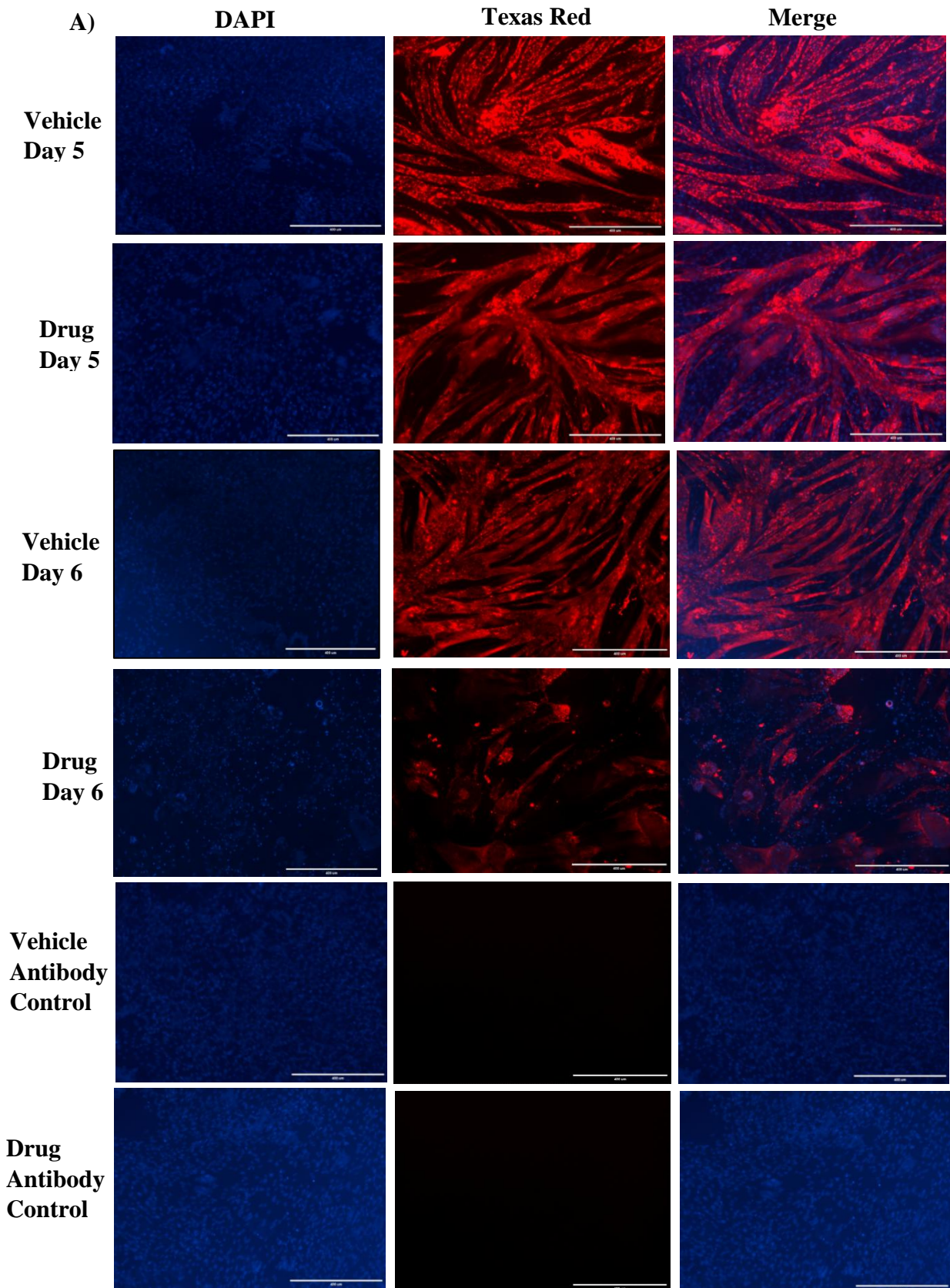
## Figure Results

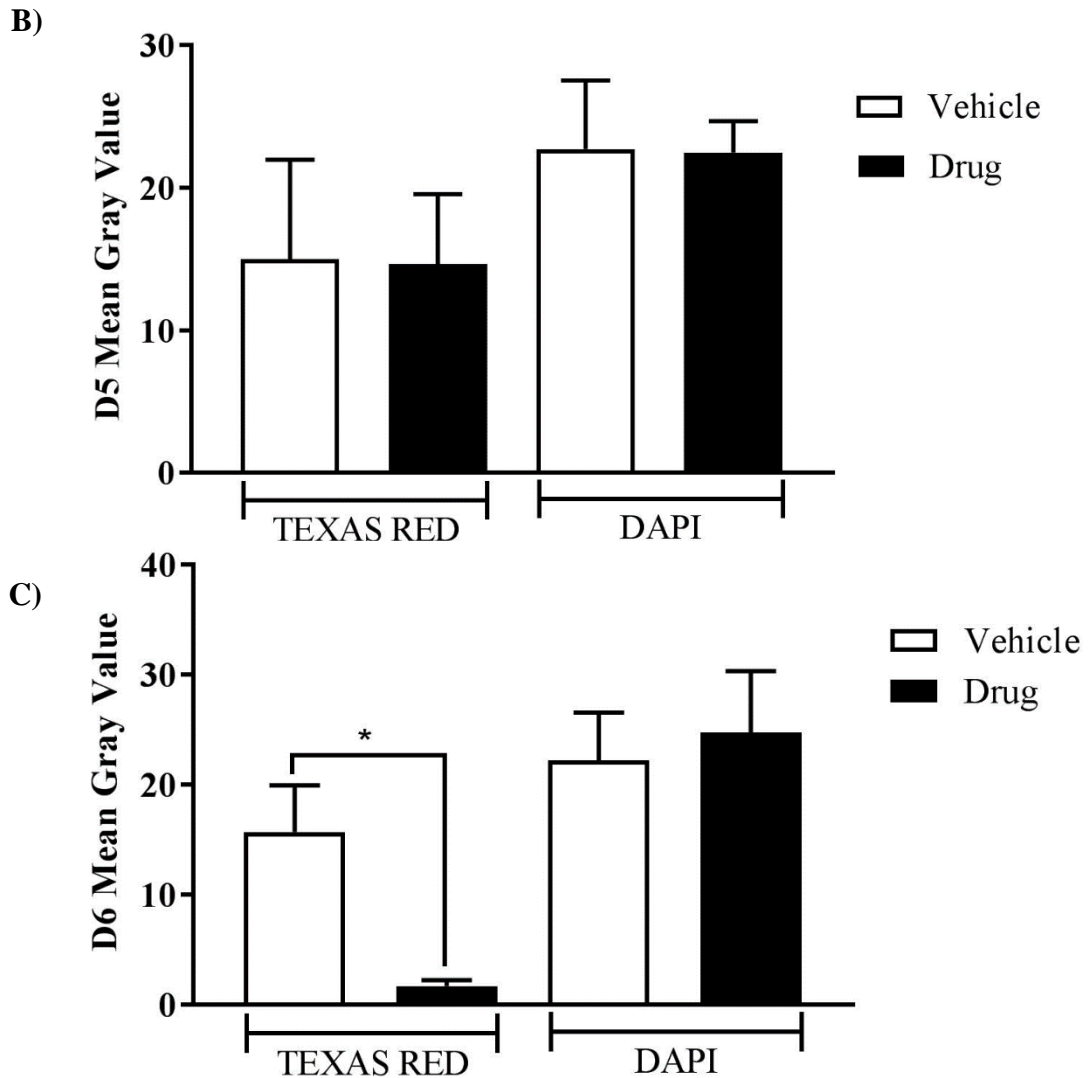
Figure 1.



**Fig 1.** A chemotherapy drug cocktail negatively regulates myotube formation and morphology. **A:** D0 L6 myoblasts were exposed to fresh DM supplemented with either Vehicle or Drug treatments. **B:** Vehicle or drug treated myoblasts differentiated for four days **C:** Formation of D4 myotubes prior to vehicle or drug treatments. **D-F:** Vehicle and drug treated myotubes on D5 (**D**), D6 (**E**) and D7 (**F**) **G:** Protein Concentration ( $\mu\text{g}/\mu\text{L}$ ) differences between D0 control myoblasts, D4 control myotubes and D5, D6 and D7 vehicle and drug treated myotubes. (n=4 independent experiments, 3 replicates per experiment). Bar graphs show mean  $\pm$  SEM.

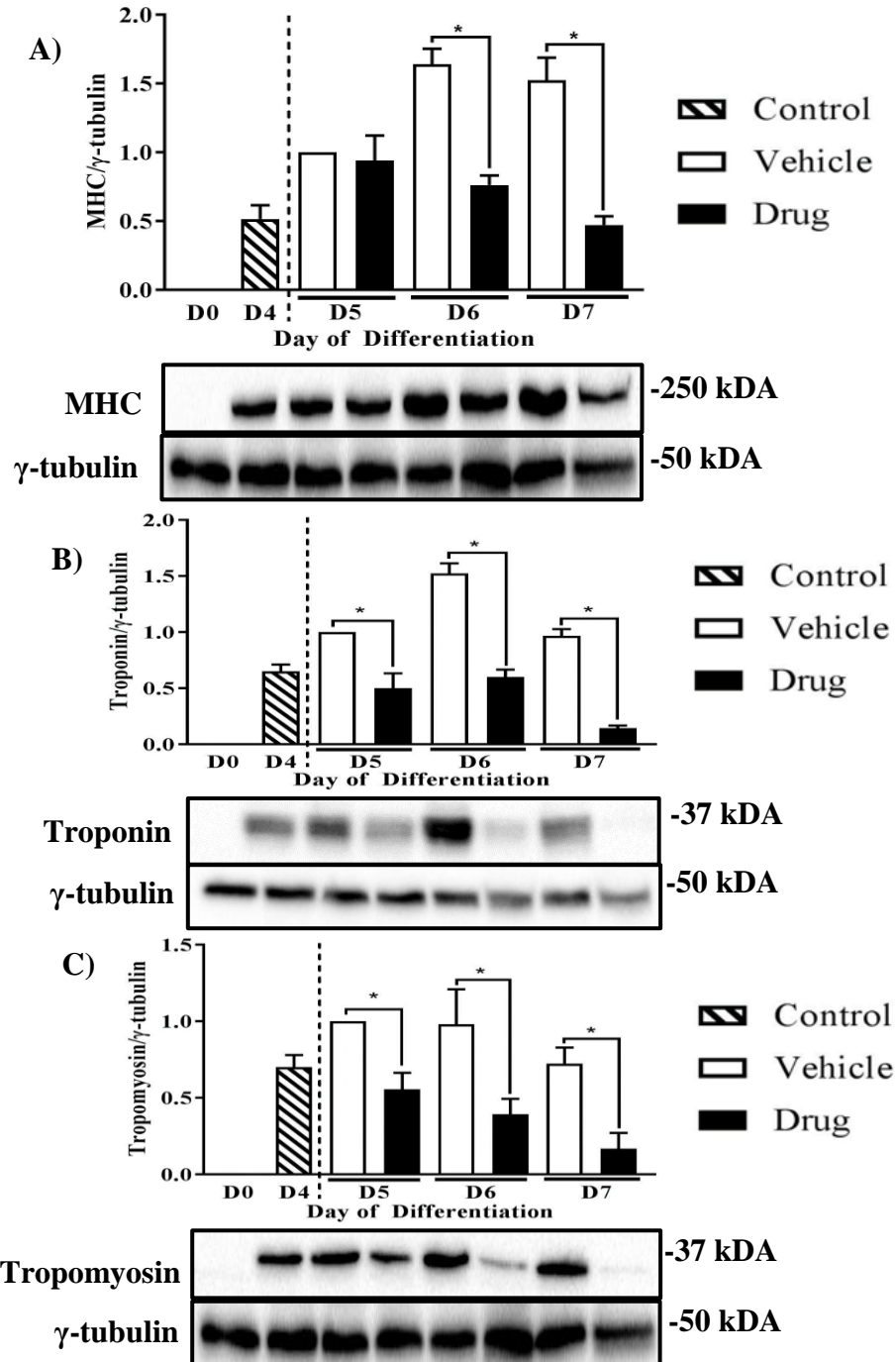
Figure 2.





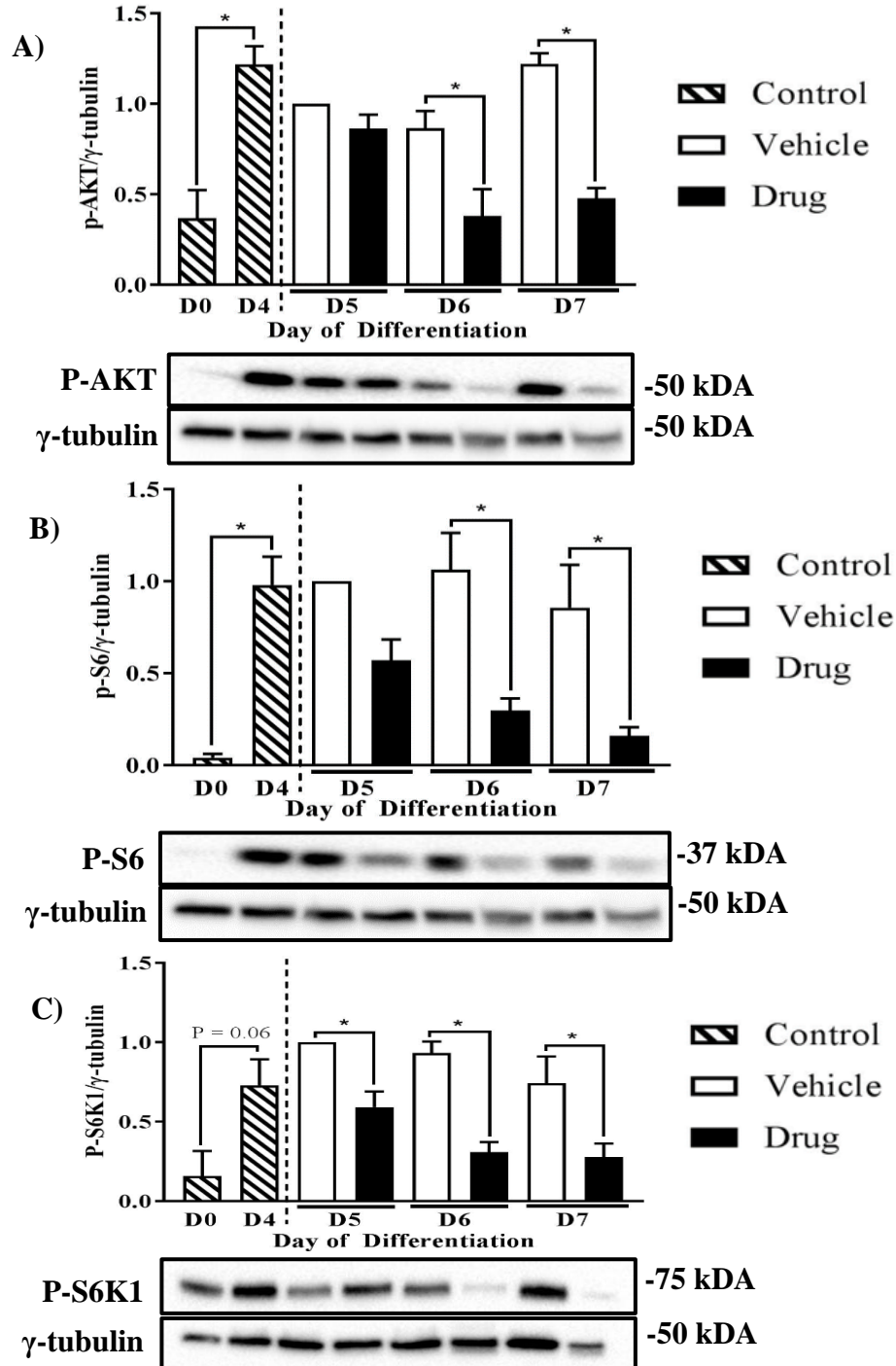
**Fig 2.** A chemotherapy drug cocktail disrupts L6 myofibrillar abundance. L6 myoblasts were differentiated until day 4. On day 4, myotubes were co-treated with fresh DM and either Vehicle or a chemotherapy drug cocktail until day 5 and 6. **A:** D5 and D6 myotubes in both treatments were fixed, permeabilized, blocked and incubated overnight in MHC primary antibody. Next, cells were exposed to Texas Red Anti-Mouse secondary antibody before mounting. DAPI was used to identify the nuclei. Bar, 400 $\mu$ m. **B-C:** Quantified mean gray value of MHC and DAPI nuclei staining in vehicle and drug treated myotubes on day 5 and 6 of differentiation. (n=4 independent experiments, 3-4 replicates per experiment, \* denotes significance,  $p < 0.05$ ). Bar graphs show mean  $\pm$  SEM.

Figure 3.



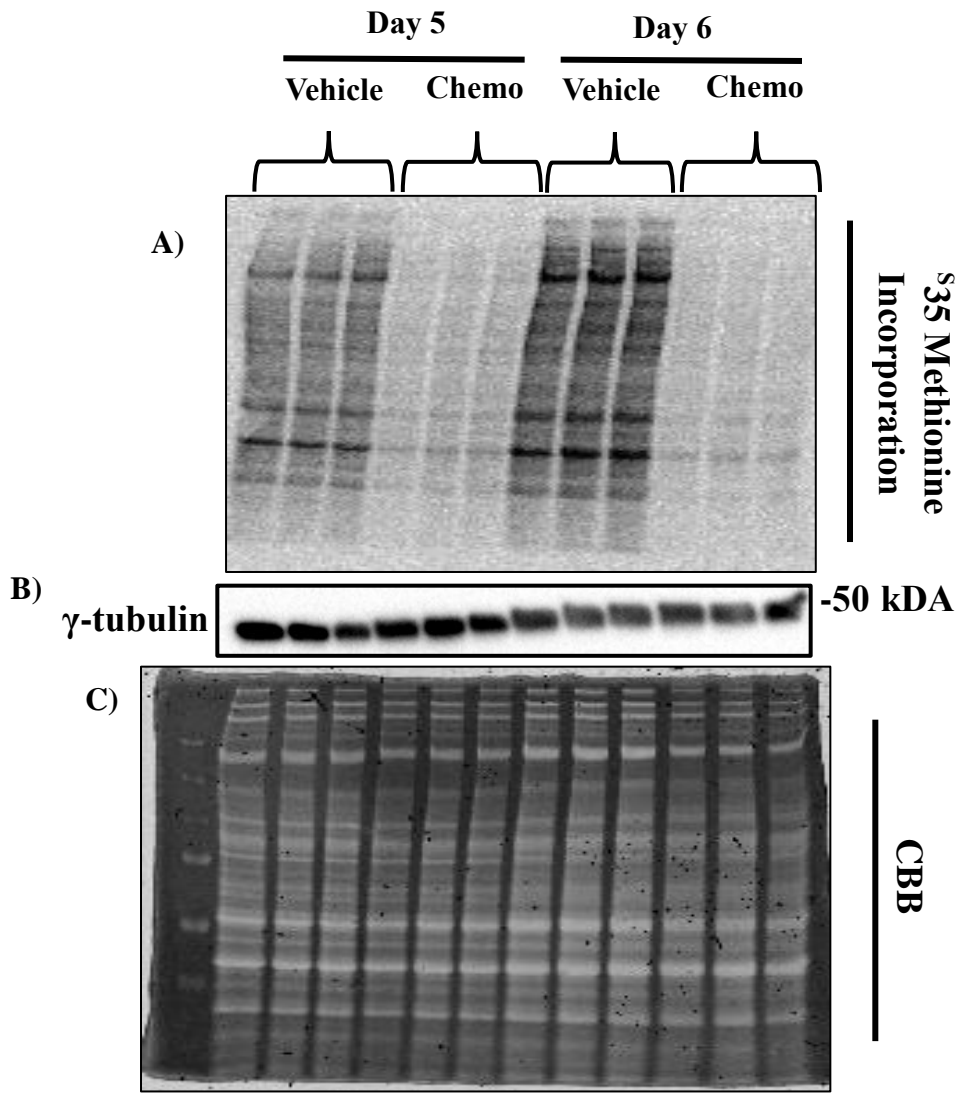
**Fig 3.** Myofibrillar protein content is decreased in myotubes treated with a chemotherapy drug cocktail. L6 myoblasts were differentiated until day 4. On day 4, myotubes were co-treated with fresh DM and either Vehicle or a chemotherapy drug cocktail until day 7. Chemotherapy drug treated myotubes had decreased abundance of myofibrillar protein content of MHC (A), Troponin (B) and Tropomyosin (C) throughout differentiation. (n=4-5 independent experiments, 3 replicates per experiment, \* denotes significance,  $p < 0.05$ ). Bar graphs show mean  $\pm$  SEM.

Figure 4.



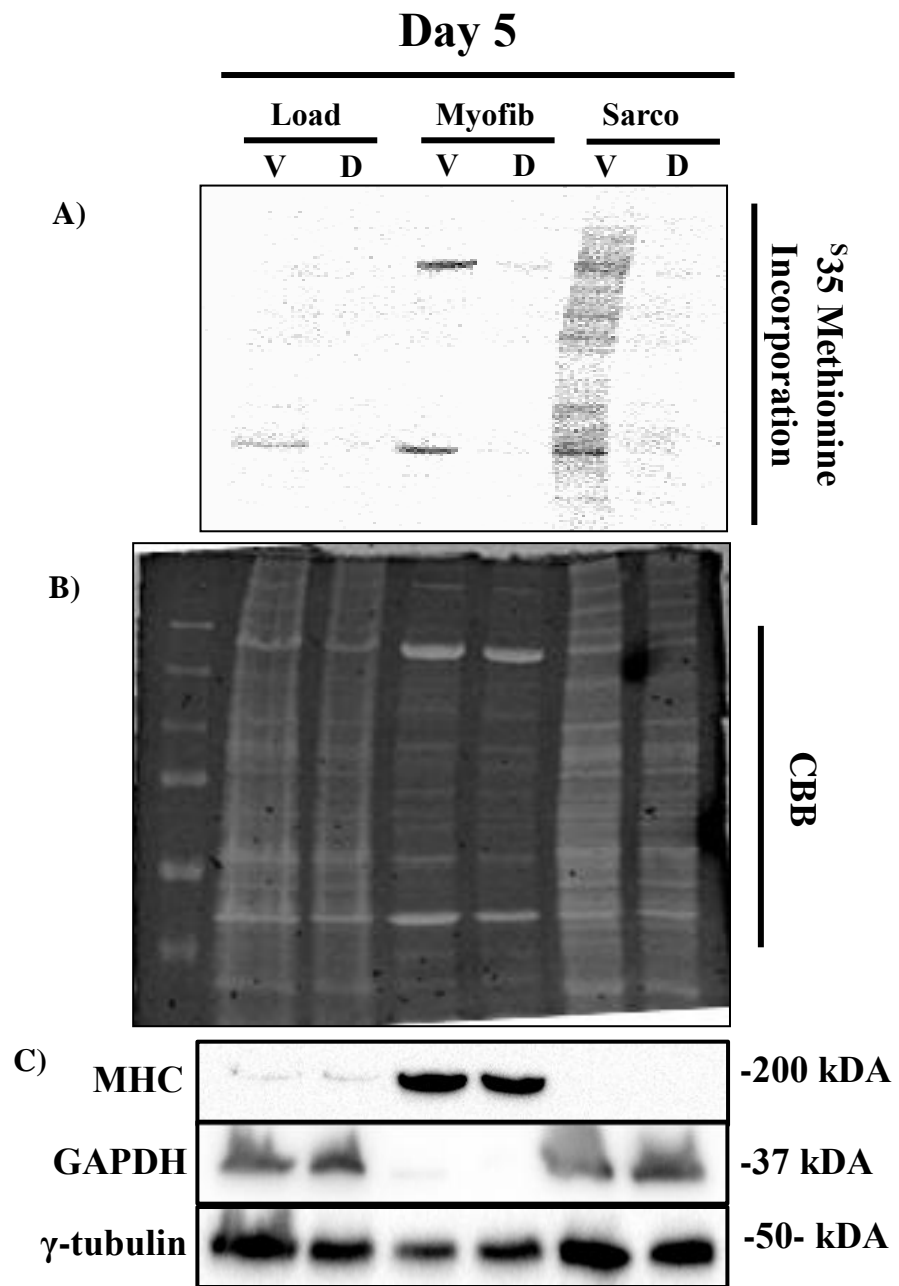
**Fig 4.** mTORC1 signalling is disrupted in myotubes treated with a chemotherapy drug cocktail. On day 4, myotubes were co-treated with fresh DM and either Vehicle or a chemotherapy drug cocktail until day 7. Phosphorylation of mTORC1's upstream activator AKT (A) was decreased in the drug group throughout differentiation. Phosphorylation of mTORC1's downstream targets S6 (B) and S6K1 (C) were decreased in the drug group throughout differentiation. (n=3-4 independent experiments, 3 replicates per experiment, \* denotes significance,  $p < 0.05$ ). Bar graphs show mean  $\pm$  SEM.

Figure 5.

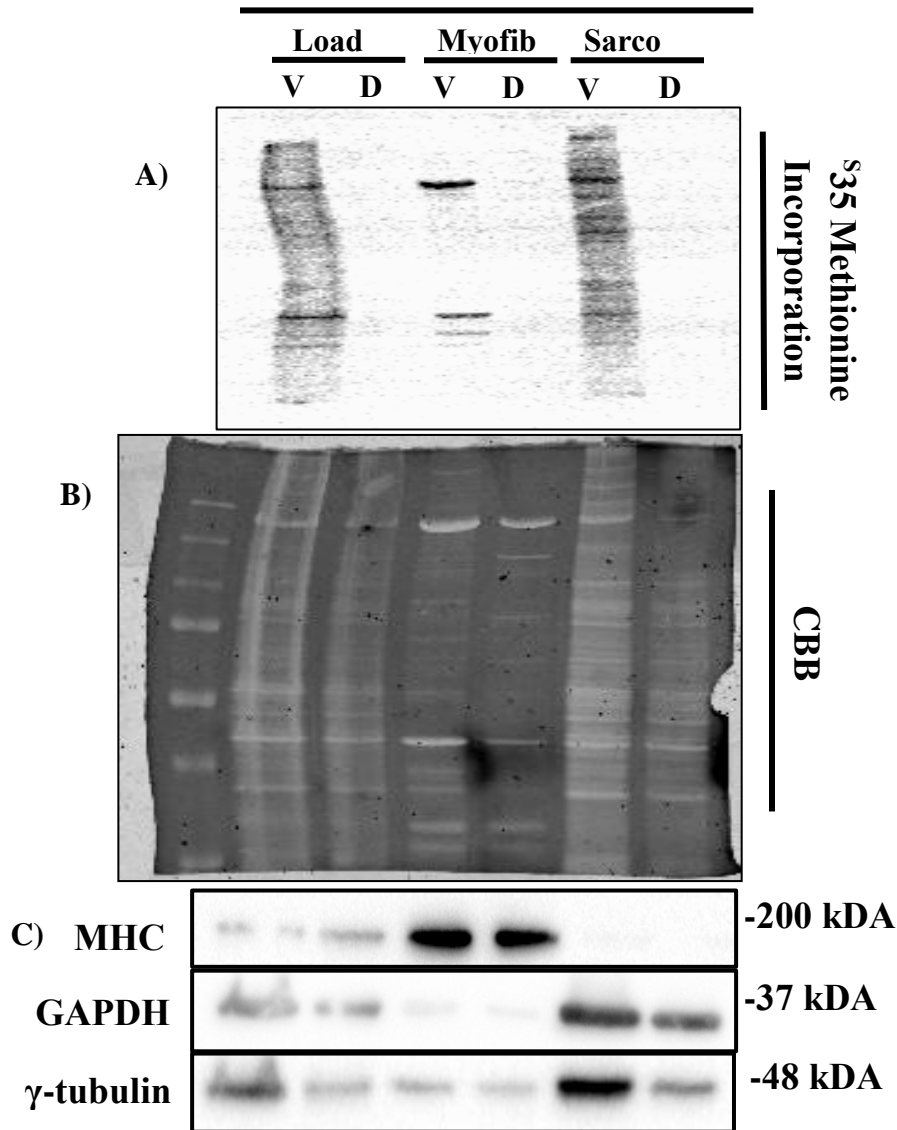


**Fig 5.** Protein Synthesis is reduced in myotubes treated with a chemotherapy drug cocktail. L6 myoblasts were differentiated until day 4. On day 4, myotubes were co-treated with fresh DM and either Vehicle or a chemotherapy drug cocktail until D6. On D5 and D6, myotubes in both treatments were incubated in a <sup>35</sup>S Methionine labelling mix for 1hour, washed 5X in 1mL/well of PBS and then harvested according to regular procedure. **A:** D5 and D6 representative blot of <sup>35</sup>S Methionine incorporation into proteins in vehicle and chemotherapy drug treated myotubes **B:** Loading control blot for  $\gamma$ -tubulin in D5 and D6 vehicle and chemotherapy drug treated myotubes. **C:** Comassie blue blot (CBB) of protein concentrations in D5 and D6 vehicle and chemotherapy drug treated myotubes. (n=5 independent experiments, 3 replicates per experiment)

Figure 6.

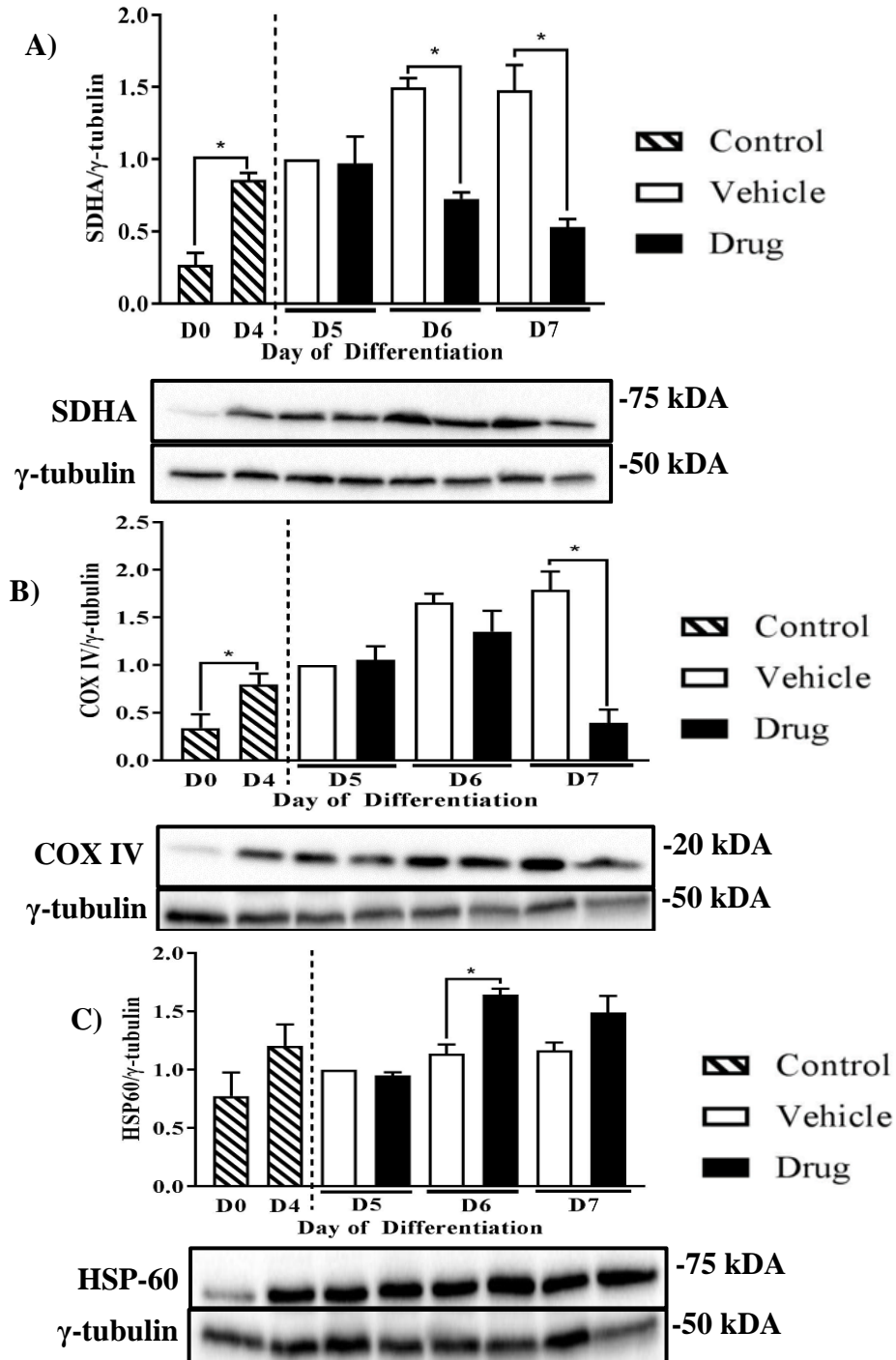


## Day 6



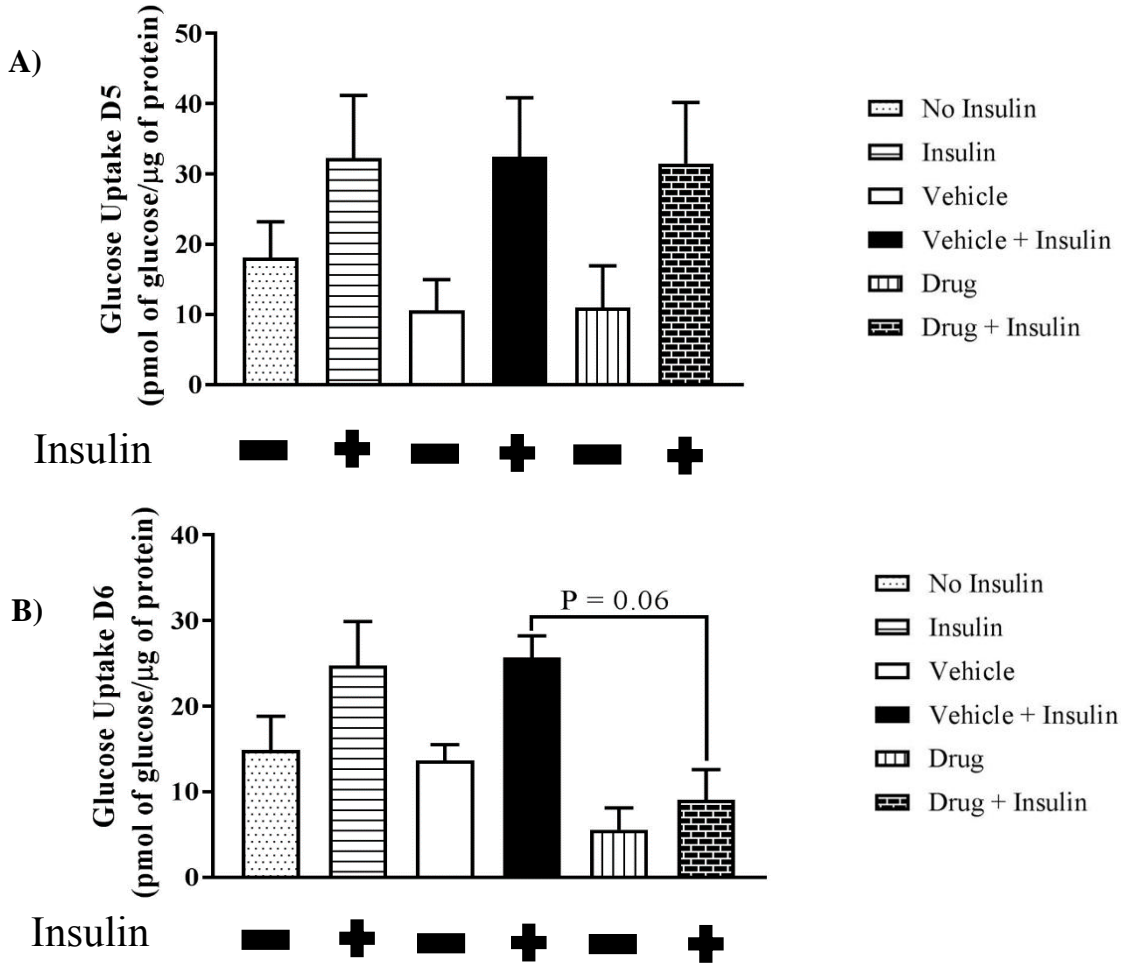
**Fig 6.** Protein synthesis is decreased in fractionated myotubes treated with a chemotherapy drug cocktail. Day 4 differentiated myotubes were co-treated with fresh DM and either Vehicle or a chemotherapy drug cocktail until day 6. On D5 and D6, myotubes in both treatments were incubated in a <sup>35</sup>S Methionine labelling mix for 1hr. Next, myotubes were fractionated into vehicle load, drug load, vehicle myofibrillar, drug myofibrillar, vehicle sarcoplasmic and drug sarcoplasmic. **A:** D5 and D6 representative blot of <sup>35</sup>S Methionine incorporation into proteins in vehicle and chemotherapy drug treated myotubes for each fractionated segment. **B:** Comassie blue blot (CBB) of protein concentrations in D5 and D6 vehicle and chemotherapy drug treated fractionated myotubes. **C:** Representative western blotting for MHC, GAPDH and γ-tubulin showing protein expression specific to each fractionated segment. (n=4 independent experiments). Myofib = Myofibrillar, Sarco = Sarcoplasmic.

Figure 7.



**Fig 7.** Mitochondrial Proteins are reduced in myotubes treated with a chemotherapy drug cocktail **A:** L6 myoblasts were differentiated until day 4. On day 4, myotubes were co-treated with fresh DM and either vehicle or a chemotherapy drug cocktail until day 7. **A-B:** By D7 of differentiation, mitochondrial proteins SDHA (**A**) and COXIV (**B**) were decreased in chemotherapy drug treated myotubes compared to vehicle. **C:** HSP60 protein content in vehicle and chemotherapy drug treated myotubes. (n=3-4 independent experiments, 3 replicates per experiment, \*denotes significance,  $p < 0.05$ ). Bar graph shows mean  $\pm$  SEM.

Figure 8.



**Fig 8.** Glucose Uptake is reduced in myotubes treated with a chemotherapy drug cocktail. L6 myoblasts were differentiated until day 4. On day 4, myotubes were co-treated with fresh DM and either Vehicle or a chemotherapy drug cocktail. On D5 (**A**) and D6 (**B**), myotubes in all conditions were starved for 3 hours, followed by incubation with or without insulin for 20 minutes. Next, cells were washed in hepes buffer and incubated in transport solution for 5 minutes. Cellular glucose uptake was stopped using ice cold saline and cells were harvested using NaOH. (n=5 independent experiments, 2-5 replicates per experiment). Bar graph shows mean  $\pm$  SEM.

## Chapter Eight: Discussion

The findings from this study suggest that common chemotherapeutic agents cisplatin and 5-Flu, normally used for the treatment of a spectrum of different cancers, leads to abnormal myotube morphology and protein metabolism. The observed myotube abnormalities under drug treatment are associated with reductions in the abundance of myofibrillar proteins, anabolic signalling, protein synthesis, mitochondrial content and glucose uptake.

To our knowledge, this study is the first to investigate the effects of a common chemotherapeutic drug cocktail on myofibrillar protein content in L6 cells. In this, the present study has found evidence of chemotherapy-related effects on myofibrillar protein integrity in myotubes. Compared to vehicle, I have shown that myotubes treated with the drug cocktail exhibit concurrent loss in the immunofluorescent expression of MHC (Fig 2). I next measured and quantified DAPI nuclei staining in both treatments to ensure that cell number was similar and that the above finding was not due to factors such as cell death or unspecific binding. Via western blotting of MHC, troponin and tropomyosin, I further confirmed the reductions in myofibrillar protein abundance in myotubes treated with the drug cocktail (Fig 3). Due to the observation that chemotherapy treatment decreases body weight, associated with reductions in muscle mass and function<sup>160</sup>, this finding is potentially critical as myofibrillar proteins are necessary for muscle maintenance and contraction over time<sup>187</sup>.

I suggest that the reduction in myofibrillar proteins induced by the administration of chemotherapy drugs, can be attributed to reductions in anabolic signalling pathways. Both upstream and downstream markers in the IGF-1/AKT/mTORC1 pathway were decreased in myotubes following the administration of chemotherapy drugs (Fig 4). Our findings for decreased activity through the IGF-1/AKT/mTORC1 pathway in myotubes following drug

administration is in opposition to other cachectic models. In cachectic tumour-bearing models, upregulation of AKT is associated with progressive tumour growth and inhibiting AKT does not affect mTORC1/S6 signalling<sup>188</sup> in muscle. Similarly, the phosphorylation of AKT is also significantly upregulated in denervation-induced muscle atrophy, but mTORC1's downstream substrate S6K1 is downregulated<sup>189</sup>. Our results in accordance with these past reports, present clear complexities on the effect of cachexia on skeletal muscle anabolism through mTORC1 regulation. These findings suggest that the IGF-1/AKT/mTORC1 pathway may be differentially regulated by AKT substrates or by separate oncogenic and protein degradation networks during cachexia.

Since mTORC1 regulation is involved in both augmenting skeletal muscle anabolism and inhibiting protein degradation<sup>185</sup>, I investigated whether the deregulated mTORC1 following drug administration had an effect on protein synthesis in myotubes. Using <sup>35</sup>S methionine incorporation (Fig. 5), I suggest that the reductions in activity through the AKT/mTORC1 pathway is associated with decreases in protein synthesis. I further confirmed our myofibrillar protein findings (Fig. 2-3), by fractionating myotubes into myofibrillar and sarcoplasmic segments. In accordance to decreases in total protein synthesis (Fig. 5), I found evidence of reduced protein synthesis in myofibrillar and sarcoplasmic portions of myotubes (Fig. 6). These findings coincide with the effects of other chemotherapeutic drugs, such as doxorubicin, which also impairs skeletal muscle protein synthesis *in vivo*<sup>190, 191</sup>.

Findings from this study also found support for chemotherapy-induced effects on mitochondrial content in myotubes. Following drug treatment, myotubes exhibited mitochondrial complex depletion of COXIV and SDHA (Fig 7). COXIV and SDHA are two subunits within the electron transport chain that allow for essential generation of ATP. Dysregulation within the

complexes of the electron transport chain, leads to the insufficient production of ATP and the formation of reactive oxygen species<sup>192</sup>, a well-known factor in the progression of cachexia<sup>93,96</sup>. Our mitochondria observations are consistent with previous work whereby cachexia-induced chemotherapy treatment led to skeletal muscle alterations associated with mitochondrial abnormalities<sup>160</sup>. Although mitochondria protein content can often be correlated with mitochondrial activity, our study did not investigate this mechanism and elucidations cannot be made at this time. In contrast, the previous study mentioned found both mitochondria number and activity to be downregulated in response to chemotherapy drugs. Further, I also found evidence of increased HSP60 protein content in myotubes administered the drug cocktail (Fig. 7). Within healthy or unstressed mitochondria, HSP60 is a chaperone mediating protein involved in transportation and re-folding of proteins from the cytoplasm to the mitochondrial matrix<sup>193</sup>. Interestingly, similar to the increase in HSP60 following drug administration, past reports have found evidence of increases in the levels of heat shock proteins in cellular stressing conditions, such as exercise and oxidative stress<sup>197, 198</sup>, but few past reports have studied HSPs following chemotherapy treatment. From these past reports, HSP60 mRNA expression was closely related to the development of cisplatin resistance in vitro<sup>251</sup>. In addition, inhibition of heat shock protein 27 (HSP27) phosphorylation resulted in increased 5-FLU sensitivity in-vitro<sup>252</sup>.

Lastly, via glucose uptake measurement assays, I find evidence of myotube alterations in insulin stimulated glucose uptake following chemotherapy drug administration. The mechanism of glucose uptake in skeletal muscle is a tightly regulated process involving multiple signalling events and proteins. Activation of IRS-1 by the binding of insulin to the  $\alpha$ -subunit of its cognate insulin receptor leads to the activation of the PI3K pathway<sup>194</sup>. Via the phosphorylation of AKT<sup>195</sup>, the PI3K pathway culminates the translocation of glucose transporter 4 to the cell

surface, thereby promoting glucose uptake<sup>196</sup>. Due to the vital role of AKT in insulin mediated glucose uptake and the fact that chemotherapy drugs decreased the phosphorylation of this kinase (Fig 4), I investigated glucose uptake in myotubes treated with the chemotherapy drug cocktail. Similarly to the phosphorylation of AKT, insulin stimulated glucose uptake was reduced in myotubes following drug treatment (Fig 8). This finding is similar to past reports whereas doxorubicin treatment decreased insulin-stimulated glucose uptake in L6 cells<sup>253</sup>, but this study did not explore a mechanism related to AKT in-vitro. This finding is particularly important since individuals receiving chemotherapy treatment with pre-existing diabetes are at an increased risk of developing glycemic issues in accordance with an increased risk of death<sup>199</sup>. I suggest that the mechanism of decreased glucose uptake following administration of chemotherapy drugs in myotubes may be a result of decreased phosphorylation of AKT, but may also be partly due to a decrease in muscle protein status.

The present report does not come without study limitations that should be addressed. Although protein concentrations do not differ significantly, L6 myotubes often struggle to continually differentiate past 7 days. This provides a limited period of time to measure proteins and markers of interest. Nonetheless, we were still able to measure proteins and markers of interest on day 5, 6 and 7. Another possible limitation is the fact that the chemotherapy drugs and their effects were not studied individually and the singular effects of these drugs on myotube morphology and protein metabolism cannot be elucidated at this time. Whereas others have studied the effects of singular drugs<sup>156, 179</sup>, the goal of my study was to investigate the combined effects of chemotherapy drugs in myotubes. In addition, due to the fact that total protein levels for AKT, S6K1 and S6 were not investigated, it is a possibility that the observed decreases in the phosphorylation of these signals is due to a decrease in total protein content. Further, due to the

decreases in  $\gamma$ -tubulin following drug treatment on day 6 and 7, findings from this study could be attributed to the effect of the chemotherapy drug cocktail on cell death. Although this effect of cell death may be true, all findings were normalized to their respective  $\gamma$ -tubulin values. In addition, significant decreases were still found for troponin, tropomyosin and p-S6K1 by day 5 of differentiation, when  $\gamma$ -tubulin values did not differ between treatments. In regards to our cachexia model, using an in-vitro approach does not allow for elucidation of how these chemotherapy drugs effect mammalian body systems. In addition, our chemotherapy-induced cachexia model may underlie cachexia severity, as cachexia development is often caused by multiple factors such as tumour burden, malnutrition and muscle disuse. Nonetheless, our in-vitro model allows for the investigation of specific mechanisms underlying chemotherapy-induced cachexia progression and development in isolated conditions.

Nonetheless, data from this study finds evidence of chemotherapy related effects on myofibrillar protein abundance, anabolic signalling, protein synthesis, mitochondrial content and glucose metabolism. Findings shed light on a possible mechanism of chemotherapy-driven cachexia development and progression. Interventions aimed at the maintenance of muscle mass during chemotherapy treatment may increase body weight, associated with increases in treatment efficacy, quality of life and chance of survival.

## Chapter Nine: Future Research

Future investigations should include:

- 1) Since we explored and found decreases in anabolic signaling (mTORC1) and protein synthesis ( $^{35}\text{S}$  methionine incorporation), future studies should investigate markers and pathways of protein degradation in myotubes treated with the chemotherapy drug cocktail. Experiments investigating protein content (western blotting) and mRNA expression (RT-PCR) of autophagy (ULK-1, LC3B I/II, Beclin-1) and muscle atrophy (MuRF-1, MAFbx) related markers should be conducted in myotubes treated with the chemotherapy drug cocktail.
- 2) Due to the fact that we used  $^{35}\text{S}$  methionine (an amino acid) to measure protein synthesis in myotubes, future studies should confirm these results by investigating amino acid uptake and transport in myotubes treated with the chemotherapy drug cocktail. These experiments could be conducted by using high pressure liquid chromatography to measure both the transport and concentration of amino acids in myotubes treated with the chemotherapy drug cocktail.
- 3) In accordance with seeing a decrease in mitochondrial proteins (SDHA, COXIV), future studies should also measure mitochondrial activity in myotubes treated with the chemotherapy drug cocktail. Since disruptions in mitochondria activity are associated with increases in ROS<sup>262</sup> and ROS is a factor regulating cachexia<sup>93</sup>, investigating mitochondrial activity will help to determine whether myotubes treated with the chemotherapy drug cocktail are affected by ROS.
- 4) Investigate mechanisms of chemotherapy-induced cachexia in an in-vivo model. By investigating similar mechanisms of our in-vitro study within an animal model,

findings could elucidate the mechanisms of chemotherapy-induced cachexia in mammalian body systems. Using an animal model also allows the investigation of chemotherapy-induced cachexia on age and gender.

## References

1. Frontera WR et al. 2015. Skeletal Muscle: a brief review of structure and function. *Calcified Tissue International* 96 (3): 183-195.
2. Buczkowska E et al. 2003. The role of skeletal muscle in the regulation of glucose homeostasis. *Endokrynol Diabetol Chor Przemiany Materii Wieku Rozw* 9: 93-97.
3. Stump CS et al. 2006. The metabolic syndrome: role of skeletal muscle metabolism. *Annals of Medicine* 38: 389-402.
4. Atherton P et al. 2016. Control of Skeletal Muscle Atrophy in Response to Disuse: Clinical/Preclinical Contentions and Fallacies of Evidence. *American Journal of Physiology Endocrinol Metab* 311(3): E594-604.
5. Phillips S et al. 2016. Protein requirements beyond the RDA: implications for optimizing health. *Applied Physiology, Nutrition and Metabolism* 41 (5): 565-572.
6. Burd NA et al. 1985. Exercise training and protein metabolism: influences of contraction, protein intake and sex based differences. *Journal of Applied Physiology* 106 (5): 1692-1701.
7. Churchward-Venne TA et al. 2012. Nutritional regulation of muscle protein synthesis with resistance exercise: strategies to enhance anabolism. *Nutritional Metabolism* 9: 1-8.
8. Dreyer HC et al. 2006. Resistance exercise increases AMPK activity and reduces 4E-BP1 phosphorylation and protein synthesis in human skeletal muscle. *Journal of Physiology* 576: 613-624.
9. MacDougall et al. 1995. The Time Course for Elevated Muscle Protein Synthesis Following Heavy Resistance Exercise. *Canadian Journal of Applied Physiology* 20 (4): 480-486.
10. Phillips et al. 1997. Mixed muscle protein synthesis and breakdown after resistance exercise in humans. *American Journal Physiology* 273: 99-107.
11. Moore et al. 2009. Ingested protein dose response of muscle and albumin protein synthesis after resistance exercise in young men. *American Journal of Clinical Nutrition* 89 (1): 161-168.
12. Areta et al. 2013. Timing and distribution of protein ingestion during prolonged recovery from resistance exercise alters myofibrillar protein synthesis. *Journal of Physiology* 591(9): 2319-2331.
13. Macnaughton LS et al. 2016. The response of muscle protein synthesis following whole-body resistance exercise is greater following 40 g than 20 g of ingested whey protein. *Physiology Representative* 15.
14. Syed S et al. 2015. Intake of low-dose leucine-rich essential amino acid stimulates muscle anabolism equivalently to bolus whey protein in older women at rest and after exercise. *American Journal Endocrinology Metabolism* 308: 1056-1065.
15. West D et al. 2011. Rapid aminoacidemia enhances myofibrillar protein synthesis and anabolic intramuscular signaling responses after resistance exercise. *American Journal of Clinical Nutrition* 94: 795-803.

16. Witard OC et al. 2014. Myofibrillar muscle protein synthesis rates subsequent to a meal in response to increasing doses of whey protein at rest and after resistance exercise. *American Journal of Clinical Nutrition* 99 (1): 86-95.
17. Phillips SM et al. 2008. Insulin and muscle protein turnover in humans: stimulatory, permissive, inhibitory, or all of the above? *Am J Physiol Endocrinol Metab* 295: E731.
18. Fujita S et al. 2006. Effect of insulin on human skeletal muscle protein synthesis is modulated by insulin-induced changes in muscle blood flow and amino acid availability. *Am J Physiol Endocrinol Metab* 291 (4): E745-E754.
19. Gelfand RA et al. 1987. Effect of physiologic hyperinsulinemia on skeletal muscle protein synthesis and breakdown in man. *J Clin Invest* 80: 1-6.
20. Everman S et al. 2016. Insulin does not stimulate muscle protein synthesis during increased plasma branched-chain amino acids alone but still decreases whole body proteolysis in humans. *Am J Physiol Endocrinol Metab* 311 (4): E671-E677.
21. Griggs RC et al. 1989. Effect of testosterone on muscle mass and muscle protein synthesis. *J Appl Physiol* 66(1): 498-503.
22. Srinivas S et al. 2010. Effects of Testosterone on Muscle Strength, Physical Function, Body Composition, and Quality of Life in Intermediate-Frail and Frail Elderly Men: A Randomized, Double-Blind, Placebo-Controlled Study. *The Journal of Clinical Endocrinology & Metabolism* 95: 639-650.
23. Brodsky ID et al. 1996. Effects of testosterone replacement on muscle mass and muscle protein synthesis in hypogonadal men--a clinical research center study. *J Clin Endocrinol Metab* 81(10): 3469-75.
24. Bengtsson B et al. 2000. The Treatment of Growth Hormone Deficiency in Adults. *J Clin Endocrinol Metab* 85(3): 933-937.
25. Gostelli P et al. 1994. Expression and regulation of insulin like growth factor I (IGF-I) and IGF binding protein messenger ribonucleic acid levels in tissues of hypophysectomized rats infused with IGF-I and growth hormone. *Endocrinology* 135:2558-2567.
26. Velloso C et al. 2008. Regulation of muscle mass by growth hormone and IGF-I. *B J Pharmacol* 154(3): 557-568.
27. Yuan L et al. 2015. Muscle-specific E3 ubiquitin ligases are involved in muscle atrophy of cancer cachexia: an in vitro and in vivo study. *Oncol Rep* 33(5):2261-8.
28. Schiaffino S et al. 2011. Regulation of skeletal muscle growth by the IGF1-Akt/PKB pathway: insights from genetic models. *Skeletal Muscle* 1: 4.
29. Manning BD et al. 2007. AKT/PKB signaling: navigating downstream. *Cell* 129: 1261-1274.
30. Dibble CC et al. 2013. Signal integration by mTORC1 coordinates nutrient input with biosynthetic output. *Nat Cell Biol* 15:555-564.
31. Garami A et al. 2003. Insulin activation of Rheb, a mediator of mTOR/S6K/4E-BP signaling, is inhibited by TSC1 and 2. *Mol Cell* 11(6): 1457-66.
32. Inoki K et al. 2002. TSC2 is phosphorylated and inhibited by Akt and suppresses mTOR signaling. *Nat Cell Biol* 4 (9): 648-57.

33. Manning, BD et al. 2002. Identification of the tuberous sclerosis complex-2 tumor suppressor gene product tuberin as a target of the phosphoinositide 3-kinase/akt pathway. *Mol Cell* 10 (1): 151-62.
34. Burd NA et al. Resistance exercise volume affects myofibrillar protein synthesis and anabolic signaling molecule phosphorylation in young men. *J Physiol* 588 (16): 3119-3130.
35. Marabita M et al. 2016. S6K1 is required for increasing skeletal muscle force during hypertrophy. *Cell Rep* 17 (2): 501-513
36. Dyachok A et al. 2016. Amino Acids Regulate mTORC1 by an Obligate Two-step Mechanism. *J Bio Chem* 291: 22414-22426.
37. Laplante M et al. 2013. Regulation of mTORC1 and its impact on gene expression at a glance. *J Cell Sci* 126:1713-9.
38. Walsh DW et al. 2010. Extracellular BMP-antagonist regulation in development and disease: tied up in knots. *Trends Cell Biol* 20: 244-256.
39. Miyazono K et al. 2002. Id: a target of BMP signaling. *Sci STKE* pe40.
40. Sartori R et al. 2013. BMP signaling controls muscle mass. *Nat Gen* 45: 1309-1318.
41. Winbanks C et al. 2013. The bone morphogenetic protein axis is a positive regulator of skeletal muscle mass. *J Cell Biol* 203 (2): 345-357.
42. Xue QL et al. 2011. Prediction of risk of falling, physical disability, and frailty by rate of decline in grip strength: the women's health and aging study. *Arch Intern Med* 171: 1119-1121.
43. Milanovic Z et al. 2013. Age-related decrease in physical activity and functional fitness among elderly men and women. *Clin Interv Aging* 8: 549-556.
44. Robinson S et al. 2012. Nutrition and sarcopenia: a review of the evidence and implications for preventive strategies. *J Aging Res* 2012:510801.
45. Bradlee M et al. 2017. High-Protein Foods and Physical Activity Protect Against Age-Related Muscle Loss and Functional Decline. *The Journals of Gerontology. Series A, Biological Sciences and Medical Sciences* 0 (0), 1-7.
46. Nilwik R et al. 2013. The decline in skeletal muscle mass with aging is mainly attributed to a reduction in type II muscle fiber size. *Exp Gerontol* 48 (5): 492-498.
47. Verdiik LB et al. 2012. Reduced satellite cell numbers with spinal cord injury and aging in humans. *Med Sci Sports Exerc* Epub ahead of print.
48. Conley KE et al. 2000. Oxidative capacity and ageing in human muscle. *J Physiol* 1:526.
49. Sakuma K et al. 2012. Sarcopenia and age-related endocrine function. *Int J Endocrinol* 2012:127362.
50. Wall B et al. 2013. Disuse impairs the muscle protein synthetic response to protein ingestion in healthy men. *J Clin Endocrinol Metab* 2089.
51. Boer de et al. 2007. The temporal responses of protein synthesis, gene expression and cell signaling in human quadriceps muscle and patellar tendon to disuse. *J Physiol* 585:241-251.
52. Krawiec BJ et al. 2005. Hindlimb casting decreases muscle mass in part by proteasome-dependent proteolysis but independent of protein synthesis. *Am J Physiol Endocrinol Metab* 289: E969-E980.

53. Katz et al. 1962. Diseases of the heart in the works of Hippocrates. *Br Heart J* 24: 257-264.
54. Aoyagi et al. 2015. Cancer cachexia, mechanism and treatment. *World J Gastrointest Oncol* 7 (4): 17-29.
55. Evans WJ et al. Cachexia: a new definition. *Clin Nutr* 27: 793-799.
56. Yoshida T et al. 2015. Mechanisms of Cachexia in Chronic Diseased States. *Am J Med Sci* 350 (4): 250-256.
57. Fearon K et al. 2011. Definition and classification of cancer cachexia: an international consensus. *Lancet Oncol* 12(5): 489-495.
58. Tan B et al. 2009. Sarcopenia in an overweight or obese patient is an adverse prognostic factor in pancreatic cancer. *Clin Cancer Res* 15 (22): 6973-6979.
59. Ross PJ et al. 2004. Do patients with weight loss have a worse outcome when undergoing chemotherapy for lung cancers? *Br J Cancer* 90 (10): 1905-1911.
60. Teunissen SCCM et al. 2007. Symptom prevalence in patients with incurable cancer: a systematic review. *J Pain Symptom Manag* 34 (1): 94-104.
61. Strasser F et al. 2006. The silent symptom early satiety: a forerunner of distinct phenotypes of anorexia/cachexia syndromes. *Support Care Canc* 14 (7): 869-692.
62. Ovesen L et al. 1993. Effect of dietary counseling on food intake, body weight, response rate, survival, and quality of life in cancer patients undergoing chemotherapy: a prospective, randomized study. *J Clin Oncol* 11 (10): 2043-2049.
63. Evans WK et al. 1987. A randomized study of oral nutritional support versus ad lib nutritional intake during chemotherapy for advanced colorectal and non-small-cell lung cancer. *J Clin Oncol* 5 (1): 113-124.
64. Balstad TR et al. 2014. Dietary treatment of weight loss in patients with advanced cancer and cachexia: a systematic literature review. *Crit Rev Oncol Hematol* 91: 210-221.
65. Ahlberg K et al. 2003. Assessment and management of cancer-related fatigue in adults. Review. *Lancet* 362: 640-650.
66. Stewart G et al. 2006. Cancer cachexia and fatigue. *Clin Med* 6: 140-3.
67. Takayama K et al. 2016. Quality of life and survival survey of cancer cachexia in advanced non-small cell lung cancer patients—Japan nutrition and QOL survey in patients with advanced non-small cell lung cancer study. *Sup Care Cancer* 24: 3473-3480.
68. Von Haehling S et al. 2010. Cachexia as a major underestimated and unmet medical need: facts and numbers. *J Cachexia Sarcopenia Muscle* 1: 1-5.
69. Fearon KC et al. 2006. Definition of cancer cachexia: effect of weight loss, reduced food intake, and systemic inflammation on functional status and prognosis. *Am J Clin Nutr* 83 (6): 1345-50.
70. Fouladiun M et al. 2007. Daily physical-rest activities in relation to nutritional state, metabolism, and quality of life in cancer patients with progressive cachexia. *Clin Cancer Res* 13 (21): 6379-6385.
71. Illman J et al. 2005. Are inflammatory cytokines the common link between cancer-associated cachexia and depression? *J Support Oncol* 3 (1): 37-50.

72. Chochinov HM et al. 2001. Depression in cancer patients. *Lancet Oncol* 2 (8): 499-505.
73. McClement S et al. 2005. Cancer anorexia–cachexia syndrome: psychological effect on the patient and family. *J Wound Ostomy Continence Nurs* 32 (4): 264-268.
74. McClement SE et al. 2004. Family responses to declining intake and weight loss in a terminally ill relative. Part 1: fighting back. *J Palliat Care* 20 (2): 93-100.
75. Barber MD et al. 2001. Cancer cachexia and its treatment with fish-oil-enriched nutritional supplementation. *Nutrition* (9): 751-755.
76. Tijerina AJ et al. 2004. The biochemical bases of metabolism in cancer cachexia. *Dimens Crit Care Nurs* 23 (6): 237-243.
77. Banks WA et al. Anorectic effects of circulating cytokines: role of the vascular blood-brain barrier. *Nutrition* 17: 434-437.
78. Li YP et al. 2005. TNF-alpha acts via p38 MAPK to stimulate expression of the ubiquitin ligase atrogin1/MAFbx in skeletal muscle. *FASEB J* 19 (3): 362-70.
79. Goossens V et al. 1995. Direct evidence for tumor necrosis factor-induced mitochondrial reactive oxygen intermediates and their involvement in cytotoxicity. *Proc Natl Acad Sci* 92: 8115-8119.
80. Garg AK et al. 2002. Reactive oxygen intermediates in TNF signaling. *Mol Immunol* 39: 509-517.
81. Llovera M et al. 1998. Role of TNF receptor 1 in protein turnover during cancer cachexia using gene knockout mice. *Mol Cell Endo* 142 (1-2): 183-9.
82. Tisdale MJ et al. 1997. Biology of cachexia. *J Natl Canc Inst* 89 (23): 1763-1773.
83. Dunn AJ. 1988. Systemic interleukin-1 administration stimulates hypothalamic norepinephrine metabolism paralleling the increased plasma corticosterone. *Life Sci* 43 (5): 429-435.
84. Blundell J et al. 1998. Serotonin and Appetite Regulation: Implications for the Pharmacological Treatment of Obesity. *CNS Drugs* 9: 473-495.
85. Strassmann G et al. 1992. Evidence for the involvement of interleukin 6 in experimental cancer cachexia. *J Clin Invest Am Soc Clin Invest* 89 (5): 1681-1684.
86. Moses AGW et al. 2009. Pro-inflammatory cytokine release by peripheral blood mononuclear cells from patients with advanced pancreatic cancer: relationship to acute phase response and survival. *Oncol Rep* 21 (4): 1091-5.
87. Maltoni M et al. 1997. Serum levels of tumour necrosis factor alpha and other cytokines do not correlate with weight loss and anorexia in cancer patients. *Supp Care Canc* 5 (2): 130-5.
88. Barber MD et al. 2001. Effect of a fish oil-enriched nutritional supplement on metabolic mediators in patients with pancreatic cancer cachexia. *Nutr Canc* 40 (2): 118-124.
89. Mittler R et al. 2017. ROS are good. *Cell Press* 22.
90. Bandyopadhyay U et al. 1999. Reactive oxygen species: oxidative damage and pathogenesis. *Curr Sci* 77 (5): 658-666.
91. Barzilai A et al. 2004. DNA damage responses to oxidative stress. *DNA Repair* 3 (8-9): 1109-15.

92. Arthur PG et al. 2008. Oxidative stress as a therapeutic target during muscle wasting: considering the complex interactions. *Curr Opin Clin Nutr Metab Care* 11 (4): 408-416.
93. Russell S.T et al. 2007. Role of reactive oxygen species in protein degradation in murine myotubes induced by proteolysis-inducing factor and angiotensin II. *Cellular Signalling* 19: 1797-1806.
94. Sullivan-Gunn MJ et al. 2011. Decreased NADPH oxidase expression and antioxidant activity in cachectic skeletal muscle. *J Cachexia Sarc Muscle* 2 (3): 181-188.
95. Rubin H. 2003. Cancer cachexia: its correlations and causes. *Proc Natl Acad Sci USA* 100 (9): 5384-9.
96. Barreiro E et al. 2005. Both oxidative and nitrosative stress are associated with muscle wasting in tumour-bearing rats. *FEBS Lett* 579 (7): 1646-52.
97. Morley JE et al. 2006. Cachexia: pathophysiology and clinical relevance. *Am J Clin Nutr* 83 (4): 735-43.
98. Cattadori G et al. 2018. Exercise and heart failure. *ESC Heart Fail* 5: 222-232.
99. Suzuki T et al. Skeletal muscle wasting in chronic heart failure. *ESC Heart Fail* 5 (6): 1099-1107.
100. Ponikowski P et al. 2016. ESC guidelines for the diagnosis and treatment of acute and chronic heart failure: The Task Force for the diagnosis and treatment of acute and chronic heart failure of the European Society of Cardiology (ESC) Developed with the special contribution of the Heart Failure Association (HFA) of the ESC. *Eur Heart J* 37 (27): 2129-2200.
101. Anker SD et al. 1997. Wasting as independent risk factor for mortality in chronic heart failure. *Lancet* 349:1050-1053.
102. Anker SD et al. 2002. The syndrome of cardiac cachexia. *Int J Cardiol* 85 (1): 51-66.
103. Arambula- Garza E et al. 2016. Association of cardiac cachexia and atrial fibrillation in heart failure patients. *Int J Cardiol* 223:863-866.
104. Fraser SD et al. 2016. Chronic kidney disease: identification and management in primary care. *Pragmat Obs Res* 7: 21-32.
105. Fraser SD et al. 2015. The burden of comorbidity in people with chronic kidney disease stage 3: a cohort study. *BMC Nephrol* 16: 193.
106. Kalantar-Zadeh K et al. 2003. Malnutrition–inflammation complex syndrome in dialysis patients: causes and consequence. *Am J Kidney Dis* 42: 864-881.
107. Cheung WW et al. 2005. Role of leptin and melanocortin signaling in uremia-associated cachexia. *J Clin Invest* 115:1659-65.
108. Mak RH et al. 2006. Leptin and inflammation-associated cachexia in chronic kidney disease. *Kidney Int* 69: 794-797.
109. Cheung WW et al. 2010. Ghrelin in chronic kidney disease. *Int J Pept pii*: 567343.
110. Cheung WW et al. 2010. Inflammation and cachexia in chronic kidney disease. *Pediatr Nephrol* 25: 711-724.
111. Mitch WE. 2006. Proteolytic mechanisms, not malnutrition, cause loss of muscle mass in kidney failure. *J Ren Nutr* 16: 208-211.
112. Xiaomei M et al. 2006. Global burden of cancer. *Yale J Bio Med* 79 (3-4): 85-94.

113. Melstrom LG et al. 2007. Mechanisms of skeletal muscle degradation and its therapy in cancer cachexia. *Histol Histopathol* 22: 805-814.
114. Baracos VE et al. 2018. Cancer-associated cachexia. *Nat Rev Dis Primers* 4: 17105.
115. Dewys WD et al. 1980. Prognostic effect of weight loss prior to chemotherapy in cancer patients. Eastern Cooperative Oncology Group. *Am J Med* 69: 491-497.
116. Deans C et al. 2005. Systemic inflammation, cachexia and prognosis in patients with cancer. *Curr Opin Clin Nutr Metab Care* 8: 265-269.
117. Argiles JM et al. 2009. The role of cytokines in cancer cachexia. *Curr Opin Supp Palliat Care* 3: 263-268.
118. Dworzak F et al. 1998. Effects of cachexia due to cancer on whole body and skeletal muscle protein turnover. *Cancer* 82: 42-48.
119. Acharyya S et al. 2004. Cancer cachexia is regulated by selective targeting of skeletal muscle gene products. *J Clin Invest* 114: 370-378.
120. Fredrix EW et al. 1991. Effect of different tumor types on resting energy expenditure. *Cancer Res* 51: 6138-6141.
121. Falconer JS et al. 1994. Cytokines, the acute-phase response, and resting energy expenditure in cachectic patients with pancreatic cancer. *Ann Surg* 219: 325-331.
122. Shellock FG et al. 1986. Brown adipose tissue in cancer patients: possible cause of cancer-induced cachexia. *J Cancer Res Clin Oncol* 111: 82-85.
123. Wang J et al. 2018. Tumor-infiltrating neutrophils predict prognosis and adjuvant chemotherapeutic benefit in patients with biliary cancer. *Cancer Sci* 109 (7): 2266-2274.
124. Desoize B et al. 2002. Particular aspects of platinum compounds used at present in cancer treatment. *Crit Rev Oncol Hematol* 42: 317-325.
125. Alfarouk K et al. 2015. Resistance to cancer chemotherapy: failure in drug response from ADME to P-gp. *Cancer Cell Int* 15:71.
126. Loadman PM et al. 1994. Pharmacokinetic drug interactions with anticancer drugs. *Clin Pharmacokinet* 26: 486-500.
127. Mihich E et al. 1977. Multiple basis of combination chemotherapy. *Cancer* 40: 534-43.
128. Chen D et al. 2009. Metal complexes, their cellular targets and potential for cancer therapy. *Curr Pharm Des* 15: 777-791.
129. Kelland L et al. 2007. The resurgence of platinum-based cancer chemotherapy. *Nat Rev Cancer* 7: 573-584.
130. Eljack ND et al. 2014. Mechanisms of cell uptake and toxicity of the anticancer drug cisplatin. *Metallomics* 6 (11): 2126-33.
131. Pinto AL et al. 1985. Binding of the antitumor drug cis-diamminedichloroplatinum (II) (cisplatin) to DNA. *Biochim Biophys Acta* 780 (3): 167-80.
132. Siddik Z. 2003. Cisplatin: mode of cytotoxic action and molecular bases of resistance. *Oncogene* 22, 7265-7279.
133. Tsang R et al. 2009. Cisplatin overdose: toxicities and management. *Drug Saf* 32 (12): 1109-1122.
134. Schiller JH et al. 1989. Inadvertent administration of 480mg/m<sup>2</sup> of cisplatin. *Am J Med* 86 (5): 624-5.

135. Reed E. 1998. Platinum-DNA adduct, nucleotide excision repair and platinum based anti-cancer chemotherapy. *Cancer Treat Rev* 24: 331-344.
136. Kohno K et al. 2005. Transcription factors and drug resistance. *Eur J Cancer* 41: 2577-2586.
137. Liang XJ et al. 2008. SIRT1 contributes in part to cisplatin resistance in cancer cells by altering mitochondrial metabolism. *Mol Cancer Res* 6: 1499-1506.
138. Johnson SW et al. 1996. Cross resistance, cisplatin accumulation, and platinum-DNA adduct formation and removal in cisplatin-sensitive and -resistant human hepatoma cell lines. *Exp Cell Res* 226: 133-139.
139. Shen D et al. 1998. Cross-resistance to methotrexate and metals in human cisplatin-resistant cell lines results from a pleiotropic defect in accumulation of these compounds associated with reduced plasma membrane binding proteins. *Cancer Res* 58: 268-275.
140. Hall MD et al. 2008. The role of cellular accumulation in determining sensitivity to platinum-based chemotherapy. *Annu Rev Pharmacol Toxicol* 48: 495-535.
141. Shen D et al. 2012. Cisplatin Resistance: A Cellular Self-Defense Mechanism Resulting from Multiple Epigenetic and Genetic Changes. *Pharmacol Rev* 64: 706-721.
142. Heidelberger C et al. 1957. Fluorinated pyrimidines: a new class of tumor-inhibitory compounds. *Nature* 179: 663-666.
143. Lokich J et al. 1998. Infusional 5-FU: historical evolution, rationale, and clinical experience. *Oncology* 12: 19-22.
144. Grem J. 1996. 5-Fluoropyrimidines, in Chabner BA, Longo DL (eds): *Cancer Chemotherapy and Biotherapy Principles and Practice*. Ed 2: pp 149-211.
145. Domin BA et al. 1993. Transport of 5-fluorouracil and uracil into human erythrocytes. *Biochem Pharmacol* 146: 503-510.
146. Rose MG et al. 2002. Thymidylate synthase: a critical target for cancer chemotherapy. *Clin Colorectal Cancer* 1 (4): 220-9.
147. Sobrero AF et al. 1997. Fluorouracil in colorectal cancer-a tale of two drugs: implications for biochemical modulation. *J Clin Oncol* 15: 368-381.
148. Chu E et al. 1990. Resistance of a human ovarian cancer line to 5-fluorouracil associated with decreased levels of 5-fluorouracil in DNA. *Mol Pharmacol* 138: 410-417.
149. Berger SH et al. 1985. Thymidylate synthase overproduction and gene amplification in fluoride-oxyuridine-resistant human cells. *Mol Pharmacol* 28: 461-467.
150. Chu E et al. Autoregulation of human thymidylate synthase messenger RNA translation by thymidylate synthase. *Proc Natl Acad Sci USA* 88: 8977-8981.
151. Barbour KW et al. 1990. Single amino acid substitution defines a naturally occurring genetic variant of human thymidylate synthase. *Mol Pharmacol* 37: 515-518.
152. Grem J et al. 1997. Mechanisms of Action and Modulation of Fluorouracil. *Semin Rad Oncol* 7: 249-259.
153. Baek J et al. 2006. Unpredicted Severe Toxicity after 5-Fluorouracil Treatment due to Dihydropyrimidine Dehydrogenase Deficiency. *Korean J Intern Med* 21 (1): 43-45.

154. Focaccetti C et al. 2015. Effects of 5-Fluorouracil on Morphology, Cell Cycle, Proliferation, Apoptosis, Autophagy and ROS Production in Endothelial Cells and Cardiomyocytes. *PLOS one* 10 (2).
155. Borrás E et al. 2012. High-resolution melting analysis of the common c.1905+1G>A mutation causing Dihydropyrimidine dehydrogenase deficiency and lethal 5-fluorouracil toxicity. *Frontiers in Gen* 3: 312-312.
156. Sotos GA et al. Preclinical and clinical aspects of biomodulation of 5-fluorouracil. *Cancer Treat Rev* 20: 11-49.
157. Buyse M et al. 2000. Relation between tumour response to first-line chemotherapy and survival in advanced colorectal cancer: a meta-analysis. Meta-Analysis Group in Cancer. *Lancet* 356: 373-378.
158. Sakai H et al. 2014. Mechanisms of cisplatin-induced muscle atrophy. *Toxic Appl Pharma* 278: 190-199.
159. Caj D et al. 2004. IKKbeta/NF-kappaB activation causes severe muscle wasting in mice. *Cell* 199: 285-98.
160. Barreto R et al. 2016. Chemotherapy-related cachexia is associated with mitochondrial depletion and the activation of ERK1/2 and p38 MAPKs. *Oncotarget* 7: 28.
161. Collins G et al. 2017. The Logic of the 26S Proteasome. *Cell* 169.
162. Giordano A et al. Skeletal muscle metabolism in physiology and in cancer disease. *J Cell Biochem* 90 (1): 170-186.
163. Bodine SC et al. 2001. Identification of ubiquitin ligases required for skeletal muscle atrophy. *Science* 294: 1704-1708.
164. Khal J et al. 2005. Expression of the ubiquitin–proteasome pathway and muscle loss in experimental cancer cachexia. *Br J Cancer* 93 (7): 774-780.
165. Khal J et al. 2005. Increased expression of proteasome subunits in skeletal muscle of cancer patients with weight loss. *Int J Biochem Cell Biol* 37 (10): 2196-2206.
166. Gomes MD et al. 2001. Atrogin-1, a muscle-specific F-box protein highly expressed during muscle atrophy. *Proc Natl Acad Sci USA* 98: 14440-14445.
167. Lecker SH et al. 2004. Multiple types of skeletal muscle atrophy involve a common program of changes in gene expression. *FASEB J* 18: 39-51.
168. Senf SM et al. 2010. FOXO signaling is required for disuse muscle atrophy and is directly regulated by Hsp70. *Am J Physiol Cell Physiol* 298: C38-C45.
169. Satchek JM et al. 2007. Rapid disuse and denervation atrophy involve transcriptional changes similar to those of muscle wasting during systemic diseases. *FASEB J* 21: 140-155.
170. Sandri M et al. 2004. Foxo transcription factors induce the atrophy-related ubiquitin ligase atrogin-1 and cause skeletal muscle atrophy. *Cell* 117: 399-412.
171. Stitt TN et al. 2004. The IGF-1/PI3K/Akt pathway prevents expression of muscle atrophy-induced ubiquitin ligases by inhibiting FOXO transcription factors. *Mol Cell* 14: 395-403.
172. Reed SA et al. 2012. Inhibition of FoxO transcriptional activity prevents muscle fiber atrophy during cachexia and induces hypertrophy. *FASEB J* 26: 987-1000.

173. Chen J et al. 2013. Regulation of NF- $\kappa$ B by Ubiquitination. *Curr Opin Immunol* 25 (1): 4-12.
174. Vaughan V et al. 2013. Cancer cachexia: impact, mechanisms and emerging treatments. *J Cach Sarc Musc* 4 (2): 95-109.
175. Cornwell E et al. 2011. The role of NF- $\kappa$ B in cancer cachexia-induced skeletal muscle wasting. *FASEB J*.
176. Russell ST et al. 2007. Role of reactive oxygen species in protein degradation in murine myotubes induced by proteolysis inducing factor and angiotensin II. *Cell Signal* 19: 1797-1806.
177. Zimmers TA et al. 2002. Induction of cachexia in mice by systemically administered myostatin. *Science* 296: 1486-1488.
178. McFarlane C et al. 2006. Myostatin induces cachexia by activating the ubiquitin proteolytic system through an NF $\kappa$ B independent Foxo1-dependent mechanism. *J Cell Physiol* 209: 510-514.
179. Damrauer JS et al. 2008. Chemotherapy-induced muscle wasting: association with NF- $\kappa$ B and cancer cachexia. *Basic Appl Myol* 18: 139-148.
180. Gilliam LA et al. 2011. Chemotherapy-induced weakness and fatigue in skeletal muscle: the role of oxidative stress. *Antioxid Redox Signal* 15: 2543-2563.
181. Antoun S et al. 2010. Low body mass index and sarcopenia associated with dose limiting toxicity of sorafenib in patients with renal cell carcinoma. *Ann Oncol* 21: 1594-1598.
182. Jung HW et al. 2015. Effect of muscle mass on toxicity and survival in patients with colon cancer undergoing adjuvant chemotherapy. *Suppor Care Cancer* 23:687-694.
183. Thoresen et al. 2013. Nutritional status, cachexia and survival in patients with advanced colorectal carcinoma. Different assessment criteria for nutritional status provide unequal results. *Clin Nutr* 32 (1): 65-72.
184. Ozola Zalite I et al. 2015. Influence of cachexia and sarcopenia on survival in pancreatic ductal adenocarcinoma: a systematic review. *Pancreatology* 15 (1): 19-24.
185. Bodine SC et al. 2001. Akt/mTOR pathway is a crucial regulator of skeletal muscle hypertrophy and can prevent muscle atrophy in vivo. *Nat Cell Biol* 3 (11): 1009-1013.
186. Sandri M et al. 2013. Protein breakdown in muscle wasting: role of autophagy-lysosome and ubiquitin proteasome. *Int J Biochem Cell Biol* 45 (10): 2121-2129.
187. Kachur T et al. 2008. Myosin Assembly, Maintenance and Degradation in Muscle: Role of the Chaperone UNC-45 in Myosin Thick Filament Dynamics. *Int J Mol Sci* 9 (9): 1863-1875.
188. Zhang W et al. 2012. Evidence of mTOR Activation by an AKT-Independent Mechanism Provides Support for the Combined Treatment of PTEN-Deficient Prostate Tumors with mTOR and AKT Inhibitors. *Trans Oncol* 5 (6): 422-429.
189. MacDonald E et al. 2014. Denervation atrophy is independent from Akt and mTOR activation and is not rescued by myostatin inhibition. *Dis Model Mech* 7(4): 471-481.

190. Fabris S et al. 2018. Doxorubicin chemotherapy affects the intracellular and interstitial free amino acids pools in skeletal muscle. *PLOS ONE* 13 (4): e0195330.
191. Nissinen T et al. 2016. Systemic blockade of ACVR2B ligands prevents chemotherapy-induced muscle wasting by restoring muscle protein synthesis without affecting oxidative capacity or atrogenes. *Scientific Reports* 6.
192. Chen Q et al. 2003. Production of Reactive Oxygen Species by Mitochondria. *J Biol Chem* 38: 36027-36031.
193. Cheng M et al. 1989. Mitochondrial heat shock protein hsp60 is essential for assembly of proteins imported into yeast mitochondria. *Nature* 337: 620-625.
194. Roques M et al. 1999. A phosphatidylinositol 3-Kinase/p70 ribosomal S6 protein kinase pathway is required for the regulation by insulin of the p85alpha regulatory subunit of phosphatidylinositol 3-kinase gene expression in human muscle cells. *J Biol Chem* 274 (48): 34005-10.
195. Franke TF et al. 1995. The protein kinase encoded by the Akt proto-oncogene is a target of the PDGF-activated phosphatidylinositol 3-kinase. *Cell* 81 (5): 727-36.
196. Thong FS et al. 2007. The Rab GTPase-activating protein AS160 integrates Akt, protein kinase C, and AMP-activated protein kinase signals regulating GLUT4 traffic. *Diabetes* 56 (2): 414-23.
197. Salo DC et al. 1991. HSP70 and other possible heat shock or oxidative stress proteins are induced in skeletal muscle, heart, and liver during exercise. *Free Rad Biol Med* 11: 239-46.
198. Liu Y et al. 2001. Changes in skeletal muscle heat shock proteins: pathological significance. *Front Bio Sci* 6: D12-25.
199. Barone B et al. 2008. Long-term All-Cause Mortality in Cancer Patients With Preexisting Diabetes Mellitus. *JAMA* 300 (23): 2754-2764.
200. Prado CMM et al. 2007. Body composition as an independent determinant of 5-fluorouracil-based chemotherapy toxicity. *Clin Cancer Res* 13 (11): 3264-3268.
201. DeWys WD et al. 1980. Prognostic effect of weight loss prior to chemotherapy in cancer patients. *Am J Med* 69 (4): 491-497.
202. Doren BA et al. 2016. Cachexia Significantly Increases The Risk of Major Peri-Operative Complications and In-Hospital Mortality in Total Joint Replacement Patients: Results of a Matched Cohort Study. *Value in Health* 19.
203. Mason MC et al. 2016. Preoperative cancer cachexia and short-term outcomes following surgery. *J Surg Res* 205 (2): 398-406.
204. Fearon KCH et al. 2008. Cancer cachexia: developing multimodal therapy for a multidimensional problem. *Eur J Cancer* 44 (8): 1124-1132.
205. Elmore S. 2007. Apoptosis: A Review of Programmed Cell Death. *Toxicol Pharma* 35 (4): 495-516.
206. Fanzani A et al. 2012. Molecular and cellular mechanisms of skeletal muscle atrophy: an update. *J Cachexia Sarcopenia Muscle* 3 (3): 163-179.
207. Dirks A et al. 2002. Apoptosis in skeletal muscle with aging. *Am J Physiol Regul Integr Comp Physiol* 282: R519-27.

208. Siu PM et al. 2009. Response and adaptation of skeletal muscle to denervation stress: the role of apoptosis in muscle loss. *Front Biosci* 14: 432-52.
209. Belizario JE et al. 2001. Cleavage of caspases-1, -3, -6, -8 and -9 substrates by proteases in skeletal muscles from mice undergoing cancer cachexia. *Br J Cancer* 84: 1135-40.
210. Goldberg RM et al. 1995. Pentoxifylline for treatment of cancer anorexia and cachexia? A randomized, double-blind, placebo-controlled trial. *J Clin Oncol* 13 (11): 2856-2859.
211. Lissoni P et al. 1996. Is there a role for melatonin in the treatment of neoplastic cachexia? *Eur J Cancer* 32A (8): 1340-1343.
212. Mantovani G et al. 2006. A phase II study with antioxidants, both in the diet and supplemented, pharmacological support, progestagen, and anti-cyclooxygenase-2 showing efficacy and safety in patients with cancer-related anorexia/cachexia and oxidative stress. *Canc Epidemiol Biomarks Prev* 15 (5): 1030-1034.
213. Dillon E et al. 2013. Testosterone Therapy is Anti-cachectic in Cancer Patients Receiving Standard Care Chemotherapy. *J Geriatric Onco* 4: S21.
214. Wright TJ et al. 2018. A randomized trial of adjunct testosterone for cancer-related muscle loss. *J Cachexia Sarcopenia Muscle* 9 (3): 482-496.
215. Whitehouse AS et al. 2001. Mechanism of attenuation of skeletal muscle protein catabolism in cancer cachexia by eicosapentaenoic acid. *Cancer Res* 61 (9): 3604-3609.
216. Wigmore SJ et al. 1997. Down-regulation of the acute-phase response in patients with pancreatic cancer cachexia receiving oral eicosapentaenoic acid is mediated via suppression of interleukin-6. *Clin Sci* 92 (2): 215-221.
217. Smith HJ et al. Induction of apoptosis by a cachectic-factor in murine myotubes and inhibition by eicosapentaenoic acid. *Apoptosis* 8 (2): 161-169.
218. Bhoj VG et al. 2009. Ubiquitylation in innate and adaptive immunity. *Nature* 458 (7237): 430-437.
219. Li M et al. 2011. Protective effects of eicosapentaenoic acid on genotoxicity and oxidative stress of cyclophosphamide in mice. *Environ Toxicol* 26 (3): 217-223.
220. Van Norren K et al. 2009. Dietary supplementation with a specific combination of high protein, leucine, and fish oil improves muscle function and daily activity in tumour-bearing cachectic mice. *Br J Cancer* 100 (5): 713-722.
221. Wigmore SJ et al. 2000. Effect of oral eicosapentaenoic acid on weight loss in patients with pancreatic cancer. *Nutr Canc* 36 (2): 177-184.
222. Jatoi A et al. An eicosapentaenoic acid supplement versus megestrol acetate versus both for patients with cancer-associated wasting: a North Central Cancer Treatment Group and National Cancer Institute of Canada collaborative effort. *J Clin Oncol* 22 (12): 2469-2476.
223. Goll DE et al. The calpain system. *Physiol Rev* 83: 731-801.

224. Kawasaki H et al. 1993. Calpastatin has two distinct sites for interaction with calpain-- effect of calpastatin fragments on the binding of calpain to membranes. *Arch Biochem Biophys* 305 (2): 467-72.
225. Huang J et al. 1998. Role of calpain in skeletal-muscle protein degradation. *Proc Natl Acad Sci USA* 95 (21): 12100-12105.
226. Han Y et al. 1999. Tumor necrosis factor- $\alpha$ -inducible I $\kappa$ B $\alpha$  proteolysis is mediated by cytosolic m-calpain. A mechanism parallel to the ubiquitin-proteasome pathway for nuclear factor- $\kappa$ B activation. *J Biol Chem* 274: 787-794.
227. Liu ZQ et al. 1996. Proteolytic processing of nuclear factor kappa B by calpain in vitro. *FEBS Lett* 385: 109-113.
228. Smith IJ et al. 2007. Calpain activation causes a proteasome-dependent increase in protein degradation and inhibits the Akt signaling pathway in rat diaphragm muscle. *Exp Physiol* 92: 561-573.
229. Menconi MJ et al. 2004. Treatment of cultured myotubes with the calcium ionophore A23187 increases proteasome activity via a CaMK II-caspase-calpain-dependent mechanism. *Surgery* 136: 135-142.
230. Bhattacharyya J et al. 1991. Calcium-dependent and calcium-independent protease activities in skeletal muscle during sepsis. *Circ Shock* 35: 117-122.
231. Fischer DR et al. 2001. Dantrolene reduces serum TNF $\alpha$  and corticosterone levels and muscle calcium, calpain gene expression and protein breakdown in septic rats. *Shock* 15: 200-207.
232. Voisin L et al. 1996. Muscle wasting in a rat model of long-lasting sepsis results from the activation of lysosomal, Ca (2+)-activated, and ubiquitin-proteasome proteolytic pathways. *J Clin Invest* 97: 1610-1617.
233. Williams AB et al. 1999. Sepsis stimulates release of myofilaments in skeletal muscle by a calcium-dependent mechanism. *FASEB J* 13: 1435-1443.
234. Busquets S et al. 2000. Calpain-3 gene expression is decreased during experimental cancer cachexia. *Biochim Biophys Acta* 1475: 5-9.
235. Costelli P et al. 2001. Activation of Ca (2+)-dependent proteolysis in skeletal muscle and heart in cancer cachexia. *Br J Cancer* 84: 946-950.
236. Dargelos E et al. 2008. Calcium-dependent proteolytic system and muscle dysfunctions: a possible role of calpains in sarcopenia. *Biochimie* 90: 359-368.
237. Servais S et al. 2007. Prevention of unloading-induced atrophy by vitamin E supplementation: links between oxidative stress and soleus muscle proteolysis? *Free Radic Biol Med* 42: 627-635.
238. Takahashi M et al. 2006. Possible involvement of calpain activation in pathogenesis of chronic heart failure after myocardial infarction. *Cardiovasc Pharmacol* 47: 413-421.
239. Lin X et al. 2017. Calpain inhibitors ameliorate muscle wasting in a cachectic mouse model bearing CT26 colorectal adenocarcinoma. *Oncology Reports* 37: 1601-1610.
240. Ghosh J et al. 2017. Role of mTORC1-S6K1 signaling pathway in regulation of hematopoietic stem cell and acute myeloid leukemia. *Exp Hema* 50: 13-21.

241. Azad N et al. 2014. Management of chronic heart failure in the older population. *J Geriatr Cardiol* 11(4): 329-337.
242. Scheel B et al. 2015. Symptoms, signs, and tests: The general practitioner's comprehensive approach towards a cancer diagnosis. *Scand J Prim Health Care* 33 (3): 170-177.
243. Huang H et al. 2007. Dynamic FoxO transcription factors. *J Cell Sci* 120: 2479-2487.
244. Parzych K et al. 2014. An Overview of Autophagy: Morphology, Mechanism, and Regulation. *Antioxid Redox Signal* 20 (3): 460-473.
245. Yang Z et al. 2010. Mammalian autophagy: core molecular machinery and signaling regulation. *Curr Opin Cell Biol* 22:124-131.
246. Yorimitsu T et al. 2005. Autophagy: molecular machinery for self-eating. *Cell Death Differ* 12: 1542-1552.
247. Wirawan E et al. 2012. Autophagy: for better or for worse. *Cell Res* 22: 43-61.
248. Aversa Z et al. 2016. Autophagy is induced in the skeletal muscle of cachectic cancer patients. *Scientific Reports* 6: 30340.
249. Puig-Vilanova E et al. 2015. Oxidative stress, redox signaling pathways, and autophagy in cachectic muscles of male patients with advanced COPD and lung cancer. *Free Radi Bio and Med* 79: 91-108.
250. Tardif N et al. 2013. Autophagic-lysosomal pathway is the main proteolytic system modified in the skeletal muscle of esophageal cancer patients. *Am J Clin Nutr* 98: 1485-1492.
251. Nakata B et al. 1994. Association between hsp60 messenger-RNA levels and Cisplatin resistance in human head and neck-cancer cell-lines. *Int J Oncol* 5 (6): 1425-32.
252. Matsunaga A et al. 2014. Inhibition of heat shock protein 27 phosphorylation promotes sensitivity to 5-fluorouracil in colorectal cancer cells. *Oncol Lett* 8 (6): 2496-2500.
253. Alves E et al. 2016. Doxorubicin caused severe hyperglycemia and insulin resistance, mediated by inhibition in AMPk signaling in skeletal muscle. *J cachexia Sarc Musc* 7 (5): 615-625.
254. Cheong H et al. 2011. Ammonia-induced autophagy is independent of ULK1/ULK2 kinases. *Proc Natl Acad Sci U.S.A* 108: 11121-11126.
255. Chan E.Y. 2007. siRNA screening of the kinome identifies ULK1 as a multidomain modulator of autophagy. *J Biol Chem* 282: 25464-25474.
256. Ganley I et al. 2009. ULK1.ATG13.FIP200 complex mediates mTOR signaling and is essential for autophagy. *J Biol Chem* 284: 12297-12305.
257. Hosokawa N et al. 2009. Nutrient-dependent mTORC1 association with the ULK1-Atg13-FIP200 complex required for autophagy. *Mol Biol Cell* 20: 1981-1991.
258. Zachari M et al. 2017. The mammalian ULK1 complex and autophagy initiation. *Essays Biochem* 61 (6): 585-596.
259. Kim J et al. 2011. AMPK and mTOR regulate autophagy through direct phosphorylation of Ulk1. *Nat Cell Biol* 13: 132-141.
260. Lin S et al. 2012. GSK3-TIP60-ULK1 signaling pathway links growth factor deprivation to autophagy. *Science* 336: 477-481.

261. Liu Z et al. 2018. p38 $\beta$  MAPK mediates ULK1-dependent induction of autophagy in skeletal muscle of tumor-bearing mice. *Cell Stress* 2 (11): 311-324.
262. Muller F et al. 2000. The nature and mechanism of superoxide production by the electron transport chain. *J Am Aging Assoc* 23: 227-253.
263. Kim S et al. 2017. Effects of growth hormone on glucose metabolism and insulin resistance in human. *Ann Pediatr Endo Metab.* 22 (3): 145-152.
264. Mansouri A et al. 2003. Sustained Activation of JNK/p38 MAPK Pathways in Response to Cisplatin Leads to Fas Ligand Induction and Cell Death in Ovarian Carcinoma Cells. *JBC* 278: 19245-19246.
265. Morissette M et al. 2009. Myostatin inhibits IGF-I-induced myotube hypertrophy through Akt. *Am J Phys Cell Physiol* 297 (5): 1124-32.
266. Pin F et al. 2019. PDK4 drives metabolic alterations and muscle atrophy in cancer cachexia. *FASEB*.
267. McCroskery S et al. 2003. Myostatin negatively regulates satellite cell activation and self-renewal. *J Cell Biol* 162: 1135-1147.
268. Cohen S et al. 2015. Muscle wasting in disease: molecular mechanisms and promising therapies. *Nature Reviews* 14.

## Appendices

### Appendix A - Myofibrillar and Sarcoplasmic Fractionation of Myotubes

1. Suck media from each well, add 500 $\mu$ L trypsin into each well, swish around and incubate for 5 minutes.
2. May need to scrape the wells to unstick myotubes. Add 2mLs PBS into each well.
3. Combine three wells of the same condition together and add combined well into 1 15mL test tube.
4. Centrifuge each 15mL test tube at 2000rpm for 5 minutes.
5. Take out 15mL test tubes out and suck media, but leave pellet. Do this for all. Resuspend pellet in 1mL PBS and break up the pellet. Spin down again, same speed and time.
6. Take 15mL test tubes from centrifuge, suck media but leave the pellet. Resuspend pellet from each 15mL tube into 500 $\mu$ L of triton solution. Triton Solution:
  - Triton (1% Triton per mL of PBS)
  - Protease Inhibitor 10 $\mu$ L/mL
  - Phosphatase Inhibitor 10 $\mu$ L/mL
  - EDTA (Add to 1mM)
7. Each 15mL tube will now have 500 $\mu$ L of triton mixture in it. Need 2 eppendorf tubes for each 15mL test tube. 1 will be labelled protein assay/loading control, 2 is for sarcoplasmic/Myofibrillar amounts.

Pipette the full 500 $\mu$ L from the 15mL tube (mixed well) into eppendorf tube number 2. Do this for all and syringe the mixture up and down to break it up. Then take 100 $\mu$ L from eppendorf tube 2 and put in eppendorf tube 1 labelled protein assay/loading control. Place the 100 $\mu$ L aliquot (eppendorf tube 1) into -20 freezer.
8. Centrifuge eppendorf tube 2 (400 $\mu$ L) at 1200g (RCF 12.0) for 5 minutes. Use the fridge centrifuge.
9. Need more eppendorf tubes. Label them sarcoplasmic. Need a sarcoplasmic eppendorf tube for each eppendorf tube that we are centrifuging. The supernatant (400 $\mu$ L) will be the sarcoplasmic fraction while the pellet will be our Myofibrillar. Take a 400 $\mu$ L aliquot and add it into our eppendorf tube labelled sarcoplasmic and place in -80 degree. Put Myofibrillar on ice for now.
10. Grab the MPI buffer from the 4 degree fridge. Need 300 $\mu$ L of the buffer for each sample. Also need 10 $\mu$ L/mL of protease inhibitor.
11. Add 300 $\mu$ L of the buffer we made onto the Myofibrillar pellet. Break down the pellet into the buffer and leave in fridge on ice for 40 minutes. Every 10 minutes, mix the buffer with pellet up and down.
12. After 40 minutes on ice, use fridge centrifuge to spin down. 13.0 RCF for 30 minutes.
13. Need 3 more eppendorf tube per sample. Add 100 $\mu$ L of each eppendorf tube into the 3 eppendorf tube tubes after breaking up.

14. Now need filament buffer. Need 900 $\mu$ L of filament buffer for each eppendorf tube. Start by calculating how much buffer you need in total. Ratio is 1mM of EDTA to 0.1% BM in DDH<sub>2</sub>O.
15. Mix well and put in fridge on ice overnight.
16. The following day: Take out of ice box and put Myofibrillar samples in fridge centrifuge. 13.0 RCF for 30 minutes.
17. Take buffer out and throw away. We want pellet.  
Empty one eppendorf tube fully. For other two empty all but 50 $\mu$ L. Scrape the eppendorf tube to get the pellet off and switch all into 1 eppendorf tube.
18. Add 600 $\mu$ L of filament buffer to each eppendorf tube. Scrape pellet and mix well.
19. Centrifuge 13.0 rcf for 3 minutes.
20. Take out 600 $\mu$ L and throw away.
21. Add 50 $\mu$ L of 1x sample buffer to each eppendorf tube, mix well.

### **Appendix B - Immunofluorescence Microscopy**

1. Sterilize cover slips by autoclaving them. Place a single cover slip into each well of a 12-well plate.
2. Plate L6 myoblasts in the 12-well plate on top of cover slips. Include sufficient number of well so you can have a negative control. Grow myoblasts according to regular procedure.
3. When cells are confluent, change to differentiation medium.
4. Change medium every 24-48 hours until day 4 when myotubes are ready for treatment.  
On day 4, treat cells with the chemotherapy drug cocktail according to regular protocol.

The following steps take place on both day 5 and day 6 of treatment.

5. Remove medium and rinse each well 2X with 1mL of PBS.
6. FIXING: In fume hood, fix cells by incubating them in 1mL/well of paraformaldehyde (4% PFA in PBS) for 10minutes at room temperature. Use gentle swirling on a rocker. After 10minutes, remove paraformaldehyde and store in a container in hood.
7. Do 3X quick rinse in PBS with 1mL/well.
8. PERMEABILIZATION: Permeabilize the cells by adding 1mL/well of 0.03% Triton X-100 in PBS. Incubate for 5 minutes.
9. WASHING: Remove Triton solution and wash 5X, 1mL/wash, 5minutes/wash.
10. BLOCKING: Incubate with 400 $\mu$ L/well of blocking solution: 10% horse serum in PBS. Block at 37°C for 1hour with periodic swirl.
11. PRIMARY ANTIBODY: Add sufficient amount of diluted antibody, ~500 $\mu$ L/well. (MHC from Dev Hybridoma, 2.5 $\mu$ g/mL diluted in 1% BSA in PBS). Incubate overnight at 4°C with gentle rocking.
12. WASH: Decant and save primary antibody. Do one quick rinse in PBS and then 3X wash in PBS, 5minutes/wash with gentle rocking.
13. SECONDARY ANTIBODY: Dilute secondary antibody (Texas Red anti-mouse IgG, raised in horse). Dilute 1:100 with 1% BSA in PBS. After removing PBS from washing (step 12), add 500 $\mu$ L/well of the diluted secondary antibody and incubate for 2hour, room

temperature on a rocker. Make sure to keep the wells covered and protected from light using aluminum foil. This is to ensure that no photo-damage takes place on the fluorochromes of the secondary antibody.

14. WASH: Remove secondary antibody and wash 5X, 10minutes/wash in PBS.
15. MOUNTING: Take appropriately labelled microscop slides. Put a drop of mounting medium on each slide. The mounting medium contains DAPI (to stain the nucleus) and anti-oxidants to prevent oxidation of the fluorochromes.
16. With a pair of tweezers, take the cover slip out and invert the slip on the mounting medium. Ensure the side on which the cells are face the medium.
17. MICROSCOPY: Observe under the microscope.

### **Appendix C - Deoxy-Glucose Uptake in Myotubes**

Following the 20minute insulin treatment:

1. Aspirate media and do 2X wash with 400 $\mu$ L/well of Hepes Buffered Saline at room temperature. After 2X washes, aspirate any remaining media.  
HEPES BUFFERED SALINE:
  - 140 mM NaCl
  - 20 mM Hepes-Na, pH 7.4
  - 5 mM KCl
  - 2.5mM MgSO<sub>4</sub>
  - 1.0 mM CaCl<sub>2</sub>
2. For specific uptake, add 300 $\mu$ L/well of transport solution/well of the 12-well plate.  
TRANSPORT SOLUTION:
  - Prepare in Hepes Buffer
  - 10 $\mu$ M 2-Deoxy-Glucose
  - 0.5  $\mu$ Ci/mL <sup>3</sup>H 2-Deoxy-Glucose
3. Incubate for 5minutes at room temperature.
4. Working quickly, aspirate away the transport solution and do 3X washes, 1mL/well with ice-cold stop solution and aspirate to dryness.  
ICE-COLD STOP SOLUTION:
  - 0.9% Saline
5. Add 1mL/well of 0.05 NaOH, scrape and add 800 $\mu$ L for scintillation counting. The remaining 200 $\mu$ L is collected for protein assay and stored at -20°C.